CS/AR-2/2006

DAM BREAK FLOOD SIMULATION AND RESERVOIR SEDIMENTATION IN MAITHON RESERVOIR

(Part II – Dam Break Flow Simulation)

आपो हिष्ठा मयो भुव:

NATIONAL INSTITUTE OF HYDROLOGY
JAL VIGYAN BHAWAN
ROORKEE – 247667 (UTTARAKHAND)

2006

DIRECTOR

K.D. Sharma

CO-ORDINATOR

R.D. Singh

STUDY GROUP

Pankaj Mani

Biswajit Chakravorty

PREFACE

Protection of the public lives and properties from the consequences of dam failures has become important as population have concentrated in areas vulnerable to dam break disasters. The organizations responsible for the safety of dams should plan for preventive measures in case of dam failures so that damages to the lives and properties of the population living in the downstream area may be minimized. One of the preventive measures to reduce the losses due to breaking of a dam is by issuing flood warning to the downstream population. However, it is quite difficult to conduct analysis and determine the warning time and extent of inundation at the time of disaster. Therefore, pre-determination of these parameters is done by simulating a hypothetical dam break situation. The method used for such analysis gains more credibility if one can simulate the past dam break failure scenario using that method with reference to failure mode and flood wave movement downstream of the dam.

Although much academic research have been undertaken on this topic, a generalized analytical technique for simulating and routing of dam-break flows through natural channels is rarely available. The DAMBRK model developed by U.S. National Weather Service and MIKE-11 model developed by Danish Hydraulic Institute, Denmark, are two of many computer programs used to simulate such flows. These programs are capable of simulating the dam break flood wave and one-dimensional flood routing through downstream river channels as well as structures such as bridges, embankments etc. Dam break flood analysis can provide useful information about the flood inundation and warning time and help in reducing the tangible and intangible losses resulting from dam failures.

In the present study, dam break flow simulation analysis for combined flow from Maithon and Panchet dams in Damodar Valley has been carried out using the DAMBRK package of the U.S. National Weather Service. The study entitled "Dam break flood simulation and reservoir sedimentation in Maithon reservoir" was taken up in the work program of CFMS, Patna in the year 2004-2005. The study consists of two parts. The first part of the study, the estimation of reservoir sedimentation in Maithon reservoir using remote sensing technique was completed during 2004-2005 and has been reported. The second part of the study covering the simulation of dam break flow of Maithon and Panchet dam in Damodar valley has been performed in this report. The dam break flow simulation has been performed for different scenarios of dam/s failure. The maximum stage, maximum discharge and maximum flow velocity at various cross sections along the two rivers have been computed and inundation maps have been prepared. The sensitivity analysis of breach parameters for Maithon and Panchet dam has also been studies. The study has been carried out by Shri Pankaj Mani, Scientist 'C' and Shri Biswajit Chakravorty Scientist 'E1' of the Centre. We are thankful to DVC for the help and data support provided by officials of DVC for the study.

K.D. Sharma
Director

ABSTRACT

Dam break flow simulation study for various combination of failure of Maithon and Panchet dam on Barakar and Damodar river in Jharkhand state has been carried out using NWS DAMBRK model. The model simulates the development of breach in the dam section and routs the resulting flow in the downstream river valley using one dimensional Saint-Venant equation. The reservoir inflow for dam break analysis has been considered, instead of those mentioned in the completion report of two projects, based on a recent paper in which the PMF for Panchet and Maithon have been computed. The simulation has been performed for different scenarios of failure of Maithon and Panchet dams. Further, the analysis has also been performed for dam break failure under earthquake or terrorist attack by simulating a instantaneous failure of dams under nominal inflow in the reservoir. The failure of Maithon dam on Barakar river has been considered separately and its outflow at the confluence of two rivers has been considered as lateral inflow while simulating the dam break failure in Panchet dam over river Damodar. The maximum discharge, maximum stage and maximum flow velocity and its time of occurrence at various cross sections along the Damodar and Barakar river have been computed. The inundation maps showing the extent, depth and area of inundation have also been prepared in GIS environment. The sensitivity analyses of assumed breach parameters namely breach width, time of breach and slope of breach section have been performed for two dams separately.

CONTENTS

LIST OF FIGURES

LIST OF TABLES

1.0 INTRODUCTION

The dam break flood resulting due to inappropriate design or operational conditions or any other reasons, can cause catastrophe in the downstream regions having dense population and important establishments. The failure of a dam is of serious concern due to involvement of loss of lives and properties. Dam break flood analysis has become important not only for new dams but also for reviewing the existing dams designed and constructed many years ago utilizing the limited historical data and the present design standards may not be met. It is important to mention that dam break analyses of some of the dams constructed earlier have been reported to have inadequate spillways capacity. A comprehensive multistage dam break flood analysis can be justified to be useful for spillway design flood and to overcome public fears.

Water resources planners require quantitative criteria to support various decisions on engineering projects and evaluation of environmental impact and risks. In such analysis, including failure damage, different scenarios associated with flood effects are generally considered. Some of the objectives of dam break analysis are:

i. To establish the required dam spillway capacity;
ii. To evaluate environmental and safety impact of dams or other structure built in a river valley;
iii. Valley planning and flood plain zoning;
iv. To formulate emergency procedures such as warning system, evacuation plan etc.;
v. To identify and solve unexpected flood problems due to accidents;
vi. To remove fear in public and make the public aware of the risk;
vii. To analyze past accidents for advancement of the state of art.

Dam break flood is viewed under the classical unsteady flow problem of sudden release of water. However, the magnitude of the flood depths and the discharge of dam break flood event are unusually high. It is difficult to make a rigorous description of the flood propagation at the initial reach. Eye witness describes it as a violent trembling of ground followed by a brief rumble, then a strong blast of air and finally the arrival of water-first as 'a wave and then as a huge wall surging from the gorge'.

As the dam break floods (DBF) are associated with loss of lives and properties, the dam break floods analysis is very important from the point of view of flood disaster management.

Although much academic research have been undertaken on this topic, a generalized analytical technique for simulating and routing of dam-break flows through natural channels is rarely available. DAMBRK by U.S. National Weather Service and MIKE-11 by Danish Hydraulic Institute, Denmark are two of the many computer programs used to analyses such events. These programs are capable of simulating the DBF wave and routing through river channels and downstream structures like bridges, embankments, etc. These programs can provide information about the flood inundation and warning time resulting from dam failures.

1.1 Objective of the Study

The Panchet dam is located on Damodar river while Maithon dam is located on river Barakar, a tributary of Damodar. The two rivers join togather at 6.4 km d/s of Panchet dam and 12.9 km d/s of Maithon dam. In this study, it is envisaged (i) to compute the dam break flood hydrographs at Maithon and Panchet dam sections, (ii) Routing of flood hydrograph from Maithon dam upto the confluence of Damodar and Barakar, (iii) Routing of flood hydrograph from Panchet dam assuming the lateral inflow from Maithon at confluence, (iv) Preparation of flood inundation maps for different scenarios, and (iii) sensitivity analysis for breach parameters

1.2 Literature Review: Dam Break Flood Simulation Studies

The dam break modelling is an old problem in mathematical hydraulics and the concerned literature is extensive. The first solution was given in 1892 by Ritter, who used the method of characteristics to obtain a closed form solution for a dam of semi-infinite extent upon a horizontal bed with zero bed resistance. However, experimental and theoretical considerations showed that the solution is invalid in a region that starts near the leading edge of the flood wave and extends rapidly upstream with time, because of zero bed resistance assumption.

Sakkas and Strelkoff (1973), Chen and Druffel (1977) have used the method of characteristics to obtain numerical solution for dam break problems on sloping beds. These solutions were for reservoirs of finite length and included the effects of bed resistance. But in almost all of these methods, it was assumed that the breach covers the entire dam and it occurs instantaneously. U.S. Army Corps of Engineers (1960) recognized the need to assume partial breaches; however, they assumed an instantaneous failure.

In 1965, Cristofano and in 1967, Harris and Wagner incorporated the partial time dependent breach formation in their models. Cheng Lung Chen (1985) developed a numerical model on the basis of an explicit scheme of the characteristic methods with specified time intervals. He also carried out some laboratory experiments for the verification of his model. Bruce (1982) used the kinematic approximation to obtain a simple, closed form solution for the failure of a dam on a dry, sloping channel. It was found that this solution becomes asymptotically valid after the flood wave has advanced about four reservoir lengths downstream. N. D. Katopodes and D. R. Schambar (1982) formulated five mathematical models based on equations ranging from the complete dynamic system to a simple normal depth kinematic wave equation. In 1984, they have presented a theory for flow through a partial dam failure. In this, the breach section is treated as an internal boundary condition that interrupts the continuous long wave occurring upstream and downstream of the dam.

The U.S. Army Corps of Engineers, HEC-1 dam break model (HEC-1, 1981) adopts storage routing techniques for routing of flood through reservoirs as well as through channels. National Weather Service (NWS) DAMBRK Model (Fread, 1984) adopts dynamic routing techniques for routing of flood through channel and a choice of dynamic routing and storage routing for the reservoir, depending on the nature of flood wave movement in reservoir at the time of failure.

Singh and Snorrason (1982) carried out dam break flood studies using the above two models. They found that the flood stage profiles predicted by the NWS DAMBRK Model are smoother and more reasonable than those predicted by the HEC-1. For channels with relatively steep slopes, the methods compared fairly well, whereas for channels with mild slope, the HEC Model often predicted oscillatory, erratic flood stages, mainly due to its inability to route flood waves satisfactorily in non- prismatic channel.

Ralph A. Wurbs (1986) made a comparative evaluation of several dam break models. The models selected for comparison were : National Weather Service (NWS) Dam Break Flood Forecasting Model (DAMBRK); U.S. Army Corps of Engineers South-Western Division (SWD) Flow Simulation Models (FLOW SIM 1&2), U.S. Army Corps of Engineers Hydrologic Engineering Centre (HEC) Flood Hydrograph Package (HEC-1), Soil Conservation Service (SCS) Simplified Dam Breach Routing Procedure (TR66), NWS Simplified Dam break Flood Forecasting Models (SMPDBK), HEC dimensionless graphs procedure and the Military Hydrology Model (MILHY) developed by WES specially for military use. He concluded that a

dynamic routing model should be used whenever a maximum practical level of accuracy is required and adequate man power, time and computer resources are available. According to him the NWS DAMBRK is the optimal choice of model for most practical applications.

DAMBRK model uses Saint Venant's equations for routing dam break floods in channels. For reasons of simplicity, generality, wide applicability and uncertainty in the actual failure mechanism, this model allows the failure timing interval and terminal size and shape of breach as input. It gives the extent of and the time of occurrence of flooding in the downstream valley by routing the outflow hydrograph through the valley. The dynamic wave method based on the complete equations of unsteady flow is the appropriate technique to route the dam break flood hydrograph (User Manual, DAMBRK, 1989). Terzidis and Strelkoff (1970) have demonstrated the applicability of the St.Venant's equations to simulate abrupt waves such as the dam break wave.

Gundalach & Thomas (1977) analyzed the dam break flood from Teton dam using a generalized unsteady flow computer program to determine the water surface elevations resulting from various breach sizes and roughness values (n). They found that neither the size of breaches tested (30 to 40% of the size of dam) nor the rates of failures assumed were very significant in predicting peak elevation at dam axis but the calculated peak flood elevations near the dam were very sensitive to n-values. Sakkas (1980) envisaged the development of dimensionless graphs for quick estimation of dam breach flood wave characteristics. These graphs would be useful in case when either the communication system or computation facilities are not available at the time of dam breach flood wave formation. Singh and Snorrason (1984) studied the sensitivity of outflow peaks and flood stages to the dam breach parameters. They have taken an earthen dam for the study and found that the breach outflow peaks are affected significantly by the base width of breach but less so by the water level in the reservoir at the time of breach formation. They also found that the ratio of outflow peak to inflow peak and the effect of time of failure on outflow decreases as the drainage area above the dam and impounded storage increases.

Kjelds et al. (2002) has compared the modeling capability of MIKE 11, DAMBRK and FLDWAV. He also compared the simulation results from number of real application using these models. Further, he used the combined one/ two dimensional modeling approach for flood inundation mapping. He concluded that flood modeling system having one dimensional river hydraulics model and two dimensional surface water model provide a highly efficient system

with detailed modeling and accuracy without sacrificing computational or model development time.

1.3 Dam Break Flood Simulation Studies Carried out at NIH

National Institute of Hydrology has also carried out many studies related to dam break study since 1985. These include preparation of data requirements for dam break models to many case studies with actual and hypothetical dam failure data. The reports published so far based on the dam break flood simulation studies conducted by National Institute of Hydrology are tabulated below:

Name of the Study	NIH Reference No	
Dam break analysis for Machu dam-II	CS	16
Application of NWS Dam break programme using data of Gandhi Sagar Dam	CS	49
Application of dam break program MIKE 11 to Machhu II dam and its comparison with NWS DAMBRK application results	CS	89
Dam break study of MITTI dam	CS/AR	126
Dam break analysis of Machhu dam -II failure using DAMBRK and SMPDBK models of NWS	CS/AR	133
Preliminary dam break analysis of Bargi dam	CS/AR	185
Dam break study of Barna dam	CS/AR	20/96-97
Development of dimensionless flood hydrographs from Machhu dam – II failure using dambrk model;	TR	34
Effect of downstream boundary conditions on the propagation characteristics of the Dam Break flood	TR/BR	117
Development of an empirical formula for approximate dam break flood estimation	TR/BR	1147
Dam Break Study of Myntdu Leska Dam using DAMBRK Model.	CS/AR	1/2000-2001
Dam break flood simulation study of Sri Ram Sagar Dam – Consultancy work		2004
Dam break flood simulation study of Lower Manner Dam– Consultancy work		2004

Note: CS- Case Study, CS/AR- Case Study/Applied Research, TR- Technical Report, TR/BR- Technical Report/Basic Research

2.0 NWS DAMBRK MODEL

Dam failures are often caused by over topping of the dam due to inadequate spillway capacity during large inflow to the reservoir from heavy precipitation runoff. Dam failures may also be caused by seepage or piping through the dam or along internal conduits, slope embankment slides; earthquake damage and liquefaction of earthen dams from earthquakes and land slide generated waves in the reservoir. Usually the response time available for warning is much shorter than for precipitation-runoff-floods. The protection of public life and property from the consequences of dam failures has taken an increasing importance as population has concentrated in areas vulnerable to dam break disasters.

Occurrence of a series of dam failures has increasingly focused attention of project managers on the need to evaluate flash floods due to dam failure and for routing them through downstream areas, susceptible to heavy losses, so that potential hazards might be evaluated. From these inundated areas, flow depths and flow velocities can be estimated for different hypothetical dam failure situations. With the help of such studies it is possible to issue warnings to the downstream public and prepare strategies for disaster management when there is a failure of dam. The main difficulty in using the mathematical models is the failure description adopted in the model. Under these circumstances, a suitable assumption with regard to the adjustment of actual failure mode to suit the model failure mode is necessary.

The DAMBRK model developed by U. S. National Weather Services (NWS) attempts to represent the current state-of-art in understanding dam failures and utilizing hydrodynamic theory to predict the dam break wave formation and its downstream progression. The model has wide applicability. It can function with various levels of input data ranging from rough estimates to complete data specification.

2.1 Breach Description

The breach is the opening formed in the dam as it fails. The actual failure mechanisms are not well understood for either earthen or concrete dams. In earlier attempts to predict downstream flooding due to dam failures, it was usually assumed that dam failed completely and instantaneously. This was due to the reason of convenience and when applying certain mathematical techniques for analyzing dam break flood waves. These assumptions are somewhat appropriate for concrete dam but they are not appropriate for earthen dams and concrete gravity

dams. In DAMBRK the breach is always assumed to develop over a finite interval of time (τ) and will have a final size determined by a terminal bottom width parameters (b) and various shapes depending on another parameters (z). Such a parametric representation of the breach is utilized in DAMBRK for reasons of simplicity, generality, wide applicability, and the uncertainty in the actual failure mechanism.

The shape parameter (Z) identifies the side slope of the breach i.e., 1 vertical: Z horizontal. The range of Z values are from 0 to somewhat larger than unity. Its value depends on

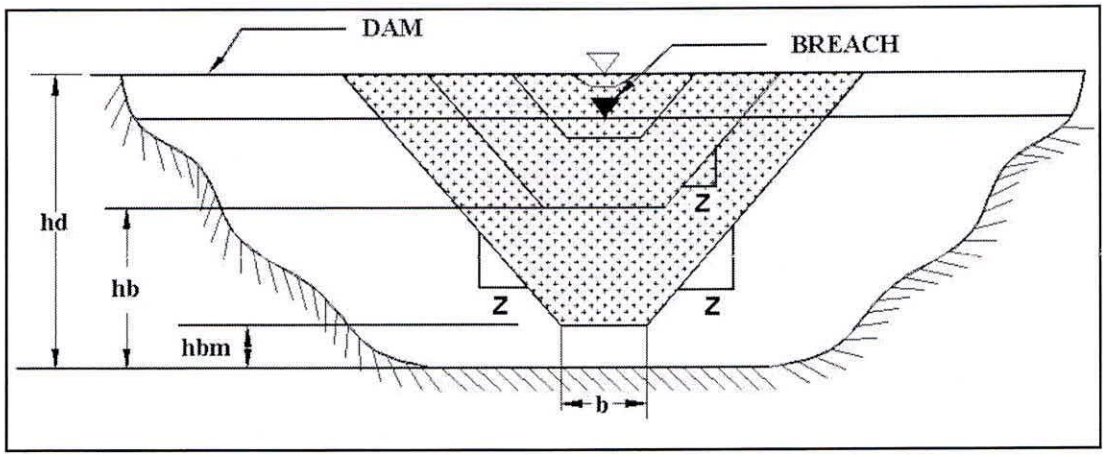

Schematic diagram showing formation of breach

the angle of repose of the compacted and wetted materials through which the breach develops. Rectangular, triangular, trapezoidal shapes may be specified by using various combinations of values for Z and b, e.g., Z=0 and b>0 produces a rectangle and Z>0 and b=0 yields a triangular-shaped breach. The terminal width b is related to the average width of the breach ($\bar{b}$) by the following:

$$b = \bar{b} - z_d \qquad (1)$$

The model assumes the breach bottom width starts at a point and enlarge at a linear or nonlinear rate over the failure time (τ) until the terminal bottom width (b) is attained and the breach bottom has eroded to the elevation h_{bm}. If τ is less than one minute, the width of the breach bottom starts at a value b rather than zero. This represents more of a collapse failure than

an erosion failure. The bottom elevation of the breach is simulated as a function of time (τ) according to the following:

$$h_b = h_d - (h_d - h_{bm})\left(\frac{t_b}{\tau}\right)^{\rho} \qquad \text{if } 0 < t_b \leq \tau \qquad (2)$$

in which h_{bm} is the final elevation of the breach bottom elevation which is usually, but not necessarily, the bottom of the bottom of the reservoir or outlet channel bottom, t_b is the time since beginning of breach formation, and ρ is the parameter specifying the degree of non linearity, e.g., $\rho = 1$ is a linear formation rate, while $\rho = 2$ is a nonlinear quadratic rate; the range for ρ is $1 \leq \rho \leq 4$; however, the linear rate is usually assumed. The instantaneous bottom width b_i of the breach is given by the following:

$$b_i = b\left(t_b / \tau\right)^{\rho} \qquad \text{if } 0 < t_b \leq \tau \qquad (3)$$

During the simulation of dam failures, the actual breach formation commences when the reservoir water surface elevation (h) exceeds a specified value h_f. This feature permits the simulation of an overtopping of a dam in which breach does not form until a sufficient amount of water is flowing over the crest of the dam. A piping failure may also be simulated by specifying the initial centerline elevation of the pipe. User may also specify the time after beginning of simulation when the breach begins to form. This is an alternative to the use of h_f as the overtopping elevation at which failure commences.

Concrete Dams- Concrete gravity dams tend to have a partial breach as one or more monolithic sections formed during the construction of the dam are forced apart and overturned by the escaping water. The time for breach formation is in the range of a few minutes. Concrete arc dams tend to fail completely and are assumed to require only a few minutes for the breach formation. The shape parameter (Z) is usually assumed zero for concrete dams

Earthen Dams- Earthen dams do not tend to completely fail nor do they fail instantaneously. The fully formed breach in earthen dams tend to have an average width ($\bar{b}$) in the range ($h \leq \bar{b} \leq 5h_d$) where h_d is the height of the dam. Breach widths for earthen dams are therefore usually much less than the total length of dam as measured across the valley. Also, the breach requires a finite interval of time (τ) for its formation through erosion of the dam materials

by the escaping water. Total time of failure (for overtopping) may be in the range of a few minutes to usually less than an hour, depending on the height of the dam, the type of materials used in construction, the extent of compaction of the materials and the magnitude and duration of the overtopping flow of escaping water. The time of failure as used in DAMBRK is the duration of time between the first breaching of the upstream face of the dam until the breach is fully formed. For overtopping failures the beginning of breach formation is after the downstream face of the dam has eroded away and the resulting crevasse has progressed back across the width of the dam crest to reach the upstream face. Piping failures occur when initial breach formation take place at some point below the top of the dam due to erosion of an internal channel through the dam by escaping water. Times of failure are usually longer for piping than overtopping failures since the upstream face is slowly eroded in the very early phase of the piping development. As the erosion proceeds larger opening is formed; this is eventually hastened by caving-in of the top portion of the dam. Poorly constructed coal-waste slag piles (dams) which impound water tend to fail within a few minutes, and have average breach widths in the upper range of the earthen dams mentioned above.

Some statistically derived predictors for $\bar{b}$ and τ have been presented by MacDonald and Langridge-Monopolis (1984) and Froelich (1987). Froelich used the properties of 43 breaches of dams ranging in height from 15 to 285 ft with all but 6 between 15 and 100 ft, the following predictive equations can be obtained:

$$\bar{b} = 9.5\, k_0 (v_r h_d)^{0.25} \tag{4}$$

$$\tau = {0.59\, v_r^{0.47}} \Big/ {h_d^{0.9}} \tag{5}$$

in which $\bar{b}$ is average breach width (ft), τ is the time of failures (hrs), k_0=0.7 for piping and 1.0 for overtopping, v_r is the volume (acre-ft) and h_d is the height (ft) of water over the breach bottom which is usually about the height of the dam. Standard error of estimate for $\bar{b}$ was ±94 ft which is an average error of ±54% of $\bar{b}$ and the standard error of estimate for τ was ± 0.9 hrs which is an average error of ±70% of τ.

Another means of determining the breach properties is the use of physically based breach erosion models. However, this procedure requires critical assumptions and specification of

unknown critical parameter values. Harris and Wanger (1967) used a sediment transport relation to determine the time for breach formation, but this procedure requires specification of breach size and shape in addition to two critical parameters for the sediment transport relation. Ponce and Tsivoglou (1981) presented a rather computationally complex breach erosion model which coupled the Meyer-Peter and Muller sediment transport equation to the one-dimensional differential equations of unsteady flow and sediment conservation.

Fread (1987) developed a breach erosion model for earthen dam. It is a physically based mathematical model which predicts the breach characteristics (size shape, time of formation) and the discharge hygrograph emanating from a breached earthen dam. The earthen dam may be man made or naturally formed by a landslide. The model is developed by coupling the conservation of mass of the reservoir inflow, spillway outflow, and breach outflow with the sediment transport capacity of the unsteady uniform flow along an erosion-formed breach channel. The bottom slope of the breach channel is assumed to be essentially that of the downstream face of the dam. The growth of the breach channel is dependent on the dam's materials properties (D_{50} size, unit weight, friction angle, cohesive strength). The model considers the possible existence of the following complexities (i) properties of construction material differ from those of the outer portions of the dam; (ii) the necessity of forming an eroded ditch along the downstream face of the dam prior to the actual breach formation by the overtopping water; (iii) the downstream face of the dam can have a grass cover or it may be composed of material of larger grain size than the outer portion of the dam; (iv) enlargement of the breach through the mechanism of one or more sudden structural collapses of portions of the dam where breaching occurs due to hydrostatic pressure force exceeding the resisting shear and cohesive forces; (v) enlargement of the breach width by collapse of breach sides according to slope stability theory; and (vi) initiation of the breach via piping with subsequent progression to a free surface breach flow. The outflow hydrograph is obtained through a time-stepping iterative solution that requires only a few seconds for computation on a mainframe computer. The model is not subject to numerical stability or convergence difficulties. The model's predictions have been favorably compared with observations of a pipe failure of the man-made Teton Dam in Idaho, the piping failure of the man-made Lawn Lake Dam in Colorado, and an overtopping activated breach of a landslide formed dam in Peru. Model sensitivity to numerical parameters is minimum, however, it is sensitive to the internal friction angle of the dam material and the extent of grass cover when simulating man-made dam and to the cohesive strength of the material composing land slide-famed dams.

Another way of checking the reasonableness of the breach parameters (b and τ) is to use the following the equations:

$$Q_p^* = 370(v_r h_d)^{0.5} \tag{6}$$

$$Q_p = 3.1\,\bar{b}\left(\frac{C}{\tau + C/\sqrt{h_d}}\right)^3 \tag{7}$$

in which Q_P^* and Q_P are the expected peak discharge (cfs) through the breach, and v_r and h_d are the reservoir volume (acre-ft) and height (ft) of dam, respectively and $C = 23.4\ A_s/\bar{b}$ in which A_s is the surface area (acres) of the reservoir at the top of the dam. Equation (6) was developed by Hagen (1982) for historical data from 14 dam failures and provides a maximum envelope of all 14 of the observed discharges.

2.1.1 Parameter sensitivity

Selection of breach parameters before a breach forms, or in the absence of observations, introduces varying degree of uncertainty in the downstream flooding results of the DAMBRK model. However, errors in the breach description and in the resulting peak outflow are damped out as the flood wave advances downstream. Using DAMBRK, it has been observed that variations in Q_P at the dam are damped-out as the flood peak advances farther and farther downstream. The extent of damping is related to the size of the downstream floodplain; the wider the floodplain, the greater will be the extent of damping. Sensitivity tests on the breach parameters are best determined using the DAMBRK model and then comparing the variation in simulated flood peaks at critical downstream locations. In this way, the real uncertainty in the breach parameter selections will be determined.

For conservative forecasts, which are on the side of larger flood waves, the values for b and Z should produce an average breach width ($\bar{b}$) in the uppermost range for a certain type of dam. Failure time (τ) should be selected in the lower range to produce a maximum outflow. Of course, observational estimates of $\bar{b}$ and τ should be used when available to update forecasts when response time is sufficient as in the case of forecast points many miles downstream the breached dam. Flood wave travel rates are often in the range of 2-10 miles per hour. Accordingly

response time for some downstream forecast points might therefore be sufficient for updated forecast to be issued.

Equation (7) can also, be used quickly and conveniently to test the sensitivity of $\bar{b}$ and τ for a specific reservoir having properties of v_r, h_d and A_s. It may be generalized that for large reservoirs Q_p is quite sensitive to $\bar{b}$ and rather insensitive to τ, while for very small reservoirs Q_p is somewhat insensitive to $\bar{b}$ and fairly sensitive to τ.

2.1.2 Hydraulic computational algorithm

The essential component of the DAMBRK model is the hydraulic computational algorithm. It is used to compute the outflow from a breached dam in conjunction with (1) a parametric description of the breach size and shape which varies with time and (2) a description of spillway characteristic. The hydraulic computational algorithms also determine the extent and time of occurrence of flooding in the downstream valley as determined by routing the outflow hygrograph through the valley. The hydrograph is modified (attenuated, lagged, and distorted) as it is routed through the valley due to the effects of valley storage, frictional resistance to flow, flood wave acceleration components, flow losses, and downstream channel constrictions and/or flow control structures. Modifications to the dam-break flood wave are manifested as attenuation of the flood peak magnitude, spreading-out or dispersion of the temporal varying flood-wave volume, and changes in the celerity (propagation speed) or travel time flood wave. If the downstream valley contains significant storage volume such as a wide floodplain, the flood wave can be extensively attenuated and its time of travel greatly increased. Even when the downstream valley approaches that of a uniform rectangular-shaped section, there is appreciable attenuation of the flood peak and reduction in one wave celerity as the wave progress through the valley

A distinguishing feature of dam-break waves is the great magnitude of the peak discharge when compared to runoff-generated flood waves having occurred in the past in the same valley. The dam-break flood is usually many times greater than the runoff flood of record. The above record discharge makes it, necessary to extrapolate certain coefficients used in various flood routing techniques and make it impossible to fully calibrate the routing technique.

Another distinguishing characteristic of dam-break floods is the very short duration time, and particularly the extremely short time from beginning of rise until the occurrence of the peak. The time to peak, in almost all instances is synonymous with the breach formation time (t) and

therefore in the range of a few minutes to a few hours. This feature along with the great magnitude of the peak discharge causes the dam-break flood wave to have acceleration components of a far greater significance than those associated with a runoff-generated flood wave.

There are two basic types of flood routing methods, the hydrologic and the hydraulic methods. The hydrologic methods usually provide a more approximate analysis of the progression of a flood wave through a river reach than do the hydraulic methods. The hydrologic methods are used for the reasons of convenience and economy. They are most appropriate, as far as accuracy is concerned, when the flood wave is not rapidly varying, i.e. the flood-wave acceleration effects are negligible compared to the effects of gravity and channel friction. Also, they are best used when the flood wave is very similar in shape and magnitude to previous flood waves for which stage and discharge observations are available for calibrating the hydrologic routing parameters (coefficients).

For routing dam-break food waves, a particular hydraulic method known as the dynamic wave method is chosen. This choice is based on its ability to provide more accuracy in simulating the dam break food wave than that provided by the hydrologic method, as well as, other less complex hydraulic, methods such as the kinematic wave and the diffusion wave methods. Of many available hydrologic and hydraulic routing techniques, only the dynamic wave method accounts for the acceleration effects associated with the dam-break wave and the influence of downstream unsteady backwater effects producers by channel constrictions, dams, bridges-road embankments and tributary inflows. Also, the dynamic wave method can be used economically i.e. computational costs can made rather insignificant if advantages of certain "implicit" numerical solution techniques are utilized. Also, the current use of PCs has reduced the significance of computational costs.

The dynamic wave method is based on the complete one-dimensional equations of unsteady flow, which are used to route the dam-break flood hydrograph through the downstream valley. This method is based on an expanded version of the original equations developed by Barre De Saint-Venant (1871). The only coefficient that must be extrapolated beyond the range of past experience is the coefficient of flow resistance. It so happens that this is usually not an extremely sensitive parameter in effecting the modifications of the flood wave due to its progression through the downstream valley.

2.1.3 Expanded Saint-Venant equations

The equations of Saint-Venant expressed in conservation form with additional terms for the effect of expansion/contraction channel sinuosity and non-Newtonian flow consists of a conservation of mass equations.

$$\frac{\partial Q}{\partial x}+\frac{\partial S_c(A+A_0)}{\partial t}-q=0 \tag{8}$$

and, a conservation of momentum equation, i.e.,

$$\frac{\partial(S_m Q)}{\partial t}+\frac{\partial(\beta Q^2/A)}{\partial x}+gA\left(\frac{\partial h}{\partial x}+S_f+S_e+S_i\right)+L=0 \tag{9}$$

where h is the water surface elevation, A is the active cross sectional area flow, A_o is the inactive (off-channel storage) cross sectional area S_c and S_m are sinuosity factors which vary with h, x is the longitudinal distance along the channel (valley), t is the time, q is the lateral inflow or outflow per linear distance along the channel (inflow is positive and outflow is negative in sign), β is the momentum coefficient for velocity distribution, g is the acceleration due to gravity, S_f is the boundary friction slope, S_e is the expansion-contraction slope, and S_i is the additional friction slope associated with internal viscous dissipation of non-Newtonian fluids such as mud/debris flows.

In Equation (9), L is the momentum effect of lateral flow assumed herein to enter or exit perpendicular to the direction of the main flow. The boundary friction slope S_f in Equation (9) is evaluated for Manning's equation for uniform steady flow, i.e.

$$S_f=\frac{n^2|Q|Q}{2.21A^2R^{4/3}}=|Q|Q/K^2 \tag{10}$$

in which n is the Manning's coefficient of frictional resistance, R is the hydraulic radius and K is the conveyance factor. When the conveyance factor (K) is used to represent S_f, the valley/ channel cross-sectional properties are designated as left floodplain, channel and right floodplain rather than as a composite channel/ valley section. The conveyance factor is evaluated as follows:

$$K_l = \frac{1.49}{n_l} A_l R_l^{2/3} \tag{11}$$

$$K_c = \frac{1.49}{n_c s_m^{1/2}} A_c R_c^{2/3} \tag{12}$$

$$K_r = \frac{1.49}{n_r} A_r R_r^{2/3} \tag{13}$$

$$K = K_l + K_c + K_r \tag{14}$$

in which the subscript l, c, and r designate left floodplain, channel and right floodplain respectively. The sinuosity factor S_c and S_m in Eqs (8), (9) and (12) represent the weighted ratio of the flow path distance along the floodplains. They vary with depth of flow according to the following relations:

$$S_{c_j} = \frac{\sum_{k=2}^{k=j} \Delta A_{l_k} + \Delta A_{c_k} s_{c_k} + \Delta A_{r_k}}{A_{l_j} + A_{c_j} + A_{r_j}} \tag{15}$$

$$S_{m_j} = \frac{\sum_{k=2}^{k=j} \Delta K_{l_k} + \Delta K_{c_k} s_{m_k} + \Delta K_{r_k}}{K_{l_j} + K_{c_j} + K_{r_j}} \tag{16}$$

in which $\Delta A = A_{m+1} - A_m$ and the sinuosity factor S_m represents the sinuosity factor for a differential portion of the flow between the m^{th} depth and the $m+1^{th}$ depth. Distances between the cross sections are measured along the mean flow path for the floodplain flow. The momentum coefficient for velocity distribution (β) is evaluated as follows:

$$\beta = \frac{1.06\left(K_l^2/A_l + K_c^2/A_c + K_r^2/A_r \right)}{(K_l + K_c + K_r)^2/(A_l + A_c + A_r)} \tag{17}$$

where β=1.06 when floodplain characteristics are not specified and the total cross section is treated as a composite section.

The term (S_e) in Equation (9) is defined as follows:

$$S_e = \frac{k_{ce}\,\Delta(Q/A)^2}{2g\,\Delta x} \qquad (18)$$

in which k_{ce} is the expansion-contraction coefficient and $\Delta(Q/A)^2$ is the difference in the term $(Q/A)^2$ at two adjacent cross sections separated by a distance Δx. A provision is made within DAMBRK to automatically change contraction to expansion coefficients and vice versa if flow direction changes from downstream to upstream in which case the computed Q values are negative.

The active cross-sectional area (A) and inactive (off-channel storage) area (A_0) are obtained from hydrographic surveys and/or topography maps. These are specified as input to DAMBRK as a table of wetted top widths (B) which varies with elevation at selected cross sections along the channel/valley. Within the model, the top width table is integrated using the trapezoidal rule to obtain a table of cross -sectional area versus elevation. Linear interpolation is used for intermediate elevations between specified tabular points. Areas associated with elevation exceeding the maximum value as specified in the table are extrapolated.

The Manning roughness (n) coefficient is specified for each reach between adjacent cross sections and varies with elevation according to user specified tabular values similar to the top widths table. Linear interpolation is used for value associated with intermediate elevations. Values for n for elevation exceeding the tabular elevations are not extrapolated; they are assigned the value associated with the maximum elevation.

2.1.4 Solution technique for Saint-Venant equation

The expanded Saint-Venant Equation (8 and 9) constitute a system of partial differential equations with two independent variables, x and t, and two dependent variables, h and Q_i; the remaining terms are either a functions of x, t, h, and or Q, or they are constants. These equations are not amenable to analytical solutions except in cases when the channel geometry and boundary conditions are uncomplicated and the nonlinear properties of the equations are either

neglected or made linear. Equations (8 and 9) may be solved numerically by performing two basic steps. First, the partial differential equations are represented by a corresponding set of finite-difference algebraic equations; and second, the system of algebraic equations is solved in conformance with prescribed initial and boundary conditions.

Equations (8 and 9) can be solved by either explicit or implicit finite-difference techniques. Explicit methods, although simpler in application, are restricted by mathematical stability considerations to very small computational time steps (on the order of a few seconds for most dam break waves). Such small time steps cause the explicit methods to be very inefficient in the use of computer time. Implicit finite differences techniques, however, have no restrictions on the size of the time step due to mathematical stability; however, convergence considerations may require its size to be limited.

Of the various implicit schemes that have been developed, the "weighted four point" scheme appears most advantageous since it can readily be used with unequal distance steps and its stability-convergence properties can be conveniently controlled. In the weighted, four-points implicit finite-difference scheme, the continuous x, t region in which solutions of h and Q are sought is represented by a rectangular net of discrete points. The net points are determined by the intersection lines drawn parallel to the x and t axis. Those parallel to the t-axis represent locations of cross sections; they have a spacing of Δx, which need not be constant. Those parallel to the x-axis represent time lines; they have a spacing of Δt, which also need not be constant. Each point in the rectangular network can be identified by a subscript (i) which designate the x-position and a superscript (j) which designate the particular time line

The time derivatives are approximated by a forward difference quotient centered between the i^{th} and $i+1^{th}$ points along the x-axis, i.e.,

$$\frac{\partial K}{\partial t} = \frac{K_i^{j+1} + K_{i+1}^{j+1} - K_i^j - K_{i+1}^j}{2\Delta t_j} \qquad (19)$$

where K represents any variable (Q, h, A, A_0, s).

The spatial derivatives are approximated by a forward difference quotient positioned between two adjacent time lines according to weighting factors of θ and $1-\theta$. i.e.,

$$\frac{\partial K}{\partial t} = \theta\left(\frac{K_{i+1}^{j+1} - K_i^{j+1}}{\Delta x_i}\right) + (1-\theta)\left(\frac{K_{i+1}^{j} - K_i^{j}}{\Delta x_i}\right) \tag{20}$$

Variables other than derivatives are approximated at, the time level when the spatial derivatives are evaluated by using the same weighting factor i.e.,

$$K = \theta\left(\frac{K_i^{j+1} + K_{i+1}^{j+1}}{2}\right)(1-\theta)\left(\frac{K_i^{j} + K_{i+1}^{j}}{2}\right) \tag{21}$$

A θ weighting factor of 1.0 yields the fully implicit or backward difference scheme. A weighting factor of 0.5 yields the box scheme. The influence of the weighting factor on the accuracy of the computations is that the accuracy tends to somewhat decreases as θ departs from 0.5 and approaches 1.0. This effect becomes more pronounced as the magnitude of the computational time step increases. Usually, a weighting factor of 0.60 is used so as to minimize the loss of accuracy associated with greater values while avoiding the possibility of a weak or pseudo instability.

When the finite-difference operators defined by Equation (19 and 21) are used to replace the derivatives and other variables in Equation (8 and 9), the following weighted four points implicit, finite difference equations are obtained:

$$\theta\left[\frac{Q_{i+1}^{j+1} - Q_i^{j+1}}{\Delta x_i}\right] - \theta q_i^{j+1} + (1-\theta)\left[\frac{Q_{i+1}^{j} - Q_i^{j}}{\Delta x_i}\right] - (1-\theta)q_i^{j} +$$
$$\left[\frac{s_{c_i}^{j+1}(A+A_0)_i^{j+1} + s_{c_i}^{j+1}(A+A_0)_{i+1}^{j+1} - s_{c_i}^{j}(A+A_0)_i^{j} - s_{c_i}^{j}(A+A_0)_{i+1}^{j}}{2\Delta t_j}\right] = 0 \tag{22}$$

$$\left[\frac{(s_{m_i}Q_i)^{j+1}+(s_{m_i}Q_{i+1})^{j+1}-s_{m_i}Q_i)^{j}-(s_{m_i}Q_{i+1})^{j}}{2\Delta t_j}\right]$$

$$+\theta\left[\frac{(\beta Q^2/A)_{i+1}^{j+1}-(\beta Q^2/A)_i^{j+1}}{\Delta x_i}+gA^{-j+1}\left(\frac{h_{i+1}^{j+1}-h_i^{j+1}}{\Delta x_i}+S_f^{-j+1}+S_e^{-j+1}+S_i^{-j+1}\right)\right] \quad (23)$$

$$+(1-\theta)\left[\frac{(\beta Q^2/A)_{i+1}^{j}-(\beta Q^2/A)_i^{j}}{\Delta x_i}+gA^{-j}\left(\frac{h_{i+1}^{j}-h_i^{j}}{\Delta x_i}+S_f^{-j}+S_e^{-j}+S_i^{-j}\right)\right]=0$$

$$\overline{A}=\frac{(A_i+A_{i+1})}{2} \quad (24)$$

$$\overline{S_f}=n^2\overline{Q}\left|\overline{Q}\right|/(2.2A^{-2}R^{4/3})=\overline{Q}\left|\overline{Q}\right|/K^2 \quad (25)$$

$$\overline{Q}=\frac{(Q_i+Q_{i+1})}{2} \quad (26)$$

$$\overline{R}=\overline{A}/\overline{B} \quad (27)$$

$$\overline{B}=\frac{(B_i+B_{i+1})}{2} \quad (28)$$

$$\overline{K}=\frac{(K_i+K_{i+1})}{2} \quad (29)$$

The term ($\overline{S_i}$) is evaluated using Equation (18) in which D=$\overline{R}$, Q= $\overline{Q}$ and A= $\overline{A}$. The terms associated with the j^{th} time-line are known from either initial conditions or previous computations. The initial conditions refer to values of h and Q at each node along x-axis for the first time line (j=1).

Equations (22) and (23) cannot be solved in an explicit or direct manner for the unknowns since there are four unknowns and only two equations. However, if Equation (22) and

(23) are applied to each of the (N-1) rectangular grids between the upstream and downstream boundaries, a total of (2N-2) equations with 2N unknowns can be formulated (N denotes the total number of nodes or cross sections). Then, prescribed boundary conditions for subcritical flows, one at the upstream boundary and one at the downstream boundary provide the necessary additional equations required for the system to be determinate. The resulting system of 2N nonlinear equations with 2N unknowns is solved by a functional iterative procedure, the Newton-Raphson method.

Computations for the iterative solution of the nonlinear system are begun by assigning trial values to the 2N unknowns. Substitution of the trial values into the system of nonlinear equations yields a set of 2N residuals. The Newton-Raphson method provides a means for correcting the trial values until the residuals are reduced to a suitable tolerance level. This is usually accomplished in one or two iterations through use of linear extrapolation for the first trial values. If the Newton-Raphson are applied only once there is no i.e. there is no iteration, the nonlinear system of difference equations degenerates to the equivalent of a quasi-linear, finite-difference formulation of the Saint-Venant equations which may require smaller time steps than the nonlinear formulation for the same degree of numerical accuracy.

A system of 2N x 2N linear equations relates the corrections to the residuals and to a Jacobean (coefficient) matrix composed of partial derivative of each equation with respect to each unknown variable in that equation. The Jacobean (coefficient) matrix of the linear system has a banded structure which allows the system to be solved by a compact, quad-diagonal, Gaussian elimination algorithm which is very efficient with respect to computing time and storage. The required storage is 2N x 4 and the required number of computational steps is approximately 38N.

When flow is supercritical, the solution technique previously described can be somewhat simplified. Instead of a solution involving 2N x 2N equations, supercritical flow can be solved via a system of only 2 x 2N equations. The unknowns h and Q at the upstream section are determined from the two boundary equations. Then progressing from upstream to downstream in a cascade manner, Equations (22) and (23) are used to obtained h_{i+1} and Q_{i+1}, at each section. Since Equations (22) and (23) are nonlinear with respect to h_{i+1} and Q_{i+1}, they are solved by the Newton-Raphson iterative technique applied to a system of two equations with two unknowns.

2.1.5 Internal boundaries

There may be locations such as a dam, bridge, or waterfall (short rapids) along a waterway where the Saint -Venant equations are not applicable. At these locations, the flow is rapidly varied rather than gradually varied. Empirical water elevation-discharge relations such as weir flow can be utilized for simulating rapidly varying flow. In DAMBRK, unsteady flow is routed along the waterway including points of rapidly varying flow by utilizing internal boundaries. At internal boundaries, cross sections are specified for the upstream and downstream extremities of the section of waterway encompassing the rapidly varying flow. The short reach length between the two cross sections can be any appropriate value from zero to the actual measured distance. Since, as with any other Δx reach, two equations (the Saint-Venant equations) are required, the internal boundary Δx reach requires two equations. The first of the required equations represents the conservation of mass with negligible time-dependent storage, and second is an empirical, rapidly varied flow equation representing weir, orifice, and/or critical flow. The internal boundary equations are:

$$Q_i = Q_{i+1} \tag{30}$$

$$Q_i = Q_s + Q_b \tag{31}$$

in which Q_s and Q_b are the spillway and breach flow, respectively. In this way the flows Q_i and Q_{i+1} and the elevations h_i and h_{i+1} are in balance with the other flows and elevations occurring simultaneously throughout the entire flow system which may consist of additional dams or bridges which are treated as additional internal boundary condition via Equations (30) and (31). In fact, DAMBRK can simulate the progression of a dam-break flood through as many as 10 dams and/ or bridges in any combination located sequentially along the valley. Any of the dams or bridge-embankments may breach if they are sufficiently topped.

Dams - A dam may be considered an internal boundary defined by a short Δx reach between sections i and i+1 in which the flow is governed by Equations (30) and (31). In Equation (31) the spillway flow (Q_s) is computed from the following expression:

$$Q_s = k_{sp}\, c_s L_s (h - h_s)^{1.5} + \sqrt{2g}\, c_g A_g (h - h_g)^{0.5} + k_d\, c_d L_d (h - h_d)^{1.5} \tag{32}$$

in which k_{sp} is a submergence correction for tailwater effects, c_s is uncontrolled spillway discharge coefficient, h_s is the uncontrolled spillway crest elevation, c_d is the fixed-gated spillway discharge coefficient, h_g is the center-line elevation of the gated spillway or it is the tailwater elevation if the latter is greater, k_d is a submergence correction for tail water effects, c_d is the discharge coefficient for flow over the crest of the dam, L_s is the spillway length, A_g is the gate flow area, L_d is the length of the dam crest less L_s and the length of the gates located along the dam crest and Q_t is a constant outflow term which is head independent. The uncontrolled spillway flow or the fixed gated spillway flow can also be represented as a table of head versus discharge value. The gate flow may also be specified as a function of time via movable gate option.

The flow through the gate may be either orifice flow and/or weir flow. Weir flow occurs when the gate is not submerged sufficiently or as overtopping flow (Q_{og}) when the reservoir elevation is sufficiently above the top of the dam (h_d). The dependent orifice gate flow is computed as follows:

$$Q_g = \sqrt{2g}\, C_0 W_g H_g (\hat{h} - H_g/2)^{0.5} + Q_{og} \qquad \text{if } \hat{h} > 1.2H_g \tag{33}$$

$$C_o = \frac{0.712}{W_g}\left[W_d - 2(0.02W_d/40 + 0.1)\hat{h}_d\right](\hat{h}/\hat{h}_d)^{0.1} \qquad 0.60 \le C_o \le 0.72 \tag{34}$$

$$\hat{h} = h - h_g \tag{35}$$

$$Q_{og} = 3.1 W_g (h - h_d - H_g)^{1.5} \qquad \text{if } h > h_d + h_g \tag{36}$$

otherwise, $Q_{og} = 0$. If the tail water (h_t) is greater than $h_g + H_g$, then $\bar{h}$ in Equation (35) is the differential head across the gate, i.e., $h - h_t$. The gate loss coefficient will usually in the range of 0.65 to 0.7.

The breach outflow (Q_b) is computed as broad-crested weir flow, i.e.

$$Q_b = c_v k_s [3.1 b_i (h - h_b)^{1.5} + 2.45 Z (h - h_b)^{2.5} \tag{37}$$

in which c_v, is a small correction for velocity of approach, b_i is the instantaneous breach bottom width as described by Equation (3) h is the elevation of the water surface just upstream of the structure, h_b is the elevation of the breach bottom which is assumed to be a function of the breach formation time as described by Equation (2), Z is the side slope of the breach and k_s is the submergence correction due to the downstream tail water e elevation (h_t), i.e.,

$$k_s = 1.0 - 27.8\left[\frac{h_t - h_b}{h - h_b} - 0.67\right]^3 \qquad \text{if } (h_t - h_b)/(h - h_b) > 0.67 \tag{38}$$

otherwise, k_s=1.0. Equation (38) is also used to evaluate k_{sp} and k_d where k_s and h_b are replaced by k_{sp}, h_g and k_d, h_d respectively. The velocity of approach correction factor is computed from the following:

$$c_v = 1.0 + 0.023 Q_i^2 / [B_d^2 (h - h_{bm})^2 (h - h_b)] \tag{39}$$

in which B_d is the reservoir width at the dam and h_{bm} is the terminal elevation of the breach bottom. If the breach is formed by piping, Z is assumed to be zero (rectangular shape) and Equation (37) is replaced by an orifice equation, i.e.

$$Q_b = 4.8 A_p (h - \bar{h})^{1/2} \tag{40}$$

where: $A_p = 2 b_i (h_p - h_b)$ (41)

in which h_p is the specified centre line elevation of the pipe and $\bar{h} = h_p$ or $\bar{h} = h_t$ if $h_t > h_p$. The breach flow ceases to be orifice flow and becomes the broad crested weir flow when the reservoir elevation (h) lowers sufficiently and/ or pipe enlarges sufficiently so that:

$$h < 3h_p - 2h_b \tag{42}$$

2.1.6 Initial conditions

In order to solve the unsteady flow equations, the state of the flow (h and Q) must be known at all cross sections at the beginning (t= 0) of the simulation. This is known as the initial

condition of the flow. The DAMBRK model assumes the flow to be steady, non-uniform flow where the flow at each cross section is initially computed as:

$$Q_i = Q_{i+1} + q_{i-1}\,\Delta x_{i-1} \qquad i = 2,3,.....N \tag{43}$$

where Q_i is the known steady discharge at t=0 at the dam, i.e., the upstream boundary of the downstream valley, and q_i is any specified lateral inflow at t=0 from tributaries existing between the specified cross sections spaced at intervals of Δx along the valley. The steady discharge at t = 0 is usually assumed to be nonzero, i.e., an initially dry downstream channel is not usually simulated in DAMBRK. An exception to this must be used when mud/ debris flows are routed. A nonzero initial flow is not an important restriction, especially when maximum flows and peak stages are of paramount interest in the dam-break flood analysis. The tributary-lateral-inflow must be specified by the user throughout the simulation period. If these flows are relatively small compared to the dam-break flood, they may be omitted in the simulation.

The water surface elevations associated with the steady flow also must be computed at t = 0. If the flow is subcritical, this is accomplished by using the iterative Newton-Raphson method to solve the following backwater equation for h_i:

$$(Q^2/A)_{i+1} - (Q^2/A)_i + g\bar{A}_i[h_{i+1} - h_i + \Delta x_i \bar{S}_f + \Delta x_i \bar{S}_i] = 0 \tag{44}$$

in which $\bar{A}$, $\overline{S_f}$ and S_i are defined by Equations (18), (24) and (25). Equation (44) is a simplified form of the momentum Equation (9) where the first term is taken as zero for steady flow, and L' is assumed to be zero. The computations proceeds in the upstream direction (i=N, N-l, ..., 3, 2, 1). The starting water surface elevation (h_N) can be obtained from the specified downstream boundary condition for either a discharge of Q_N or the elevation h_N at t=0.

2.2 Data Requirements

The DAMBRK model was developed so as to require data that is usually available to the forecaster. The input data requirements are flexible in so far as much of the data may be ignored (left blank on the input data card or omitted altogether) when a detailed analysis of a dam-break flood inundation event is not feasible due to lack of data or insufficient data preparation time. Nonetheless, the resulting approximate analysis is more accurate and convenient to obtain than

that which could be computed by most other techniques. The input data can be categorized into four groups.

The first data group consists of program control parameters. The combination of these values determines the various methodology or options available in the DAMBRK model. These parameters can be easily ascertained depending upon the study area and case for which a specified hydrograph is to be routed and the form in which the model results are to be obtained.

The second data group pertains to the dam (the breach spillway and reservoir storage volume). The breach data consists of the following parameters t (failure time of breach in hours); b (final bottom width of the breach); Z (side slope of breach); h_{bm} (final elevation of breach bottom); h_0 (initial elevation of water in reservoir); h_f (elevation of water when breach starts to form); and h_d (elevation of top of dam). The spillway data consists of the following h_s (elevation of uncontrolled spillway crest); c_s (coefficient of discharge of uncontrolled spillway); h_g (elevation of center of submerged gated spillway); c_g (coefficient of discharge of fixed-gated spillway) c_d (coefficient of discharge of crest of dam, and Q_t (constant or time dependant discharge from dam) The storage parameters consist of surface area (A_s) or volume and the corresponding elevations within the reservoir in tabular form. The forecaster must estimate the values of t, b, Z, h_{bm}, and h_f. The remaining values are obtained from the physical description of the dam, spillway and reservoir.

The third group pertains to the routing of the outflow hydrograph through the reservoir and/or downstream valley. This consists of a description of cross sections, hydraulic resistance coefficients, and expansion coefficients. The cross sections are specified by their location mileage and tables of topwidth (active and inactive) and corresponding elevations. The active topwidths may be total width as for a composite section, or they be left floodplain, right floodplain, and channel width. This may be obtained from 1:25,000 Survey of India toposheets or from actual survey of the river reach. The channel width are usually not as significant for an accurate analysis as the over bank widths (the latter are available from toposheets). The number of cross sections used to describe the downstream valley depends on the variability of the valley widths. A minimum of two must be used. Additional cross sections are created by the model via linear interpolation between adjacent cross sections specified by the forecaster. This feature enables only a minimum of cross-sectional data to be input by the forecaster according to such criteria as data availability, variation, preparation time, etc. The number of interpolated cross sections created by model is controlled by the parameter DXM which is input for each reach

between specified cross sections. The hydraulic resistance coefficients consisting of table of Manning's n versus elevation for each reach between specified cross sections. The expansion-contraction coefficients (k_{ce}) are specified as non zero value at specified Δx reach where significant expansion or contraction occur. The k_{ce} parameters may be left blank for most reaches.

The fourth data group is comprised of information pertaining to special options within the DAMBRK model. If the conveyance option is selected, the left and right floodplain topwidths and Manning's n verses elevation tables are specified.

If lateral inflows exist along the river, the sequence number of the reach in which the lateral flow enters and the time series of discharge in the lateral are specified. If a rating curve is selected for the downstream boundary condition, a table of discharge-elevation is specified; or if an elevation time series is selected for boundary condition the water surface elevations and associated time of occurrence are specified. If the time dependent gate option is selected for a dam, the gate width and gate height above the sill are specified as time series along with the times of occurance of each gate width and gate height.

2.3 Limitations of DAMBRK Model

The DAMRRK model is subjected to limitations due to its governing equations and also due to the uncertainty associated with some of the parameters used within the model.

The governing equations within DAMBRK for routing hydrographs (unsteady, flows) are the one-dimensional Saint-Venant equations. There are some instances where the flow is more nearly two dimensional than one-dimensional, i.e., the velocity of flow and water surface elevations vary not only in the x-direction along the river /valley but also in the transverse direction perpendicular to the x-direction. Neglecting the two dimensional nature of the flow can be important when the flow first expands onto an extremely wide and flat floodplain after having passed through an upstream reach, which severely constricts the flow. In many cases where the wide floodplain is bounded by rising topography, the significance of neglecting the transverse velocities and water surface variations is confined to a transition reach in which the flow changes from one-dimensional to two- dimensional and back to one-dimensional a along the x-direction. In this case, the use of radially defined cross sections along with judicious off channel storage widths can

Minimize the two-dimensional effect neglected within the transition reach. The radial cross sections appear in plan-view as concentric circles of increasing diameter in the downstream direction which is considered appropriate for radial flow expanding onto a flat plane. The cross sections became perpendicular to the x-direction for the reach downstream of the transition reach. Where the vary wide, flat floodplain appears unbounded, the radial representation of the cross sections is at best only an approximation which varies from reality the farther from the constricted section and the greater the variability of the floodplain topography and friction.

The high velocity flows associated with dam-break floods can cause significant scour (degradation) of alluvial channels. This enlargement in channel cross-sectional area is neglected in DAMBRK since the equations for sediment transport, sediment continuity, dynamic bed-form friction, and channel bed armoring are not included among the governing equations. The significance of the neglected alluvial channel degradation is directly proportional to the channel/ floodplain conveyance ratio, since the characteristics of most floodplains along with their much lower velocities causes much less degradation within the floodplain. As this ratio increases, degradation could cause a significant lowering of the in water surface elevation until the flows are well within the recession limb of the dam-break hydrograph; however, in many instances this ratio is fairly small and remains such until the dam-break flood peak has attenuated significantly at locations far downstream of the dam, and where this occurs the maximum flow velocities also have attenuated. However, narrow channels with minimal floodplains are subjected to over estimation of water elevations due to significant channel degradation. The effect of alluvial fill (aggradation) associated with the recession limb of the dam-break hydrograph and that occurring in the flood-plain are considered to have relatively small effects on one peak flood conditions.

The uncertainty associated with the selection of the Manning's n can be quite significant for dam-break floods due to: (i) the great magnitude of the flood produces flow in portions of floodplain which were very infrequently or never before inundated; this necessitates the selection of the n value without the benefits of previous evaluations of n from measured elevation/discharges or use of calibration techniques for determining the n values; (ii) the effects of transported debris can alter the Manning n. Although the uncertainty of the Manning n values may be large, this effect is considerably damped or reduced during the computation of the water surface elevations. When the range of possible Manning n values is fairly large, it is best to perform a sensitivity test using the DAMBRK model to simulate the flow, first with the lower estimated n values and then a second time with the higher estimated n values. The resulting high

water profile computed along the river/ valley for each simulation represents an envelope of possible food peak elevation within the range of uncertainty associated with the estimated n values.

Dam-break floods with a large amount of transported debris may accumulate at constricted cross sections such as bridge openings where it acts as a temporary dam and partially or completely restricts the f low. At best the maximum magnitude of this effect i.e. the upper envelope of the flood peak elevation profile can be approximated by using the DAMBRK model to simulate the blocked constriction as a downstream dam having an estimated elevation-discharge relation approximating the gradual flow stoppage and the later rapid increase due to the release of the ponded waters when the debris dam is allowed to breach.

The uncertainty associated with the breach parameters, especially $\bar{b}$ and t, also cause uncertainty in the flood peak elevation profile and arrival times. The best approach is to perform a sensitivity test using minimum, average and maximum values for $\bar{b}$ and t.

There is the uncertainty associated with volume losses incurred by flood as it propagates downstream and inundates large floodplains where infiltration and detention storage losses may occur. Such losses are difficult to predict and are usually neglected, although they may be significant. Again, a sensitivity test may be performed using estimated minimum and maximum values for (q_m). The conservative approach is to neglect such losses, unless very good reasons justify their consideration.

3.0 STUDY AREA

The river Damodar, is one of the major east flowing inter-state River of Bihar, Jharkand and West Bengal with a basin area of 22015 sq. km (about 17817 sq. km. is the catchment of the upper Damodar just below its confluence with the Hoogly below Kolkatta. The Damodar valley is located within Latitude 22^0 20' and 24^0 30' N and Longitude 84^0 45' E to 88^0 30'.

The river Damodar rises in the hills of Chota Nagpur at an altitude of about 610 m above M.S.L It flows in a generally southeast direction entering the deltaic plains below Raniganj. Near Burdwan the river abruptly changes its course to a southerly direction and joins the Hooghly about 48 km. below Kolkatta. Its slope during the first 240 km. is about 1.9 m per km., during the next 160 km. is about 0.2 m per km. and during the last 144 km about 0.2 m per km. The River is fed by six streams of which the principal tributary Barakar joins it where it emerges from the hills. The schematic diagram of main tributaries of Damodar and locations of reservoirs are shown in Fig. 3.1

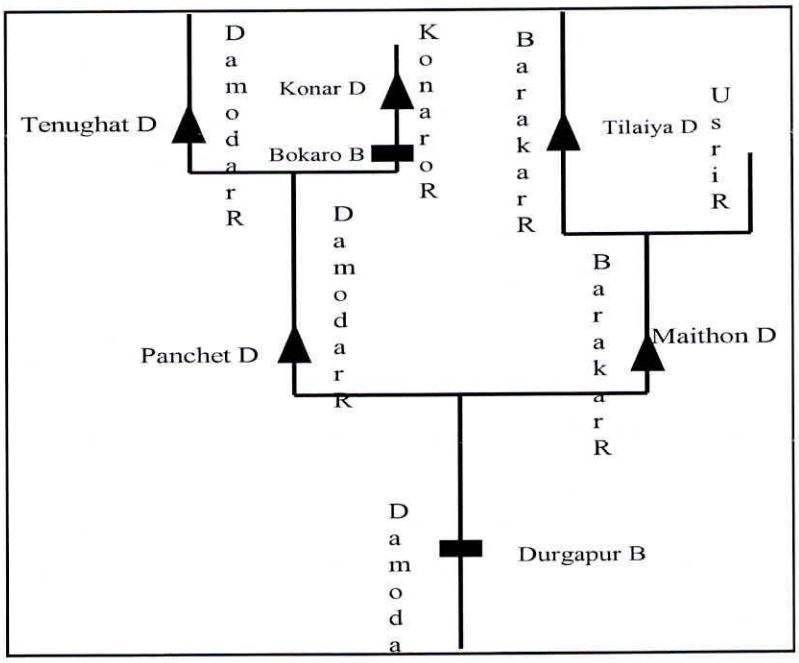

Fig. 3.1 Schematic diagram Damodar river systems

The upper portion of the catchment consists of rough hilly regions and the lower of flat deltaic plains. Considerable land erosion has taken place in the upper portion and many deep gullies have formed. In this area there is no irrigation, and cultivation is mainly dependent on monsoon rains. The lower portion, however, is silt covered and fertile. The upper valley of the Damodar covers six districts fully Hazaribagh, Kodarma, Giridih, Chatra, Dhanbad and Bokaro and four districts partially Palamau, Ranchi, Lohardaga & Dumka in the state of Jharkhand. The lower valley area covers two districts fully Burdwan & Hooghly and three districts partially Howrah, Bankura & Purulia in the state of West Bengal. The district covering the catchment of Damodar river is shown in Fig. 3.2

Fig. 3.2: Districts covered by Damodar river basin.

3.1 Development of Water Resources Projects in the Basin

The serious flood problem in the lower reaches of the river necessitated taming of this river through a comprehensive and integrated plan of development that would ensure not only flood protection but also provide other benefits of irrigation, hydropower generation, water supply for domestic and industrial purposes etc. With this objective in view, the Government of India drew an ambitious Plan to develop the entire river basin, patterned on the successful model of the Tennessee Valley Authority (TVA) of USA. The implementation of this ambitious plan

was proposed to be achieved through a semi autonomous organization called the Damodar Valley Corporation, which was established in the year 1948.

The Plan of development of the water resources of the basin envisaged construction of seven storage dams across the Damodar and its tributaries at Tilaiya, Konar, Maithon, Panchet, Bokaro, Balpahari and Aiyar; a diversion dam at Bermo and a Barrage at Durgapur (terminal structure) with canal network system. This development was to be carried out in two stages. The first stage was to cover the construction of four dams at Tilaiya, Konar, Maithon and Panchet and the barrage with canal system at Durgapur. Construction of the remaining dams was included in the second stage. The first stage was completed in 1958, and the second stage has not yet been implemented.

Subsequently, the Bihar Government has constructed a dam at Tenughat on the Damodar River, which is located upstream of the Panchet reservoir. Upstream of this dam, yet another small dam to control about 256 sq. km of catchment was constructed by the Bihar State Electricity Board to meet the requirements of Pathrathu Thermal Power Station.

Surface Water Resources of the basin

According to the Regulation Manual (2002) for Damodal valley reservoirs, the estimated average annual runoffs at different dams are:

Name of the Dam	MAF
Tilaiya	0.35
Maithon	2.12
Konar	0.45
Panchet	3.68
Tenughat	1.99

(Regulation Manual for Damodar Valley Reservoirs, CWC, 2002)

Analysis of the observed data at the above reservoir sites shows wide variation in the annual yields. The minimum and maximum yields as per analyzed data records are given in Table 3.1.

3.2 Hydro-meteorological Characteristics

The Maithon project area lies in the Dhanbad district of Jharkhand. The important climatic and other characteristics such as rainfall, temperature, relative humidity and special weather phenomenon for the Damodar Valley are explained.

Climate - Mild winters and hot wet summers characterize the climate of the area. The Damodar valley forms a part of the great Gangetic plains. Like the rest of the country, the region experiences two principal seasons. In winter, the general flow of surface air is North-Easterly. It is mainly of continental origin and hence of low humidity. This season is known as the North East Winter Monsoon. In the summer months, i.e. June to September, the general flow of wind is from the opposite direction i.e. from sea to lands and the season is named South – West Monsoon season. Between these two principal seasons is the transition period of the hot weather months i.e. April and May and retreating monsoon months i.e. October and November.

Temperature - The highest maximum temperature exceeding 46^0C was recorded over a larger part of the lower valley and around a small area near Ramgarh in Damodar catchment. In the extreme part of the valley, the absolute maximum temperature is of the order of 42^0C. The lowest minimum temperature of about 2^0C was recorded near Ramgarh. Over the major portion of the area, the lowest recorded temperature was 4^0C to 7^0C only. May is the hottest month of the year when the mean daily maximum temperature is more than 40^0C. The cold months are December and January when the mean daily maximum is about 23^0C to 26^0C.

Humidity - Mean relative humidity over the catchment is maximum during July to September when it is of the order of 80%. It is about 65% in June and 70% in October. The humidity comes down to about 40% in March, April and May. The mean diurnal variation is of the order of 10 to 15 percent. The Barakar catchment has the lowest humidity both in the morning and evening; the mean annual value being less than 60 percent and 50 percent respectively. Humidity gradually increases towards the South and South-East and the lower valley has more than 70 percent and 55 percent humidity in the morning and evening respectively.

Evaporation - The climatic conditions are conducive to high rates of evapotranspiration during the summer months. On the basis of actual measurement with pan evaporimeter, the annual evaporation losses have been estimated for the reservoirs Tilaiya, Konar, Maithon,

Panchet & Tenughat as 177 cm, 150 cm, 139 cm, 155 cm, and 170 cm respectively. Of this, about 50% is recorded in the four hot months of March, April, May and June.

Rainfall - The mean annual rainfall in Damodar valley is about 118 cm varying from a maximum of 163 cm to 76 cm. About 82 percent of mean annual rainfall occurs during the monsoon months i.e. June to September. During the pre and post monsoon seasons, the rainfall in the catchment is about 7 percent and 8 percent respectively. The upper Damodar basin generally receives a higher rainfall than any other portion of the basin. The average annual rainfall in the Maithon Project is 114.17 cm.

The salient features of the Maithon and Panchet project are given in Table 3.2 and Table 3.3

4.0 DATA USED

As described in the data requirement in the model description (section 2.2), the geometric coordinates of the cross-sections of the river downstream of the dam location are the most important inputs data for the dam break analysis. Detailed cross-sections information along the river Damodar and Barakar were collected. Fig. 4.1 below shows the availability of river cross sections along river Panchet. The figure also shows the longitudinal profile of river Damodar from Panchet dam site. The points shown along the longitudinal profile indicate that the river cross sections are available at these chainage. The river Barakar flows for a distance of 12.9 km from Maithon dam site before it meets river Damodar. The two rivers meet at a distance of 6.4 km downstream of Panchet dam. Similarly Fig. 4.2 shows the longitudinal profile of river Barakar and availability of river cross sections are indicated. The cross section profile of river along the Barakar and Damodar at various chainage is shown in Fig. 4.3 and Fig. 4.4 respectively. During the simulation/ routing of dam break flow in the river channel it has been observed that the flood level at many sections overtopped the bank level. Hence, the river sections were extrapolated. For this, the sections were initially marked over the river channel in the Survey of India toposheets (at 1: 25,000 scale), perpendiculars to flow direction and river sections were extended to the required level with the help of contours information.

For Manning's roughness constant the remarks made in the field book of survey of river cross sections are considered. In general the river is flowing in the rocky terrain in smooth natural earth channels free from vegetation growth with little curvature and occasional obstructions from large boulders, and therefore, the Manning's value within the river bank line are considered as 0.030. The affected flood plain in the area is also characterized by rocky terrain with little vegetation and sparse settlement and therefore, Manning's value for flood plain have been considered between 0.035 to 0.045 for Panchet and Maithon respectively depending on the resistance to flow as observed from satellite imageries. (Subramanya, 1986).

The physical characteristics of Maithon and Panchet reservoir are obtained from reservoir regulation manual 2002. Some of the important characteristics are already mentioned in Table 3.2 and Table 3.3. The length of Panchet reservoir as computed from satellite imagery is 24.5 km while that of Maithon reservoir is 15.8 km. The area elevation data for two reservoirs are taken from reservoir regulation manual 2002. (CWC, 2002).

For dam break analysis it is considered that dam breaks during inflow of design discharge of spillway. The reservoir regulation manual shows that the design discharge of spillway of Maithon and Panchet dams are 13,592 cumec and 16,608 cumec respectively. The completion report of Panchet dam project (1959) states that the project was designed based on the flow observations at Sudamdih gauging site, few miles upstream of Panchet dam site, for which the flow data is available since 1946 onwards. Also the flow data at Rhondia is available since 1933 onwards have been considered for estimating design flood at Panchet. The 150% of Inglish flood assuming the runoff coefficient as 90%, have been estimated as 19,256 cumecs as peak of design flood hydrograph. Similarly, the completion report of Maithon dam states the design discharge was estimated based on flow in Barakar river at Chirkunda , few miles downstream of Maithon dam site for which flow observation since 1945 is available. In this project also the flow data at Rhondia was used. The peak of design flood has been estimated assuming 150% of Inglish flood with runoff coefficient of 90% and is equivalent to 18,407 cumecs. Recently, the design floods in the Damodar valley has been estimated using unit hydrograph and PMP approach (Banerjee et al, 2003). The rainfall data of 110 storms between 1891 to 2000 with the duration of 2 to 6 days were analyzed to find out the most severe storm. The study indicates that the storm occurred on 31st July to 2nd August 1917 was most critical to produce maximum rainfall depth and is selected for transposition over the catchments to find out 3-day probable maximum precipitation (PMP) for Maithon and Panchet dam sites. The unit hydrograph at Maithon and Panchet dam site have been derived using three techniques, viz., conventional Spearman's technique, Collins technique and Nash model technique and an average unit hydrographs have been obtained. The peak of unit hydrograph for Maithon dam site has been increased by 25% to take into accounts of floods of higher magnitudes. Finally the PMP is convoluted over the unit hydrograph and after doing necessary correction for losses, the PMF at Maithon and Panchet dam sites have been estimated with the peak discharge of 26,246 cumec and 38,875 respectively. The flood hydrograph for Maithon and Panchet dam site is shown in Table 4.1 and 4.2 respectively and have been used in simulation of dam break flood.

For preparation of inundation map due to flood generated from dams break the digital elevation model (DEM) of the downstream is required. For some part of the area the toposheet map at 1: 25,000 scale with contours at 10 m is available, while for others toposheet map at 1: 50,000 scale having contours at 20 m interval have been used. Table 4.3 shows the toposheets details used for extraction of contours and preparation of DEM of the area. Fig. 4.5 shows the contours map of the downstream area of Panchet and Maithon dams.

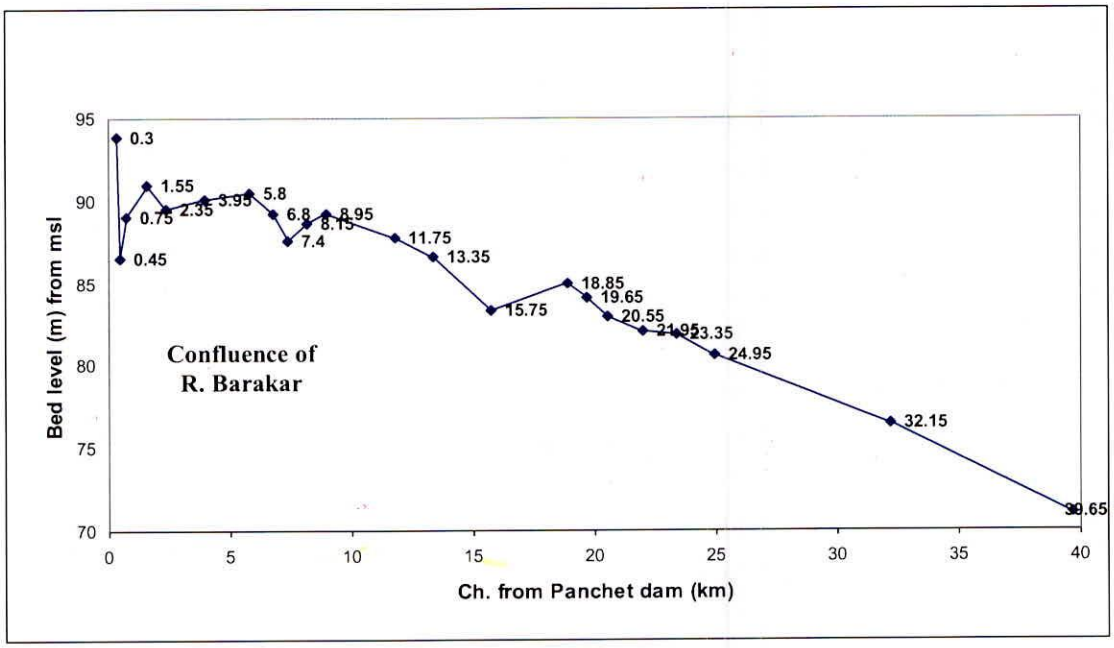

Fig. 4.1 Longitudinal profile of Damodar river d/s of Panchet dam and availability of river cross sections.

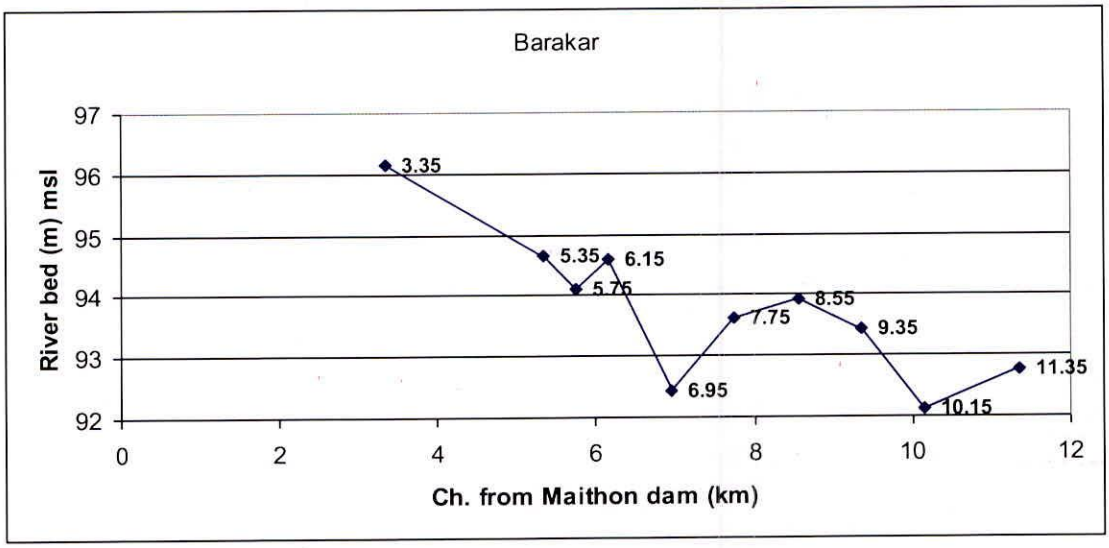

Fig. 4.2 Longitudinal profile of Barakar river d/s of Maithon dam and availability of river cross sections.

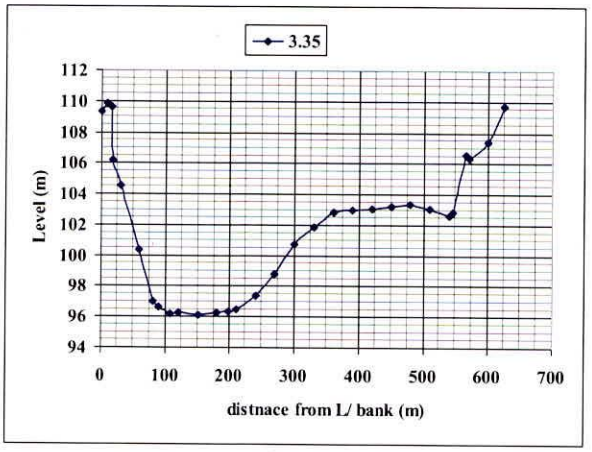

(a)

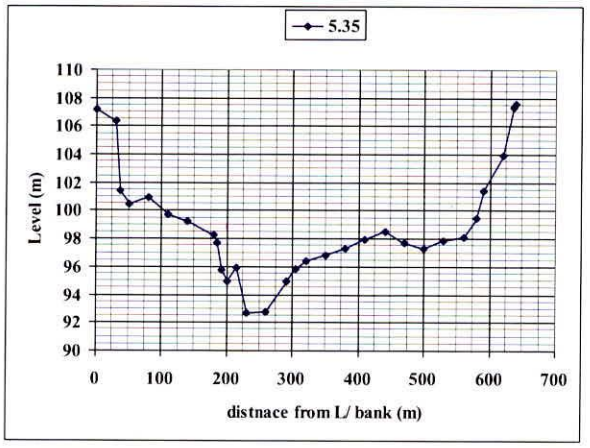

(b)

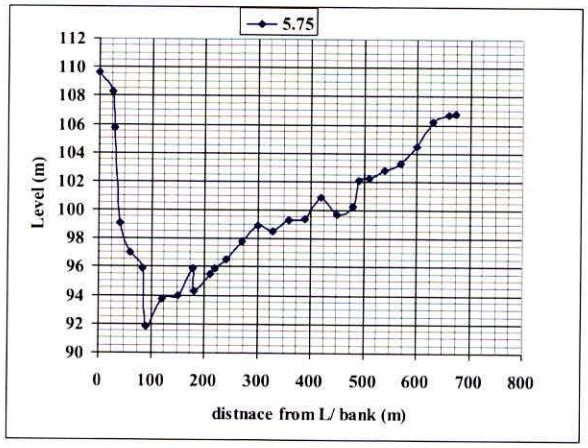

(c)

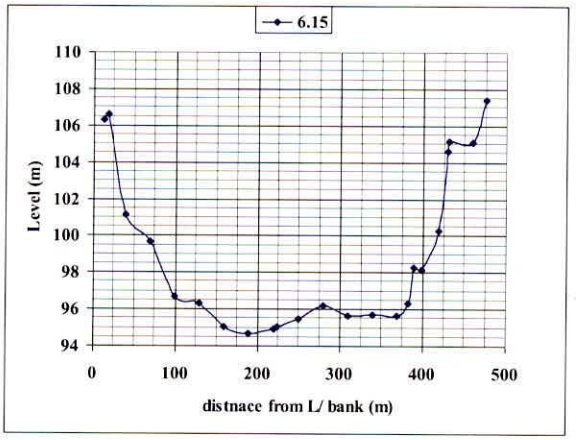

(d)

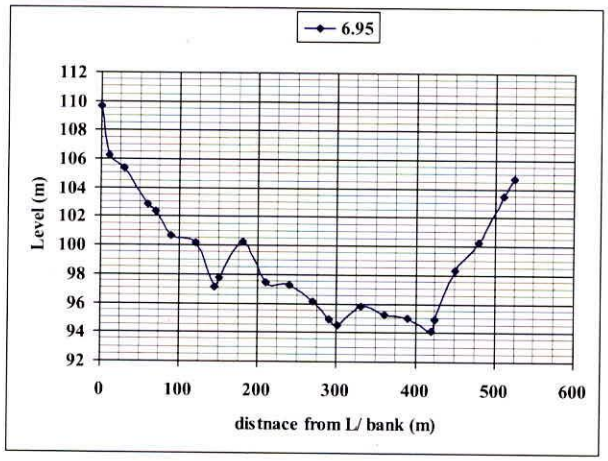

(e)

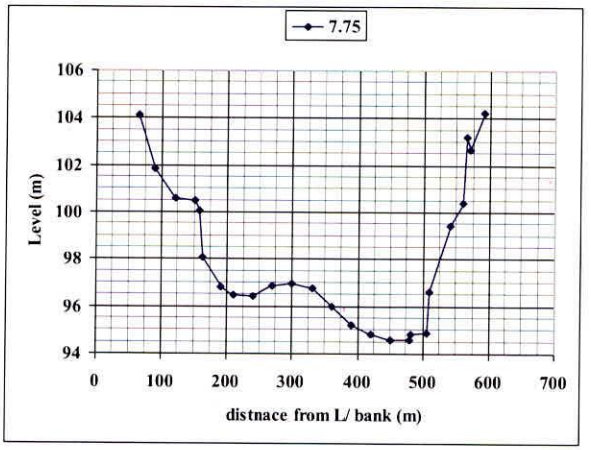

(f)

Fig. 4.3 (a) to (f) River cross sections at various chainage in Barakar river d/s of Maithon dam.

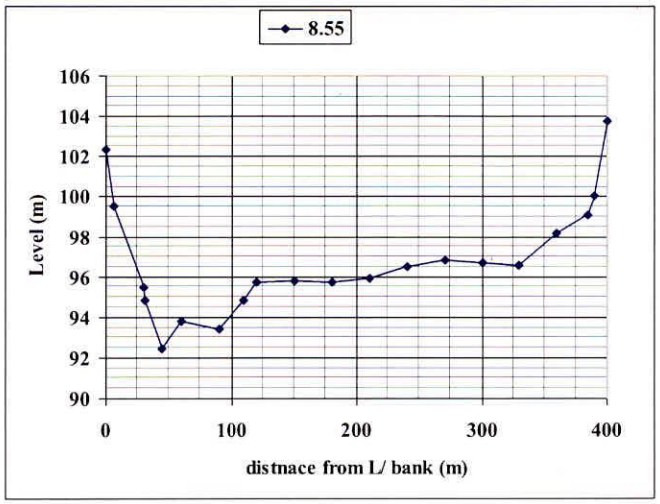

(g)

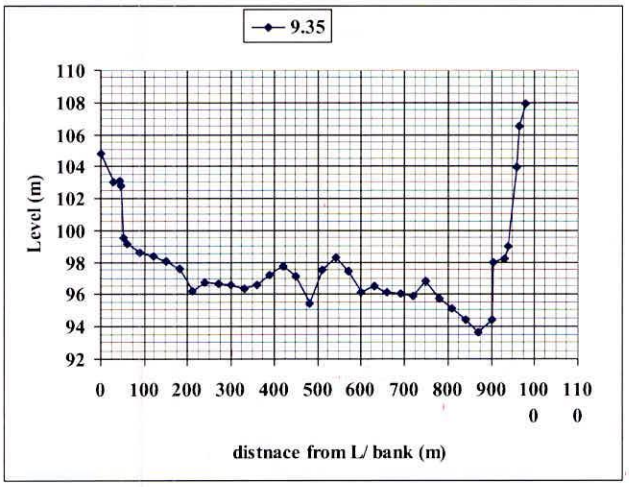

(h)

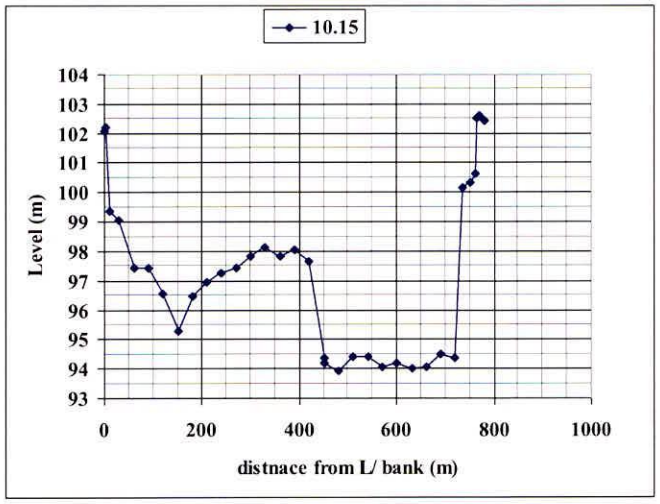

(i)

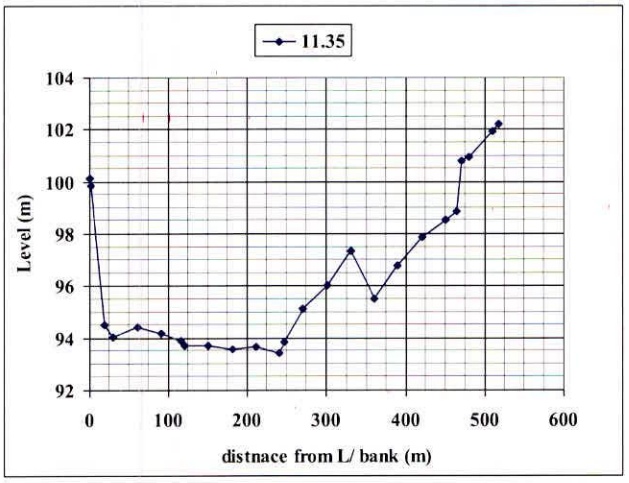

(j)

Fig. 4.3 (g) to (j) River cross sections at various chainage in Barakar river d/s of Maithon dam.

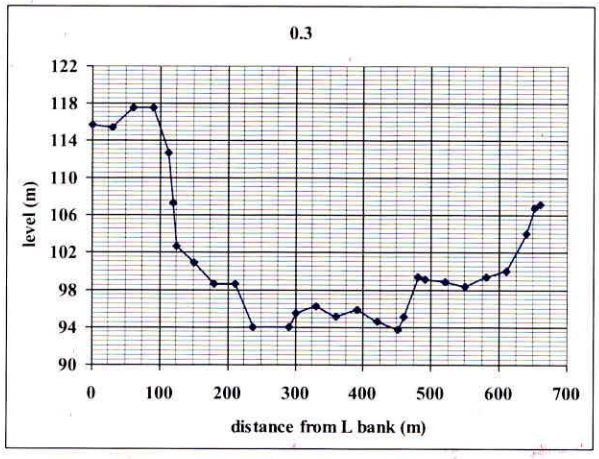

(a)

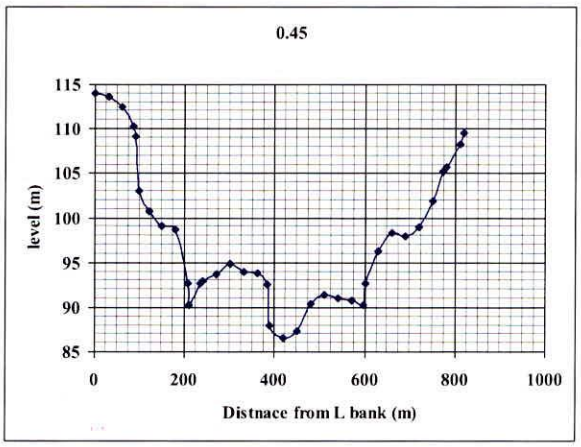

(b)

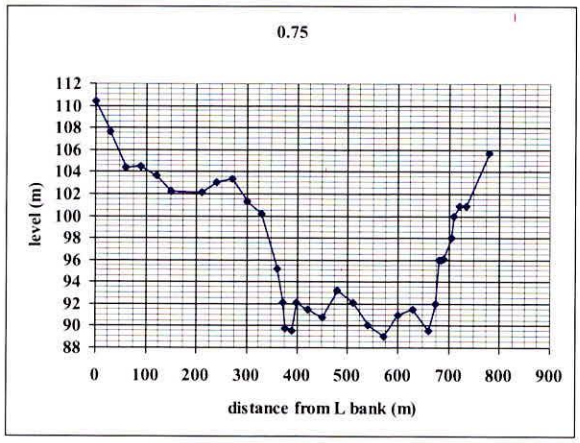

(c)

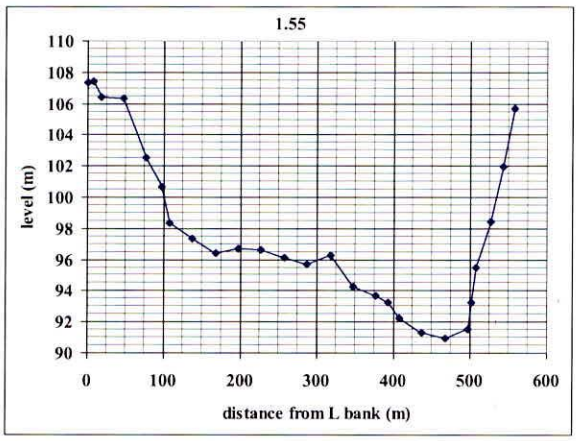

(d)

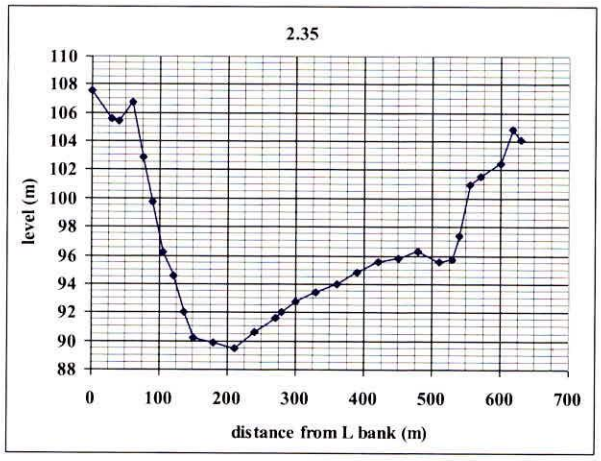

(e)

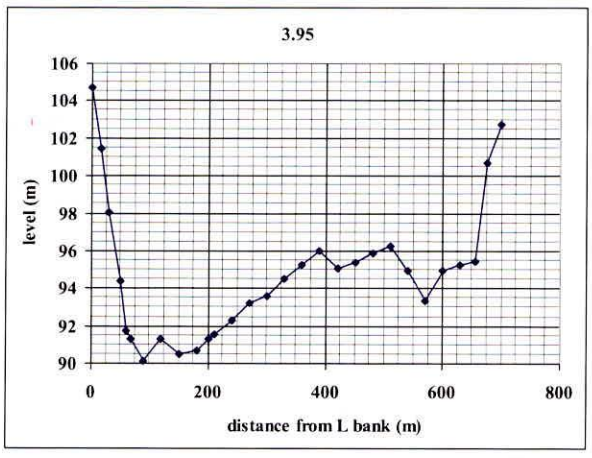

(f)

Fig. 4.4 (a) to (f) River cross sections at various chainage in Damodar river d/s of Panchet dam

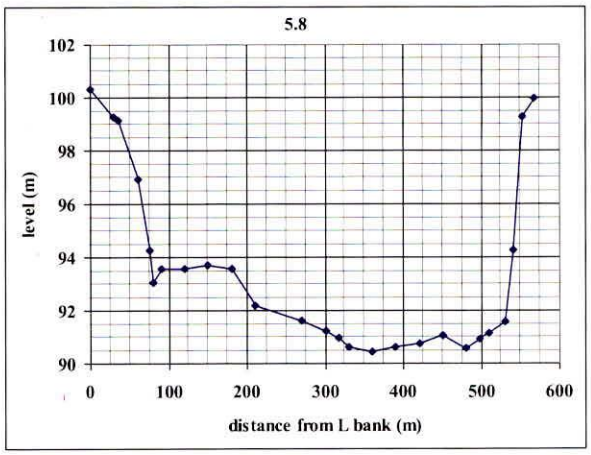

(g)

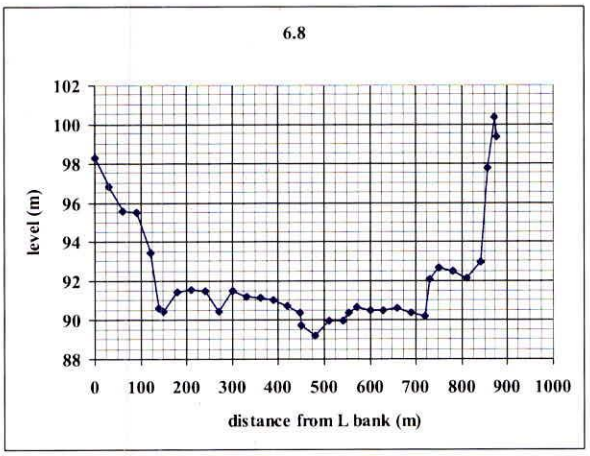

(h)

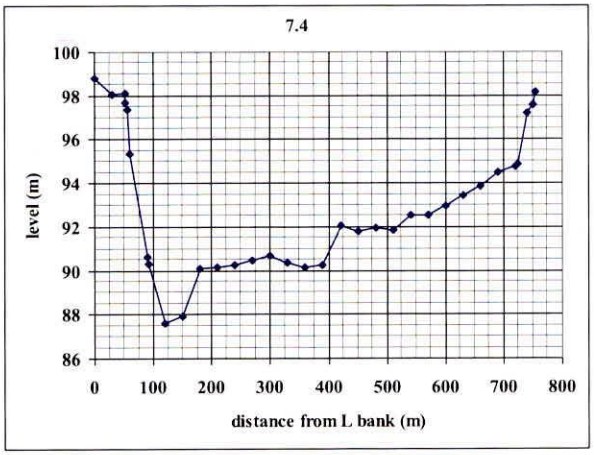

(i)

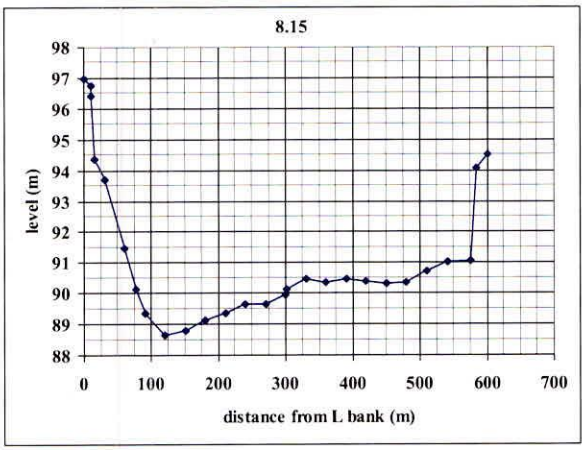

(j)

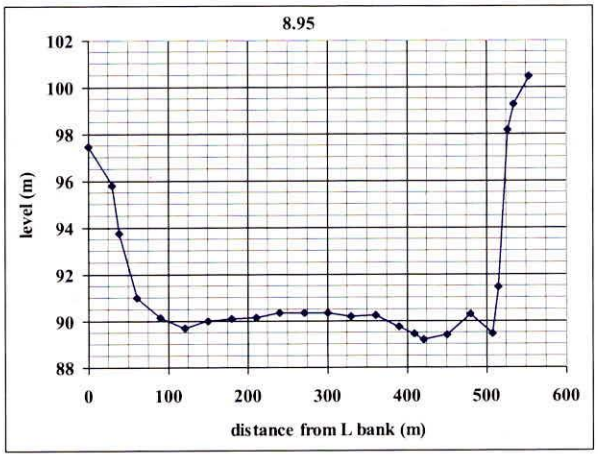

(k)

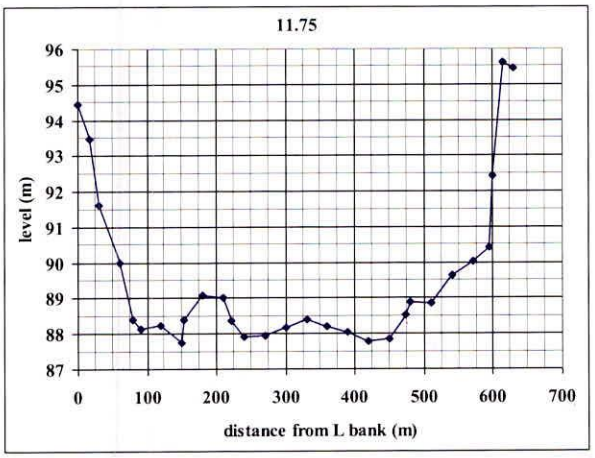

(l)

Fig. 4.4 (g) to (l) River cross sections at various chainage in Damodar river d/s of Panchet dam

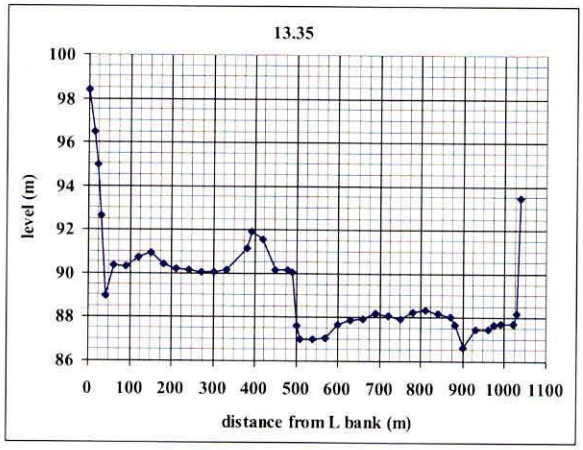

(m)

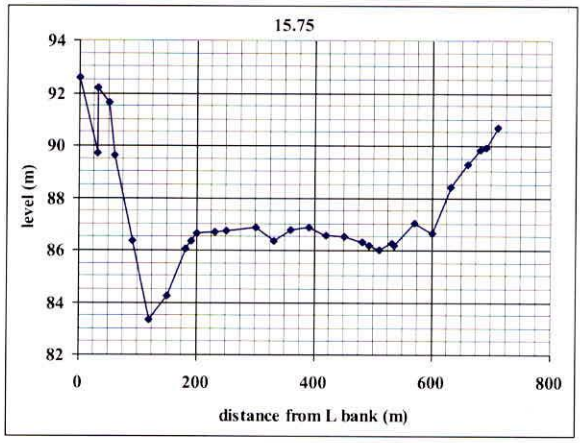

(n)

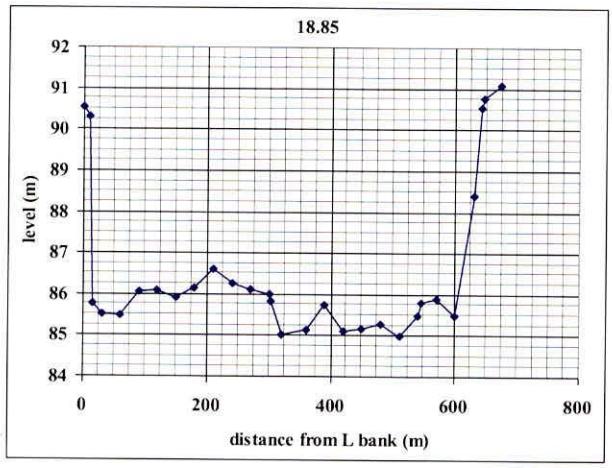

(o)

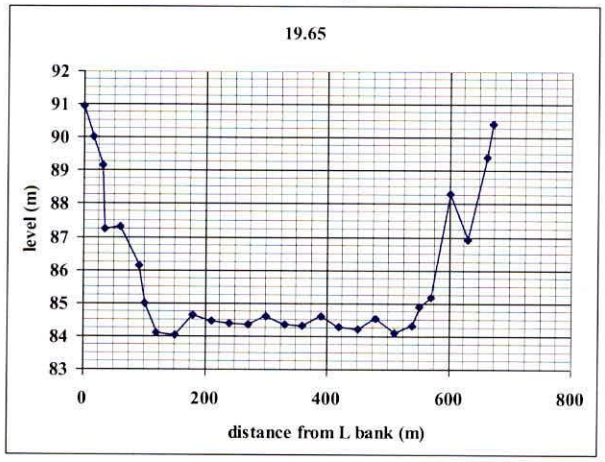

(p)

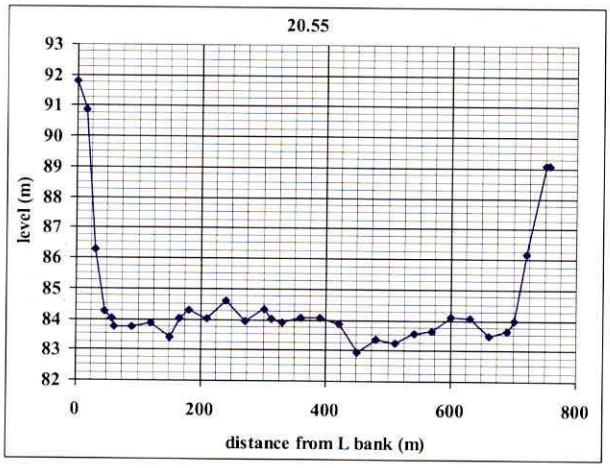

(q)

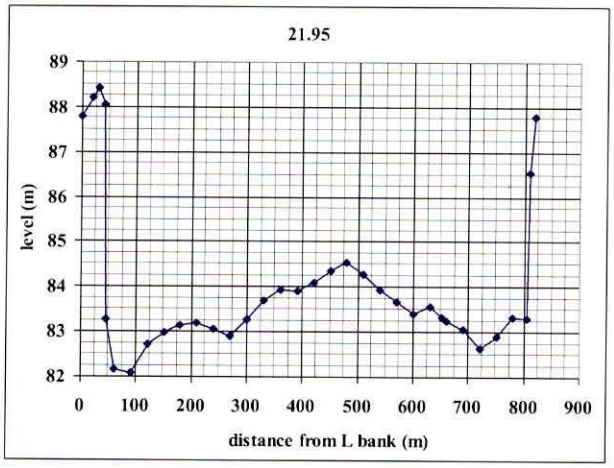

(r)

Fig. 4.4 (m) to (r) River cross sections at various chainage in Damodar river d/s of Panchet dam

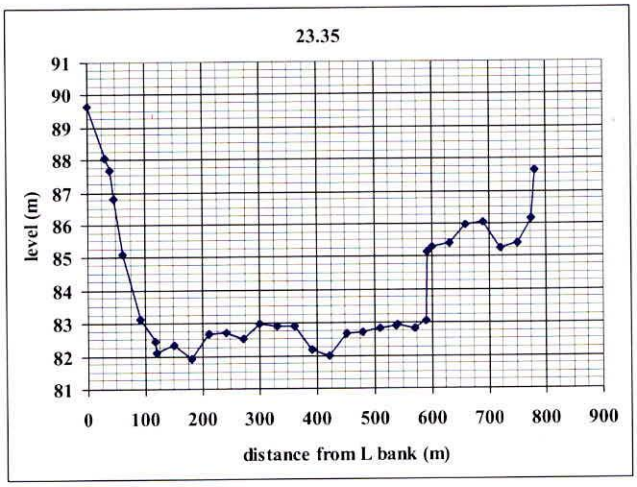

(s)

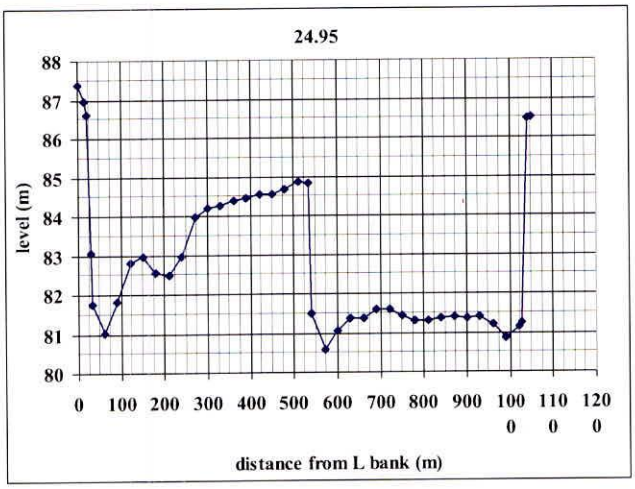

(t)

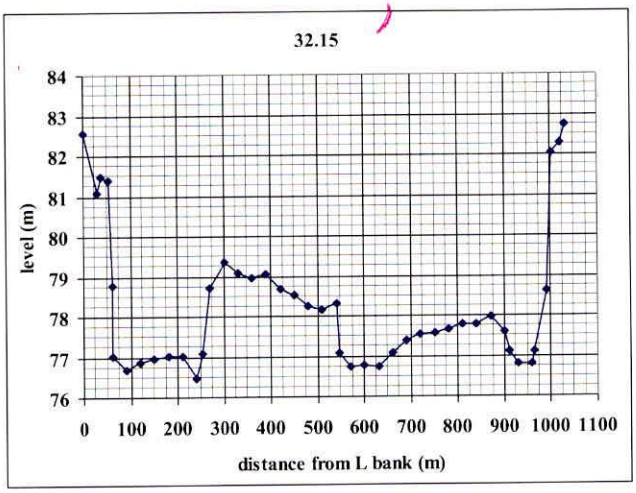

(u)

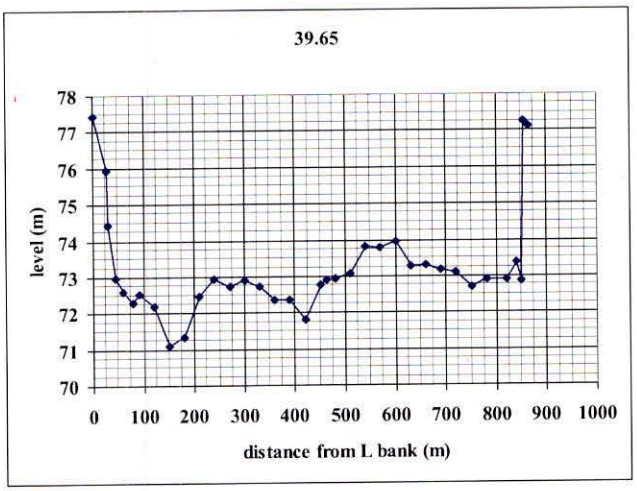

(v)

Fig. 4.4 (s) to (v) River cross sections at various chainage in Damodar river d/s of Panchet dam

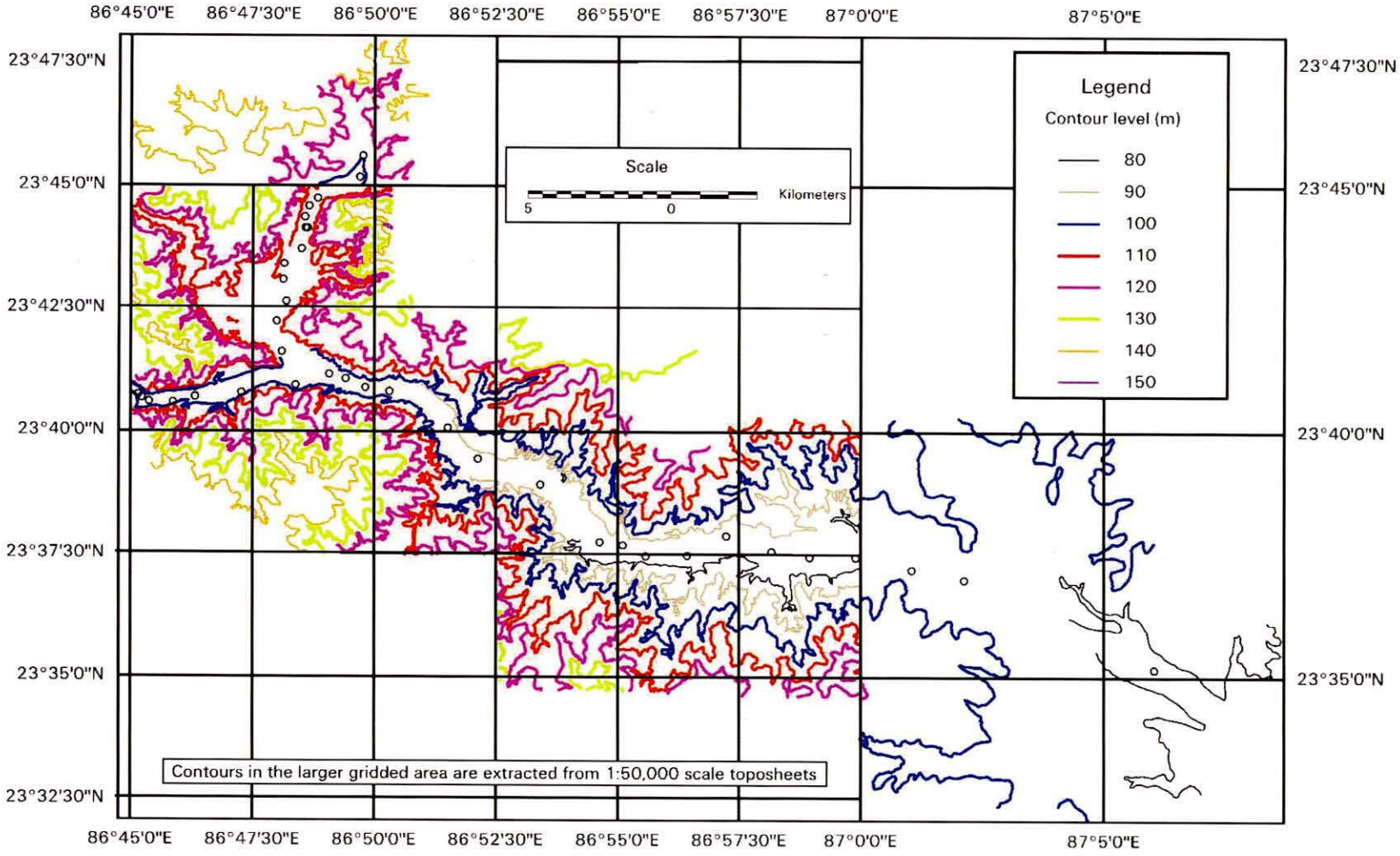

Fig. 4.5 Contour map of the downstream area

5.0 ANALYSIS AND DISCUSSIONS

For dam break situation it is considered that the reservoir is at full reservoir level (FRL) when the peak of inflow enters into the reservoir. This is the most general condition of dam break failure analysis. The water level starts rising in the reservoir when PMF enters into a reservoir. It is considered that all the gates of the dams are open at this moment and the reservoir is at FRL when peak of PMF enters into reservoir. Due to inadequate spillway designed capacity or due to some other reason if the inflow rate in the reservoir exceeds the outflow rate from spillway, water starts rising and over-tops the top of dam and spilling starts from earthen portion of dam. This condition ultimately leads to failure of dam. For dam break analysis, sometimes pipe failure of dams is also considered. In this case, the size of orifice and its location in the body of the dam is defined. In the study it is considered that the dams fail due to overtopping of reservoir water. Hence, when reservoir water spills over the dam gradually eroding its downstream side and ultimately leads to complete failure of dam within a stipulated time (breach time). The reservoir water starts oozing out from a very small circular hole and develops into a well defined opening (shape), generally assumed as trapezoidal for earthen dam. With the passage of time and under the influence of huge quantity of flow, considerable amount of dam materials is eroded away; the size of opening increases and also its base is lowered towards the bottom of the dam. Thus the three parameters are very significant in defining the breach condition in any dam. These are time of breach (T), side slope of breach section (S) and size of breach (W), i.e. final breach width. The value for each parameter is governed by type of dams, construction materials etc. Further, there are certain thumb rules which helps in deciding these values. In the study both Maithon and Panchet are earthen dams having length of 4.06 km and 6.4 km respectively. The breach time (T), breach width (W) and slope of breach section (S) have been assumed as 1 hr, 1 km and 1:1 for the dams.

The line diagram of two dams located over river Damodar and Barakar is given in Fig. 5.1. The river Barakar is one of a major tributary of river Damodar. Panchet dam is located over river Damodar while Maithon dam is located over river Barakar. The two rivers join at a point which is located 12.9 km along river Barakar from Maithon dam site and 6.4 km along river Damodar from Panchet dam site. The available sections along the Damodar river nearest to confluence are at 5.8 km and 6.8 km. For routing the flood in two rivers, first the flood in Barakar river is routed upto confluence point and the outflow hydrograph is computed. This outflow hydrograph is considered as lateral inflow between sections 5.8 km and 6.8 km while routing the flood in Damodar river. River sections at every cross sections are defined by three

parameters, i.e. location of cross section, top width of cross sections and elevation to each top width. The sections at each location are defined by 8 top width. Fig. 5.2 shows a typical cross section as defined in the DAMBRK model.

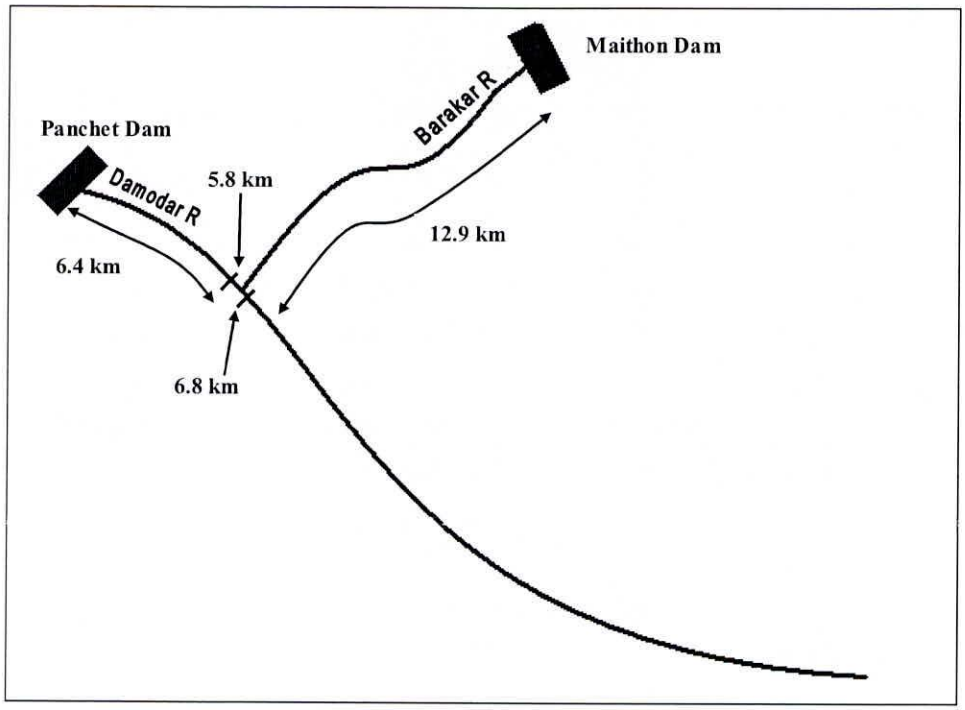

Fig. 5.1. Line diagram of river system and location of dams

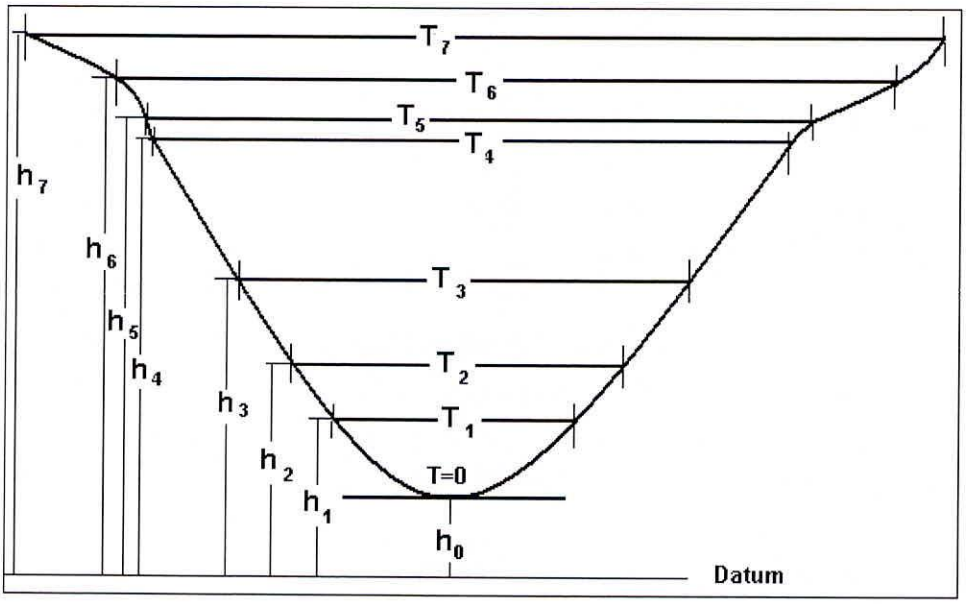

Fig. 5.2 Typical cross section definition for DAMBRK model

The survey data for cross sections are available upto both the river bank lines corresponding to normal floods only. When the floods generated from dam failure is simulated, the water level in river rises abruptly and crosses the normal bank line. In such situation, the river sections have to be extended in the flood plains and redefine the river sections so that the flow is confined to the sections. In these conditions, T_n is divided into two parts corresponding to active channel portion and off-channel portion. This generally occurs at higher top widths (say T_6 or T_7) of a river section.

For simulation of dam break floods in both dams, two types of dam failure situations are considered. In one of the situation, it is assumed that the dams are failed due to inflow of PMF in the reservoirs while in second situation it has been assumed that the dams are failed due to earthquake or by some terrorist attack. In this situation, even if PMF does not occur in the reservoirs, the dams may break and the downstream area may be submerged by the reservoir water which is at full reservoir level (FRL). The time of breach in this situation is very small and considered to be 2 minutes.

Hence, the following combinations of dam failure cases are possible and have been analyzed in the study:

Situation – A: Dams fail under the influence of PMF. In this situation, the breach parameters are T = 1 hr, W = 1000 m, and S = 1:1 for both the dams. The following cases failures of two dams are considered in this situation.

Case A1 – Only Panchet dam fails while PMF passes safely through the spillway of Maithon dam. In this condition the outflow from Maithon spillway is routed upto the confluence point where it is considered as lateral inflow into Damodar river while routing the flood due to failure of Panchet dam.

Case A2 – Only Maithon dam fails while PMF passes safely through the spillway of Panchet dam. In this condition the flood due to failure of Maithon dam is routed upto the confluence point where it is considered as lateral inflow into Damodar river while routing the spillway outflow of Panchet dam.

Case A3– In this case both Maithon and Panchet dams fail when their PMF enters into the respective reservoirs. In this condition the flood due to failure of Maithon dam is

routed upto the confluence point where it is considered as lateral inflow into Damodar river while routing the flood due to failure of Panchet dam.

Case A4– In this case the respective PMF passes safely from the spillway of Maithon and Panchet dams without any failure of dam. The outflow from Maithon spillway is routed upto the confluence point where it is considered as lateral inflow into Damodar river while routing the spillway outflow of Panchet dam.

Situation – B: Dams fail due to earthquake or some terrorist attack and the inflow in the reservoir may not be necessarily PMF. In this situation also, the flood due to dam break is significant due to sudden release of reservoir storage. This situation has been analyzed by assuming a minimum flow is inflowing into respective reservoirs when earthquake or attack occurs. The reservoirs are considered to be at their respective FRL. The time of breach in this situation is drastically reduced. In this situation, the breach parameters are T = 0.03 hr, W = 1000 m, and S = 1:1 for both the dams. The following cases failures of two dams are considered in this situation:

Case B1 – Only Panchet dam fails suddenly while a nominal outflow passes through the spillway of Maithon dam. In this condition the outflow from Maithon spillway is routed upto the confluence point where it is considered as lateral inflow into Damodar river while routing the flood due to failure of Panchet dam.

Case B2 – Only Maithon dam fails suddenly while a nominal flow passes through the spillway of Panchet dam. In this condition the flood due to failure of Maithon dam is routed upto the confluence point where it is considered as lateral inflow into Damodar river while routing the spillway outflow of Panchet dam.

Case B3– In this case both Maithon and Panchet dams fail suddenly. In this condition the flood due to failure of Maithon dam is routed upto the confluence point where it is considered as lateral inflow into Damodar river while routing the flood due to failure of Panchet dam.

Case B4– In this case none of the dams fail and only nominal outflow passes through the respective spillway. The outflow from Maithon spillway is routed upto the confluence point where it is considered as lateral inflow into Damodar river while routing the

spillway outflow of Panchet dam. In fact this is not a case of dam break analysis and no any inundation is expected. Except this case, in all other cases of dam break analysis mentioned above, there is drainage congestion at the confluence of two rivers which are very much indicated in their respective inundation maps. In this case the flood propagates in the rivers under nominal flow condition only and therefore no drainage congestion is seen in its inundation map.

5.1 Failure of Maithon Reservoir under PMF

The reservoir is at FRL (152.4 m) when PMF enters the reservoir and the water level rises even if all the gates of the spillway is open. When reservoir level increases to 156.2 m (top of dam is 156.06 m) the dam breaks. With this initial condition, the water level in the reservoir reaches 156.2 m after 7.9 hours since impingement of peak into reservoir and dam breaks at this moment. So the total outflow from the dam till 7.9 hours is outflow through spillway only. After 7.9 hours the breach starts developing and total flow from dam consists of through spillway as well as through breach section. Though the reservoir level is still rising and it rises upto 156. 32 m at 8.08 to 8.18 hours, when the flow from spillway is maximum, but by this time the breach section has not been fully developed and having width of 280 m only. The breach develop to a size of 1000 m at 8.9 hours (one hour after initial formation of breach) and also the base of breach starts lowering down towards bottom of the dam. At this time the outflow from the breach section is at maximum (values from model output).

5.2 Failure of Maithon Reservoir under Earthquake or Attack

In this case the inflow into reservoir is very nominal (base flow of PMF) and therefore the reservoir water does not rise above FRL (152.4 m) under this inflow. For dam break analysis, in this situation, orifice formation (pipe failure) is considered to be developed at FRL which leads to failure of dam completely. Here time of breach is 0.03 hours i.e. almost instantaneously; therefore, the dam outflow consists of outflow from spillway as well as from breach section. Further, the height of water above the crest of spillway (140.21 m) is comparatively small (about 12.1 m), the outflow from the spillway is almost insignificant and outflow from breach sections dominates the total outflow from dam. At 0.03 hours when the orifice develops into a full breach having width of 1000 m, the outflow is maximum.

Outflow in Barakar river at the confluence - there are four types of outflow is possible in Barakar river at the confluence due to the following conditions of inflow and Maithon dam failure condition:

C1-Maithon dam breaches under PMF condition with W=1000 m, S=1:1, and T=1 hr

Time (hr)	0	6	12	18	24	30	36	42
Flow (cumec)	1253	1456	39013	36641	28888	20656	15059	12000

C2-PMF routed safely through spillway of Maithon dam W=1000 m, S=1:1, and T=1 hr

Time (hr)	0	6	12	18	24	30	36	42	48	54
Flow (cumec)	1243	1539	8471	10142	12814	7518	5659	4328	2866	2100

C3-Maithon dam fails by earthquake or some attack when the inflow in the reservoir is very minimum (base flow of PMF) W=1000 m, S=1:1, and T=0.03 hr

Time (hr)	0	6	12	18	24	30	36	42	48	54
Flow (cumec)	1243	29958	18883	11282	7706	5807	4679	3913	3353	2924

C4-A very nominal inflow (base flow of PMF) is entering Maithon reservoirs and its corresponding spillway outflow routed at confluence.

Time (hr)	0	6	12	18	24	30	36	42	48	54
Flow (cumec)	1256	1256	1256	1256	1257	1260	1282	1262	1257	1256

Hence the lateral inflow from Barakar river considered during routing of flood in the Damodar river in various cases are summarized in Table 5.1.

5.3 Failure of Panchet Dam under PMF

The Panchet reservoir is at FRL (135.64 m) when the peak of the PMF enters into it. Though all the gates of dams are open the water level in the reservoir rises and reached 139.30 m, the top of the dam after which it starts overtopping. The dam fails when the water level reaches the height of 139.40 m. This condition develops 5.2 hours after the peak of PMF enters into the reservoir when the breach starts to form. It means upto 5.2 hours the total outflow from dam is confined to spillway section only. After 5.2 hours the outflow consists of two components, the outflow from breached section and outflow from spillway (in accordance with rating curve depending upon the reservoir level). The breach develops into its complete size (1000 m) in 1 hour (time of breach) i.e after 6.2 hours when the outflow from breached section is at its maximum value of 55,143 cumec. The total volume of water discharged from the reservoir is 3,088 M cubic meter, it includes, the volume of PMF and the reservoir storage upto FRL. The outflow from the reservoir is routed in the downstream river section assuming the lateral inflow from Barakar river at between section 5.8 to 6.8 km. Depending on the various combination of failures of Maithon and Panchet dam various cases like A1, A2, A3 and A4 as mentioned in Table 5.1 have been analyzed.

The flood hydrograph attenuates as the flood moves towards downstream from the dam site. In fact at any sections the flow hydrographs starts rising and accordingly the water level also increases and a time is reached when the discharge is its maximum value. Ideally, the water level corresponding to this discharge should also be maximum, it means the maximum water level and maximum discharges should occur at the same time. But it hardly happens, as during the stage discharge curve in the rising and falling trends are different. Fig. 5.3 (a) to (d) show the flow hydrograph and corresponding stages at selected locations along the Damodar river for various cases of dam break failure. These figures also show the time of occurrence of maximum discharge and maximum stage since the entrance of peak of the inflow hydrograph into reservoirs. The maximum discharge and maximum stage reached at a particular section is shown in the figures. It can be observed that the time of maximum discharge and maximum stage are not the same and maximum discharge occurs earlier than the maximum stage in almost all cases. As the flood waves propagates downstream in the river the time gap of occurrence of maximum stage and maximum discharge reduces. Further, the maximum stage does not give the exact information about the extent of inundation in the area, the zero gauge at all sections are also mentioned.

The NWS DAMBRK model gives the profile of maximum water level, maximum discharge. The profile of maximum water level attained by dam break flood at various sections along river Damodar downstream of Panchet dam is shown in Fig. 5.4. The four curves in the figures are corresponding to 4 cases of dam break situation under PMF condition. In the figure, it is observed that in case of A2 and A3, the maximum stage after 6 km d/s of Panchet dam suddenly falls in comparison to that of for Case A1 and A3. In fact in cases of A2 and A3, Maithon dam fails and therefore the flow in the Barakar river is very high and it creates a drainage congestion condition at the confluence, about 6 km d/s of Panchet dam. This reason may be attributed to rise in maximum water level in cases of A2 and A3 upto 6 km.

The time of occurrence of this maximum stage is shown in Fig. 5.5. These two figures should be read simultaneously to know the time of occurrence of maximum stage at any cross section. It is to mention here that the time of occurrence is for the maximum stage and it should not be confused with the time available for flood preparedness. In fact, the flood above the danger level might have occurred much before the occurrence of maximum stage at a given section.

The profile of maximum discharge at various cross sections is shown in Fig. 5.6. Information about the maximum velocity attained by the flood wave is important for determining the safety of a structure constructed in the flood plain. The DAMBRK model predicts the maximum velocity attained by the flood at various cross sections as shown in Fig. 5.7.

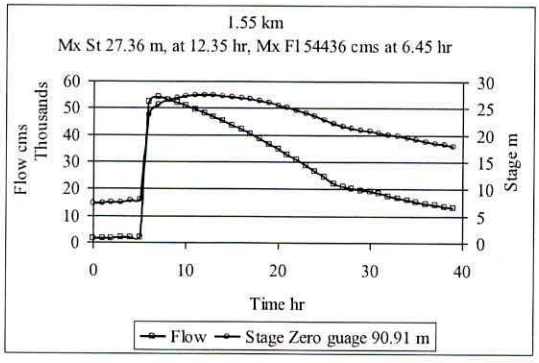

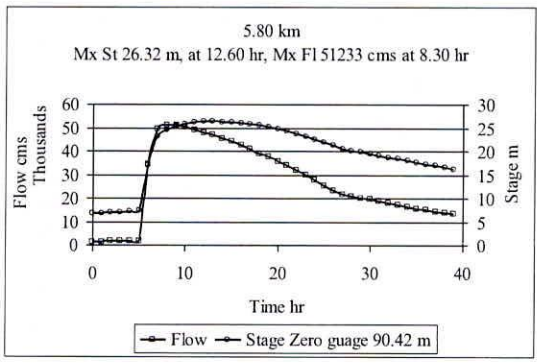

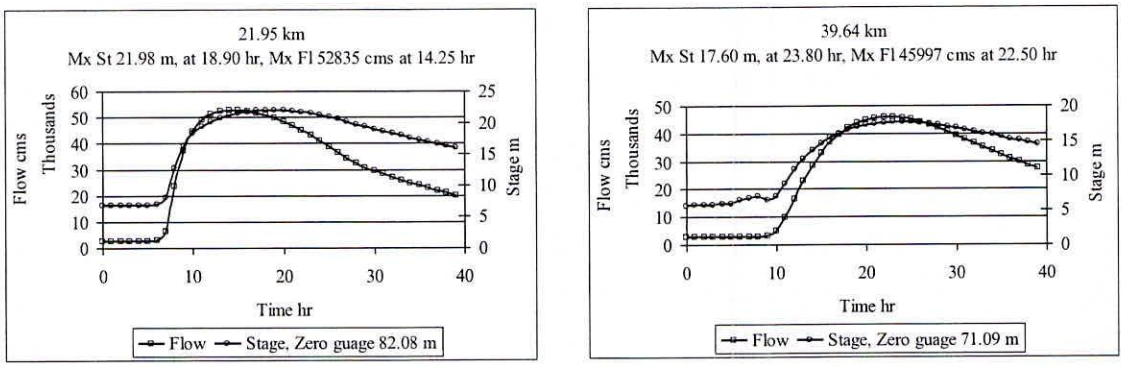

Fig. 5.3 (a) Flood and stage hydrograph at various cross sections in the Damodar river for Case A1.

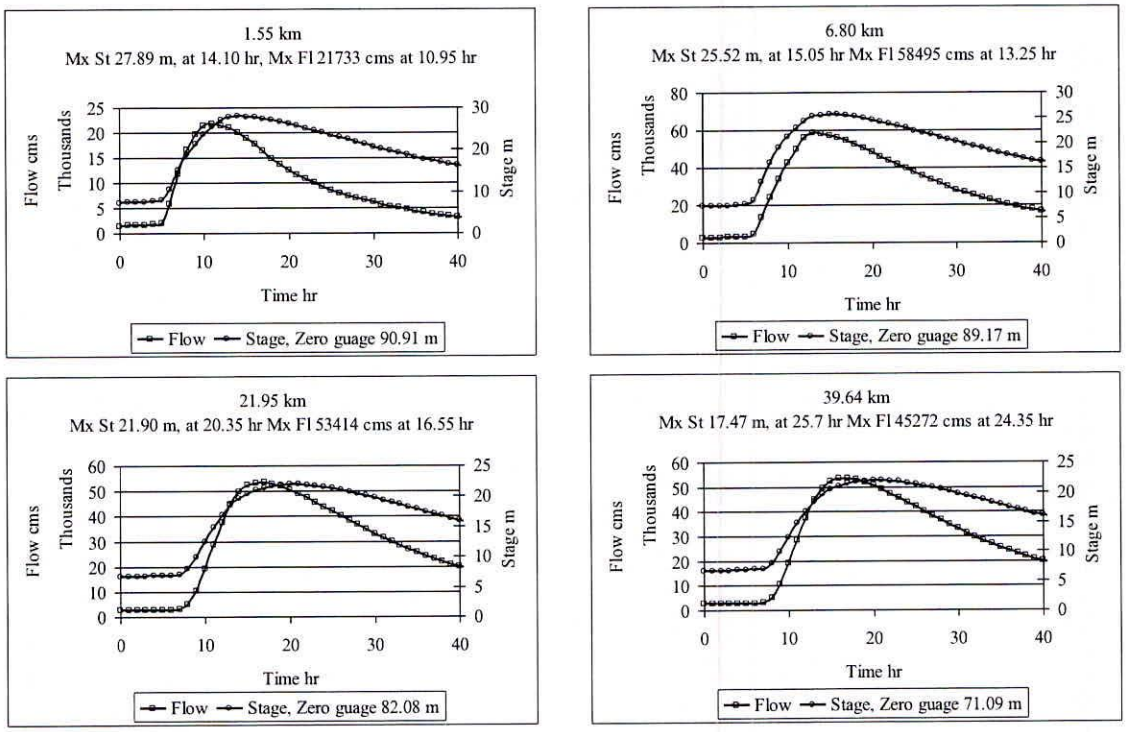

Fig. 5.3 (b) Flood and stage hydrograph at various cross sections in the Damodar river for Case A2.

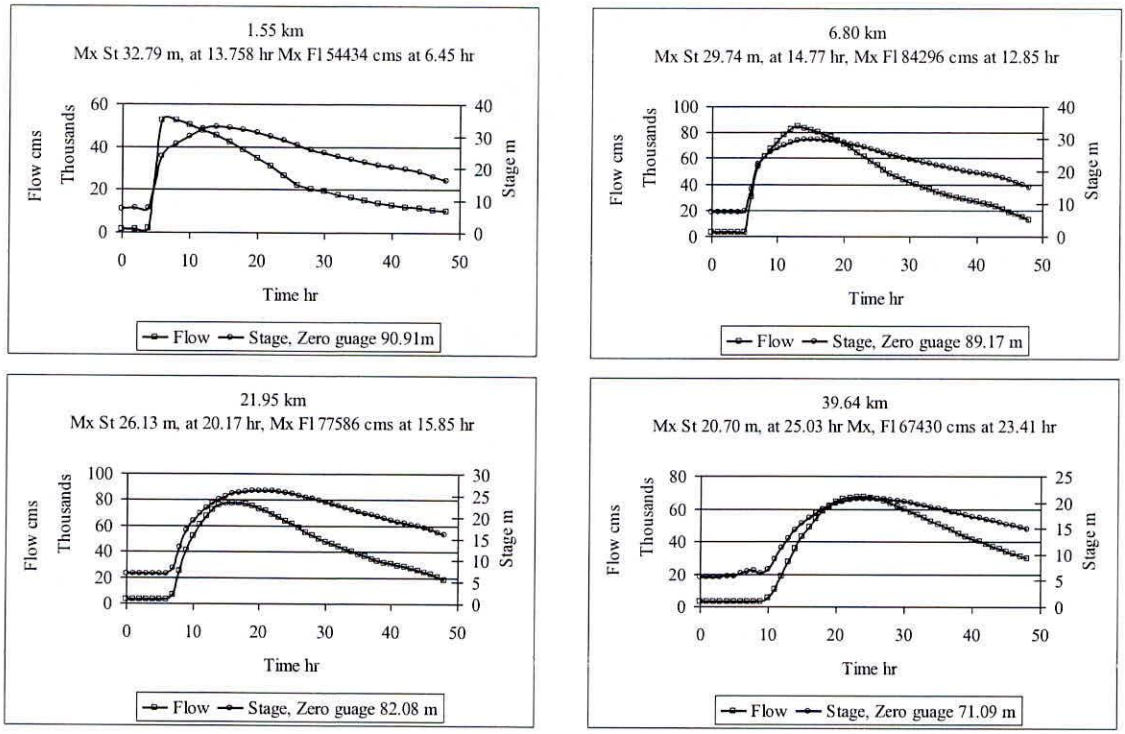

Fig. 5.3 (c) Flood and stage hydrograph at various cross sections in the Damodar river for Case A3.

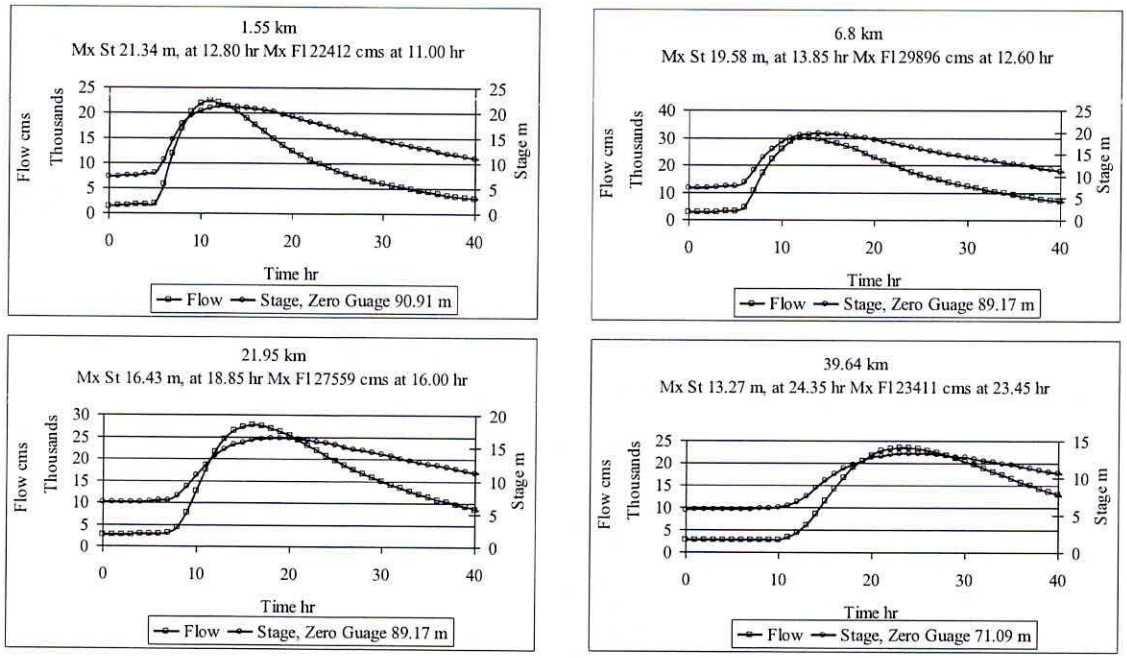

Fig. 5.3 (d) Flood and stage hydrograph at various cross sections in the Damodar river for Case A4.

The inundation maps for every case are prepared by overlaying the water-surface-profile-map of a particular failure case over the digital elevation map of the area. The digital elevation map of the area has been prepared using the contours extracted from toposheets as well as the survey data for cross sections of Damodar and Barakar rivers. The water surface profile along the river Barakar is generated separately in accordance with the case C1, C2 etc as mentioned earlier. Similarly, the water surface profile along river Damodar is generated according to cases A1, A2 etc. These two water surface profiles are added to generate a composite water surface profile along the two rivers for various cases of A1, A2 etc in accordance with Table 5.1.

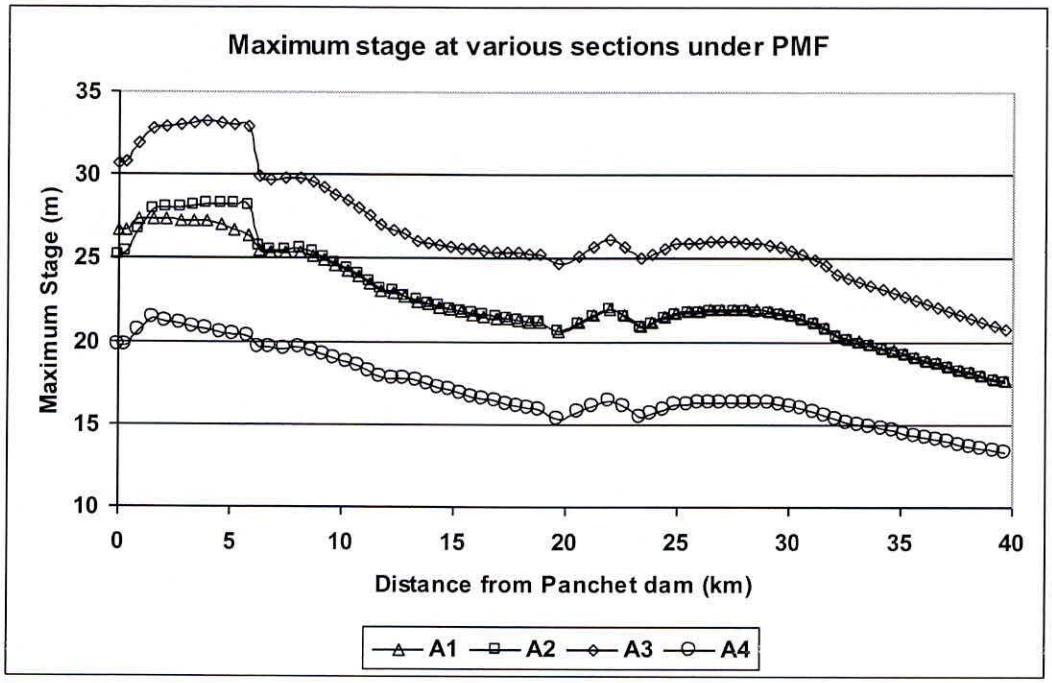

Fig. 5.4 Maximum stage occurred at sections along river Damodar d/s of Panchet dam.

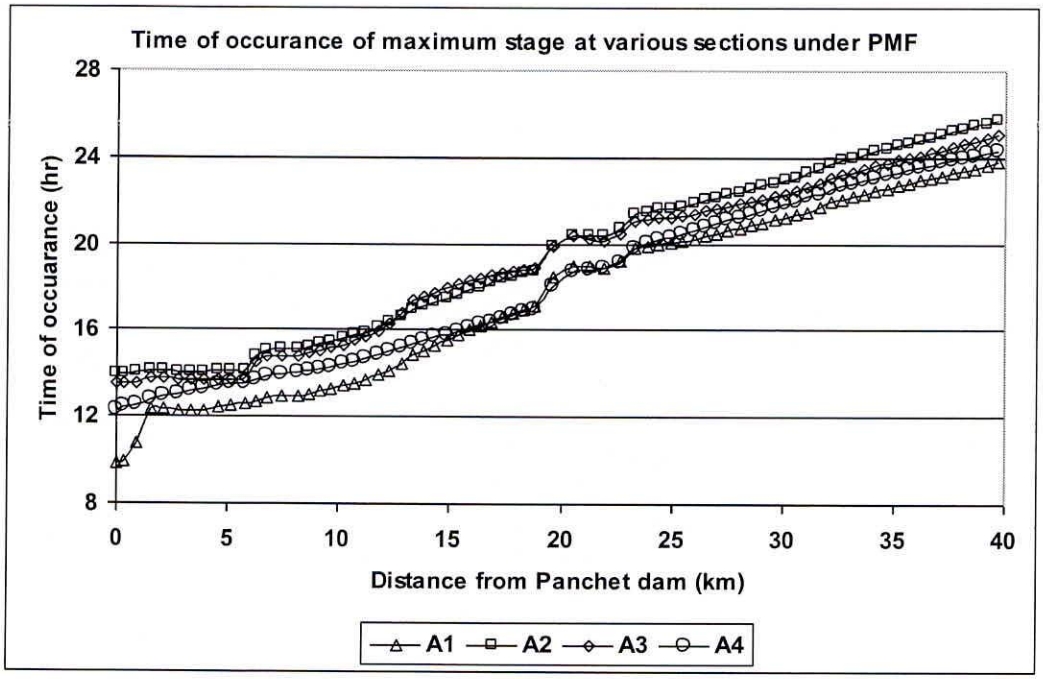

Fig. 5.5 Time of occurrence of maximum stage.

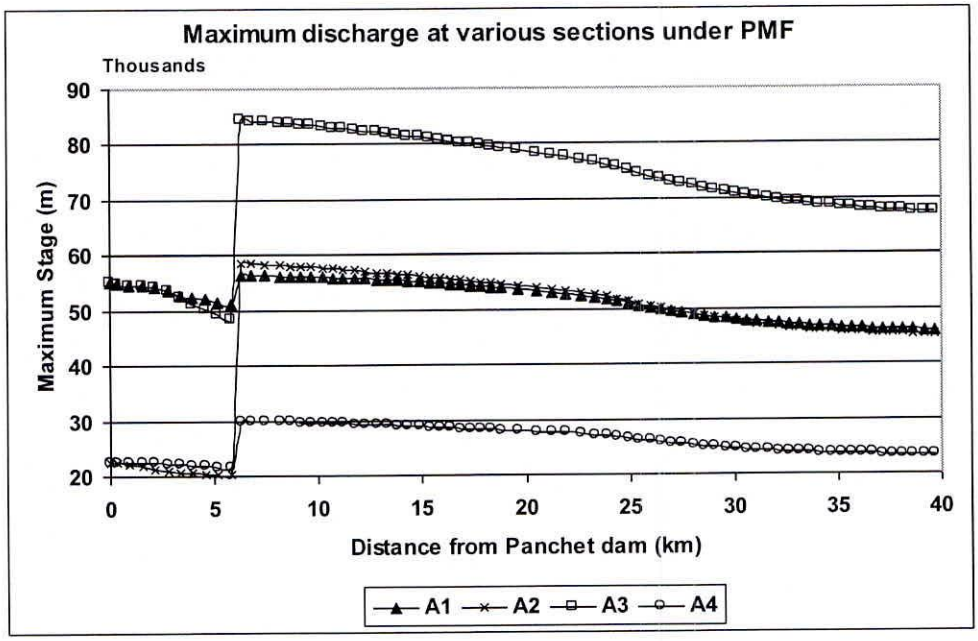

Fig. 5.6 Maximum discharge at various croo sections.

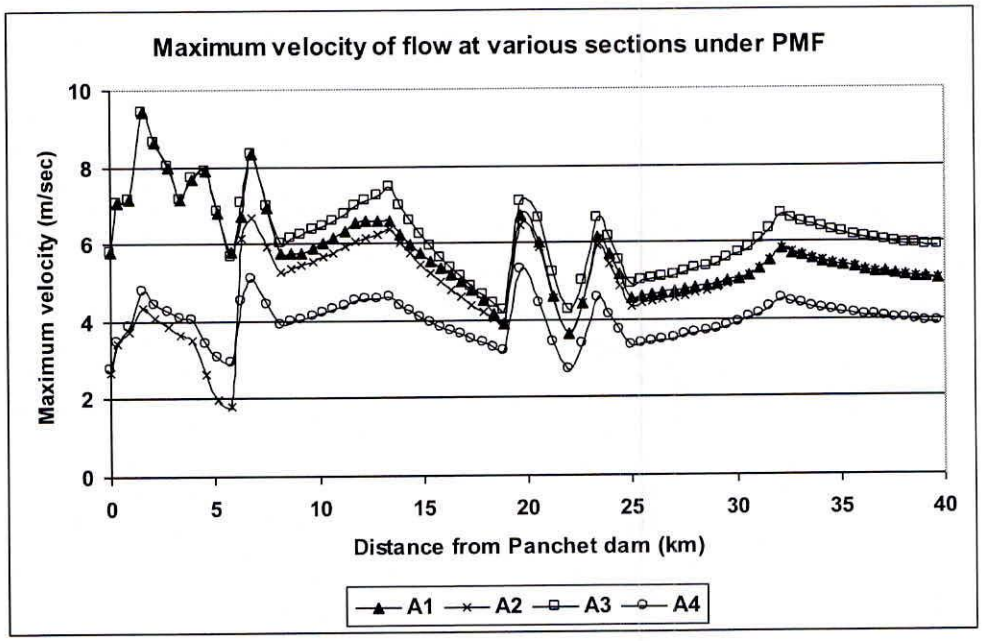

Fig. 5.7 Maximum velocity of flow at various sections.

The digital elevation model (DEM) of the area has been generated using the extracted contours from toposheets as well as survey data for river cross sections in ERDAS Imagine GIS software. Fig. 5.8 shows the DEM of the area. The two data sets, e.g. water surface profile and DEM overlaid over each other are in same geographical reference system and therefore, the difference of the two gives the depth of flood water i.e. inundation at point. The locations for which the RL of water surface is higher than the terrain level, there will be inundation otherwise; the area will be free from inundation (higher patches). All the higher patches showing water depth in negative values are grouped together and excluded from the map. For rest of the area, the water depth is further classified into 8 classes as follows:

Water Depth	Class	Water Depth	Class
0-0.25	1	2.0-5.0	5
0.25-0.5	2	5.0-10	6
0.5-1.0	3	10.0-20.0	7
1.0-2.0	4	> 20.0	8

The area for each class is represented by a unique color and its area is computed. Further, this inundation map is superimposed over a base map showing the important places and communication network as well as spread for Barakar and Damodar rivers as extracted from toposheets. Fig. 5.9 (a) to Fig. 5.9 (d) shows the inundation map for various cases of dam break failure. This map is geo referenced map and the inundation shown in the map can be very easily referred with ground locations. It can be observed from the map that the maximum inundation of > 20 m (class 8) occurs when either one or both the dams fails (Case A1, A2 or A3) but the it falls mostly on the river courses, and therefore this situation is not comparatively more alarming. But the area adjoining to the river courses are having inundation depth between 10 to 20 m (with inundation area is more than 5000 ha in all cases except A4, in which none of the dam fails). In the area away from the river the depth of inundation gradually decreases. The inundation map for case of A4 shows inundation in the lower reach of river only because in this case, none of the dams fail and only PMF is routed through the spillway. The upper reach of the rivers passes through the hilly region and therefore there is no inundation for case A4, while the lower reaches are inundated as these falls mainly in flat terrain.

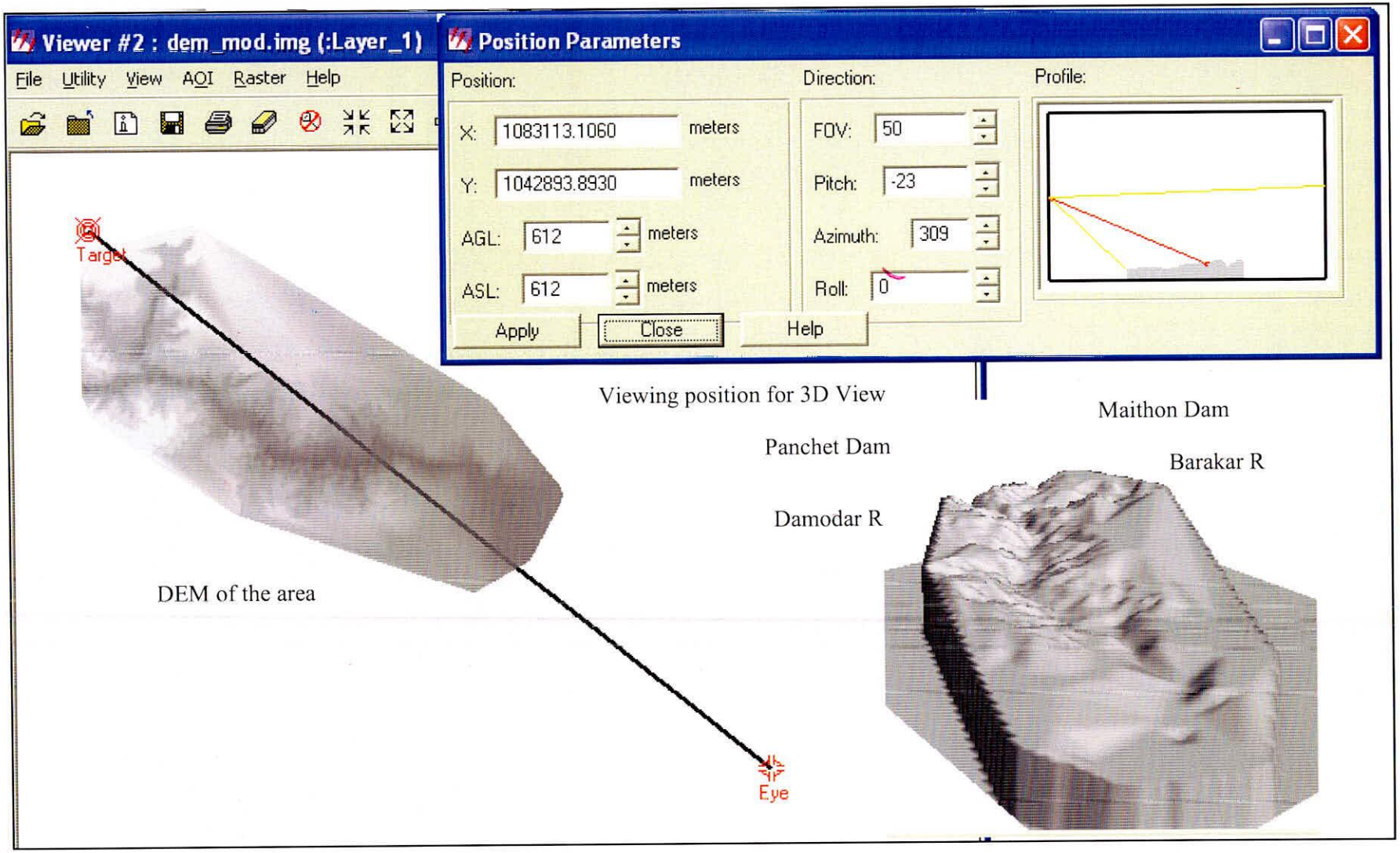

Fig. 5.8 DEM and 3D view of the study area.

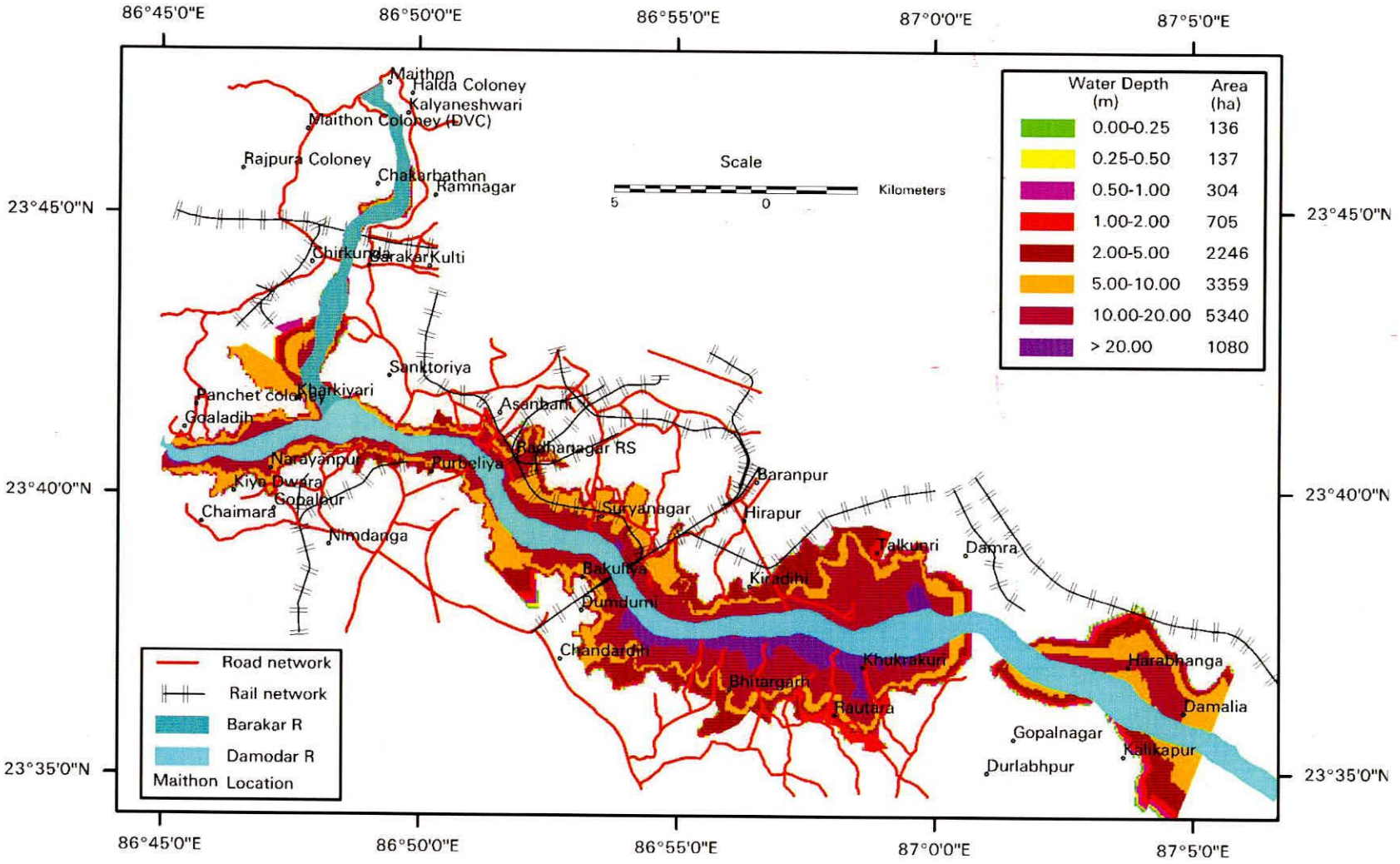

Fig. 5.9 (a) Inundation map for case A1, (Panchet dam fails while Maithon dam remains intact).

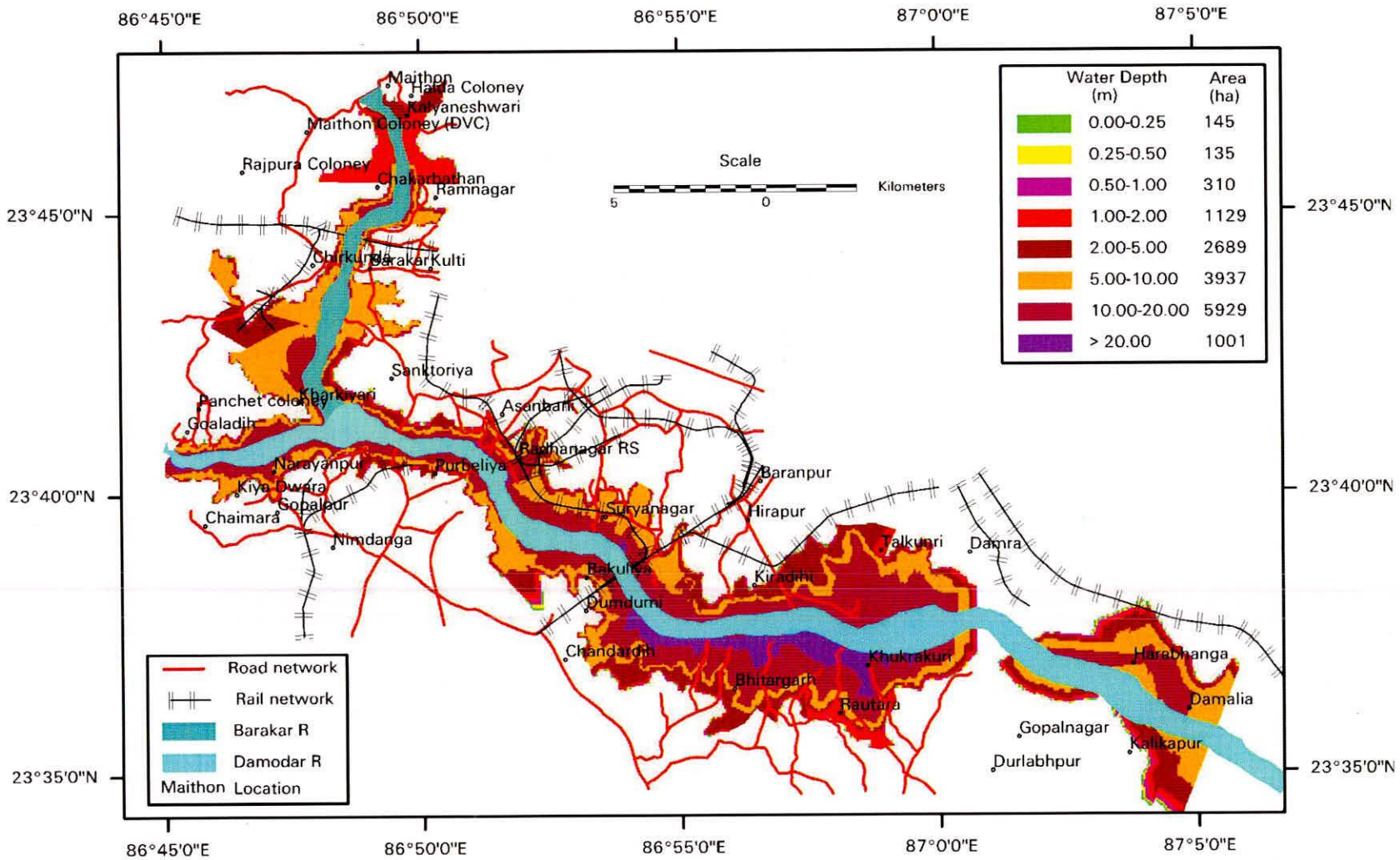

Fig. 5.9 (b) Inundation map for case A2, (Maithon dam fails while Panchet remains intact).

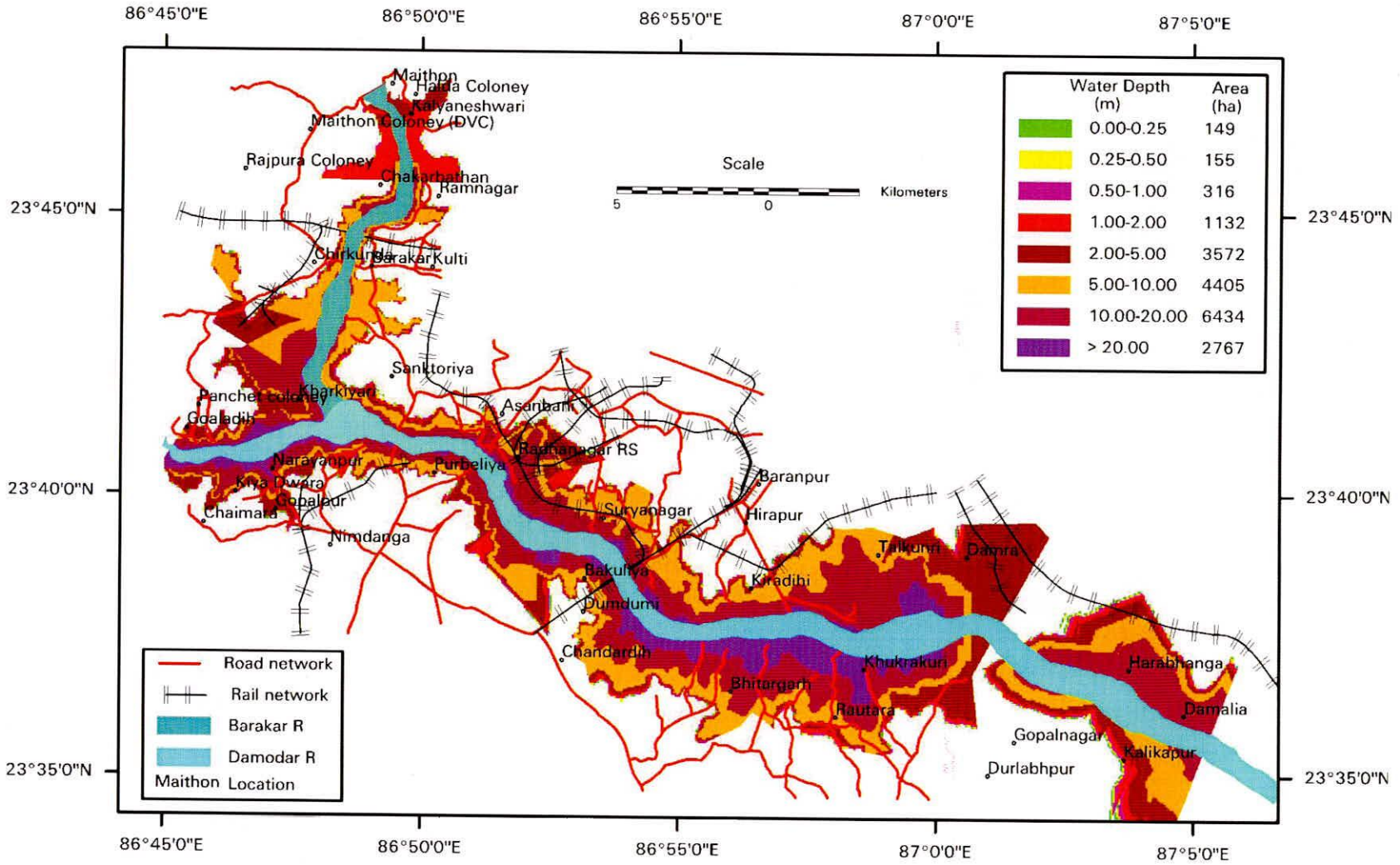

Fig. 5.9 (c) Inundation map for case A3, (both Maithon and Panchet dams fail).

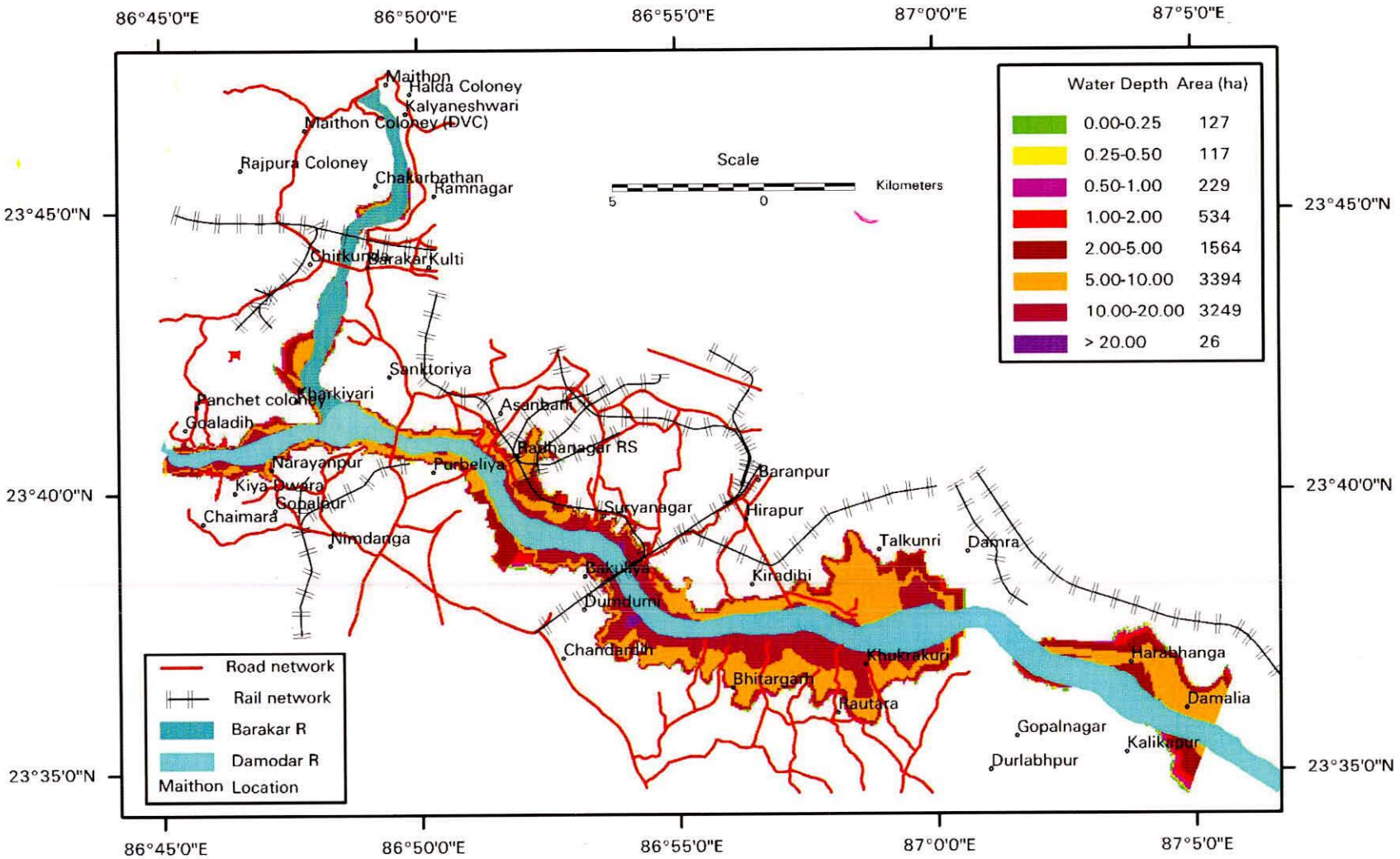

Fig. 5.9 (d) Inundation map for case A4 (Neither Panchet nor Maithon fails).

5.4 Failure of Panchet Dam under Nominal Inflow

The Panchet reservoir is at FRL (135.64 m) and a very nominal inflow is entering into reservoir, when suddenly the dam breaks due to earthquake or some human induced attack. Here overtopping of reservoir water from dam is practically impossible and therefore an instantaneous pipe failure is considered for dam break analysis. The breach develops into its complete size (1000 m) in 0.03 hour (time of breach ~ 2 min) when the outflow from breached section is at its maximum value of 46,049 cumec. The total volume of water discharged from the reservoir is 1278 M cubic meter, mainly the reservoir storage (between RL of 98 and FRL). The outflow from the reservoir is routed in the downstream river section assuming the lateral inflow from Barakar river at between section 5.8 to 6.8 km. Depending upon the various combination of failures of Maithon and Panchet dam various cases like B1, B2, B3 and B4 as mentioned in Table 5.1 have been analyzed. Fig. 5.10 (a) to (d) show the flow hydrograph and corresponding stages at selected locations along the Damodar river for various cases of dam break failure. The profile of maximum water level attained by dam break flood at various sections along river Damodar downstream of Panchet dam is shown in Fig. 5.11. The four curves in the figures are corresponding to 4 cases of dam break situation. The time of occurrence of this maximum stage is shown in Fig. 5.12. The profile of maximum discharge at various cross sections is shown in Fig. 5.13. Fig. 5.14. shows the maximum velocity attained by the flood at various cross sections along the river Damodar.

The inundation maps for every case have been prepared for this situation also. The water surface profile along the river Barakar is generated separately in accordance with the case C1, C2 etc as mentioned earlier. Similarly, the water surface profile along river Damodar is generated according to cases B1, B2 etc. These two water surface profiles are added to generate a composite water surface profile along the two rivers for various cases of B1, B2 etc in accordance with Table 5.1. In the inundated area, the water depth is classified into 8 classes as discussed earlier. The area for each class is represented by a unique color and its area is computed. Further, this inundation map is superimposed over a base map showing the important places and communication network as well as spread for Barakar and Damodar rivers as extracted from toposheets. Fig. 5.15 (a) to Fig. 5.15 (d) shows the inundation map for various cases of dam break failure. This map is geo referenced map and the inundation shown in the map can be very easily referred with ground locations. The inundation map for case B4, when none of the dams breaks also shows some inundation. These areas when overlaid on the toposheet reveals that these areas are on the river course only and therefore practically there is no inundation in this case.

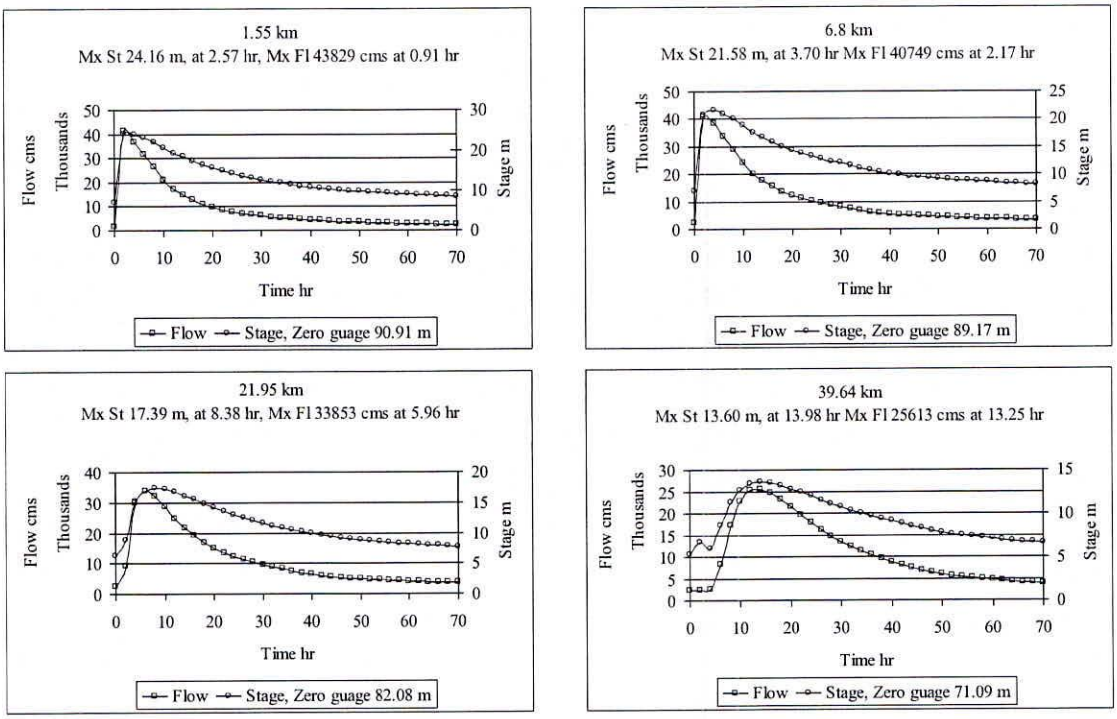

Fig. 5.10 (a) Flood and stage hydrograph at various cross sections in the Damodar river for Case B1.

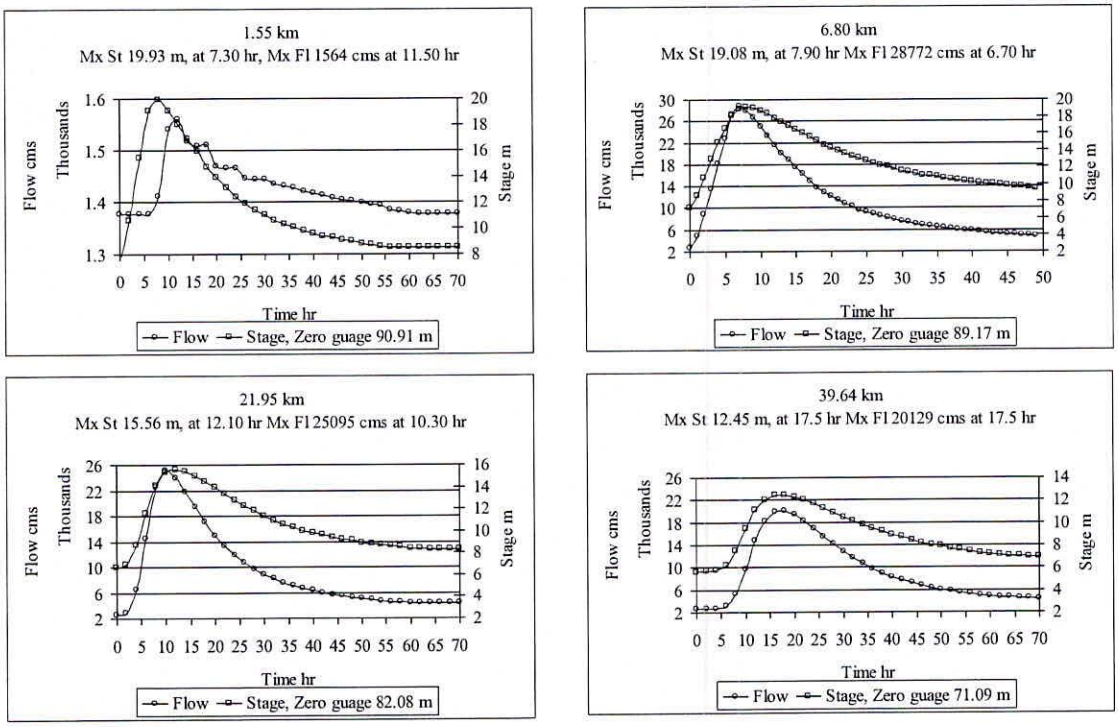

Fig. 5.10 (b) Flood and stage hydrograph at various cross sections in the Damodar river for Case B2.

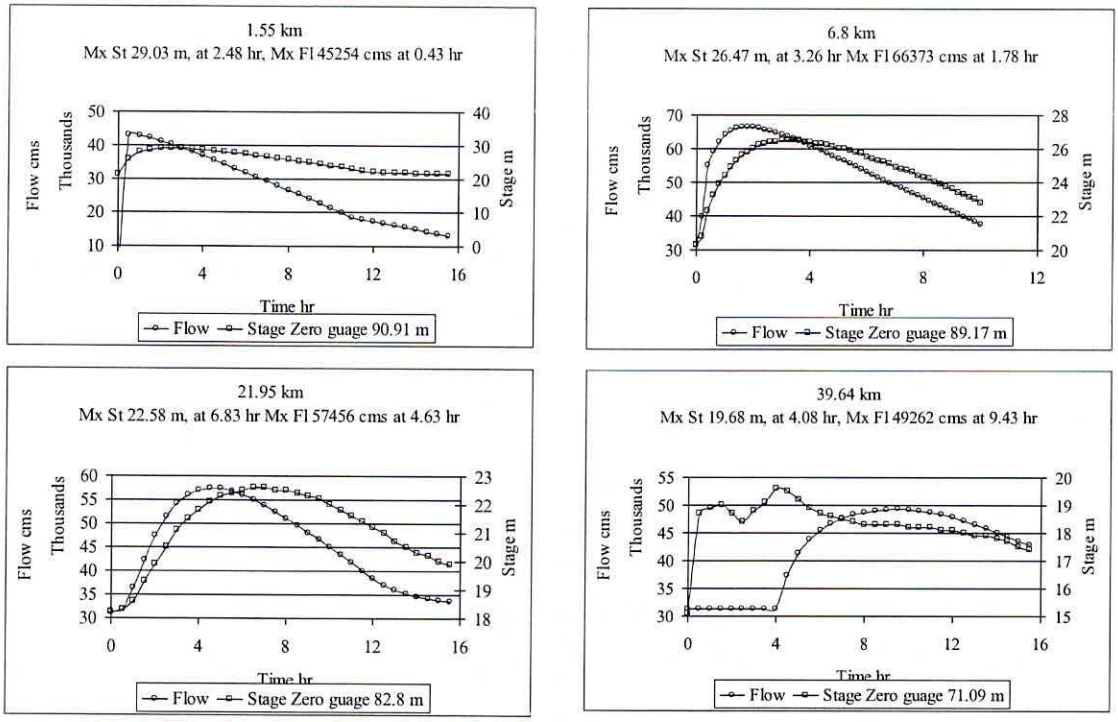

Fig. 5.10 (c) Flood and stage hydrograph at various cross sections in the Damodar river for Case B3.

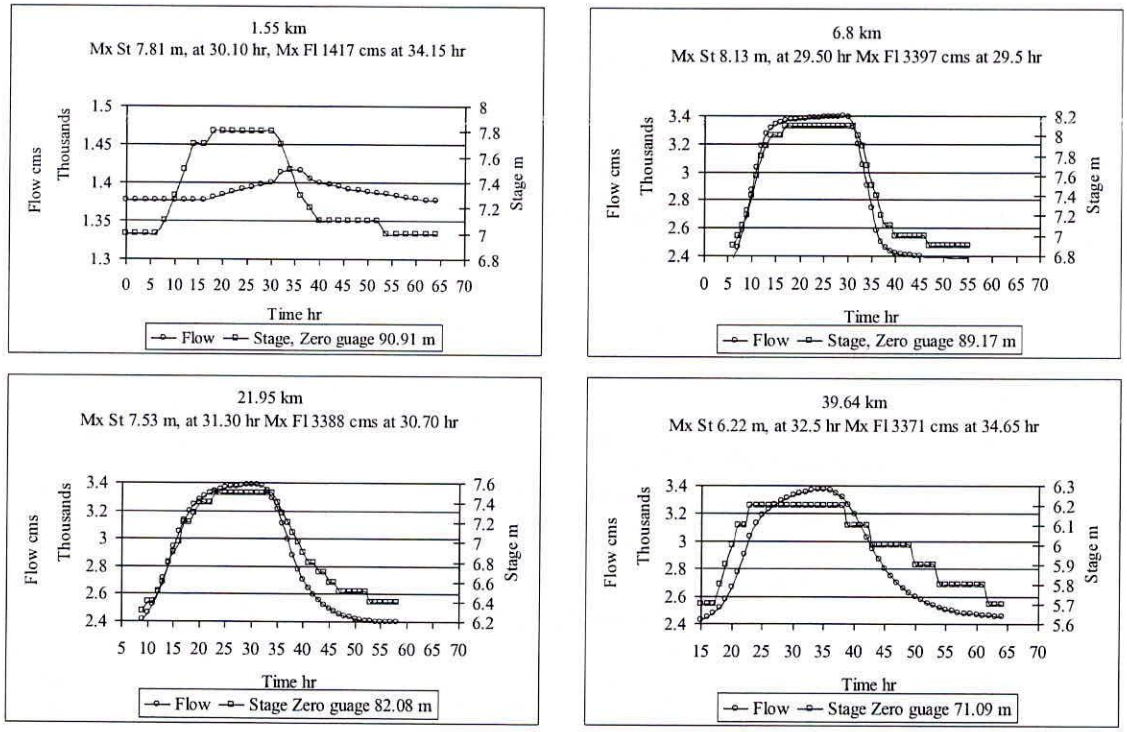

Fig. 5.10 (d) Flood and stage hydrograph at various cross sections in the Damodar river for Case B4.

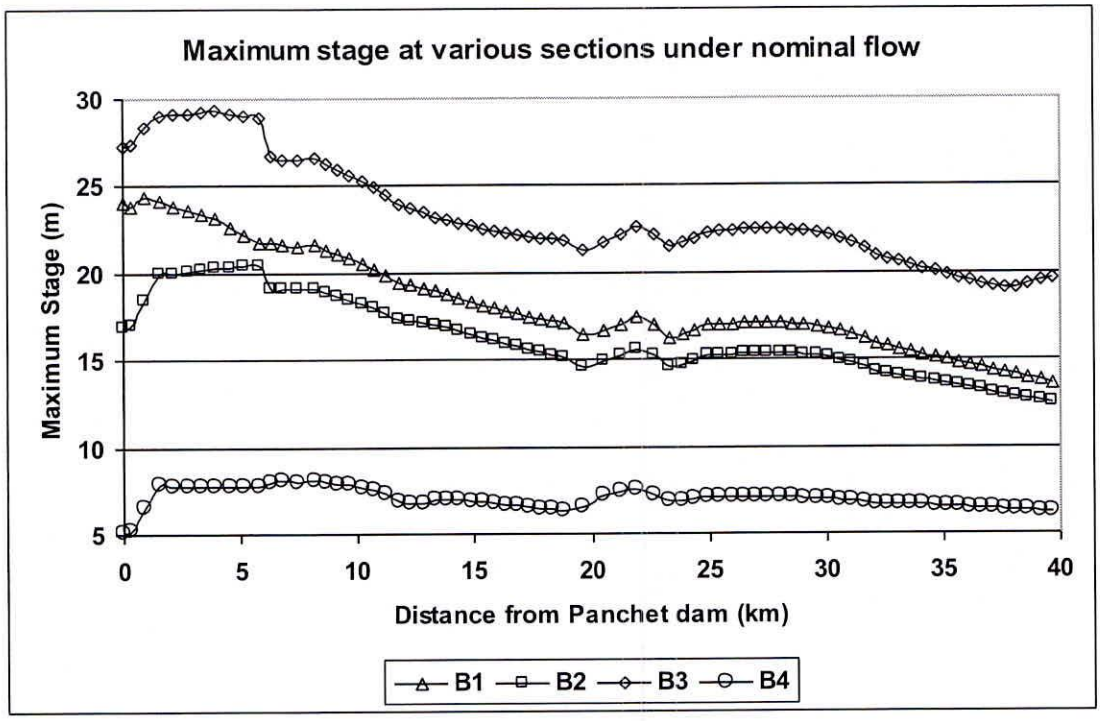

Fig. 5.11 Maximum stage occurred at sections along river Damodar d/s of Panchet dam.

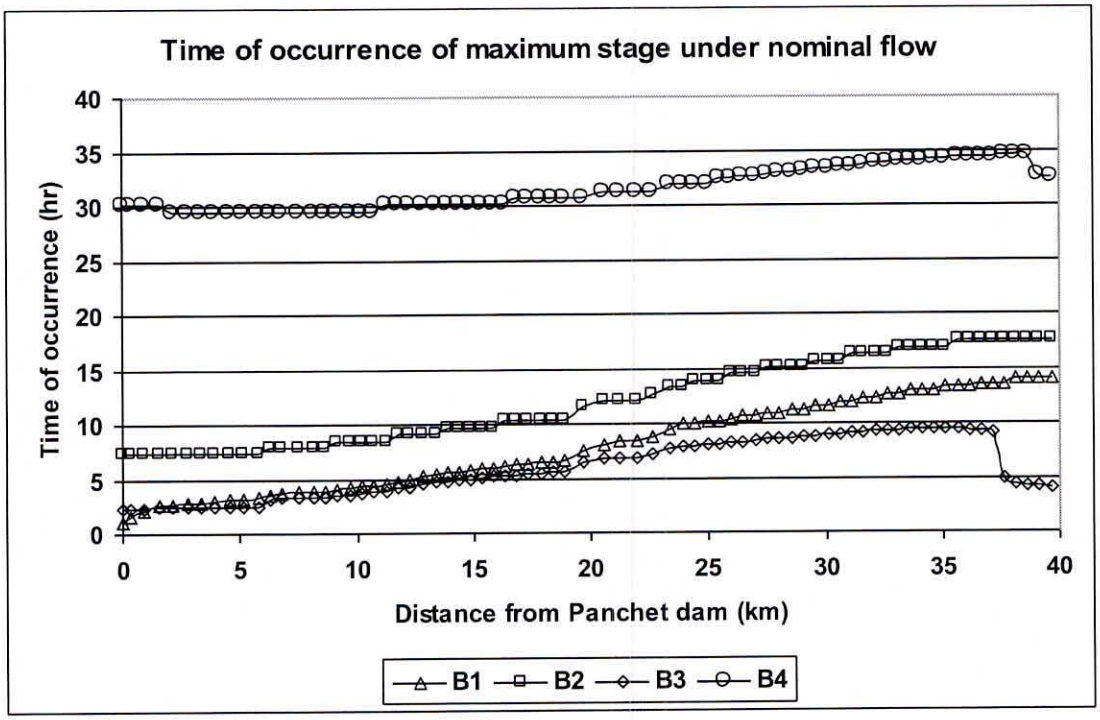

Fig. 5.12 Time of occarrence of maximum stage.

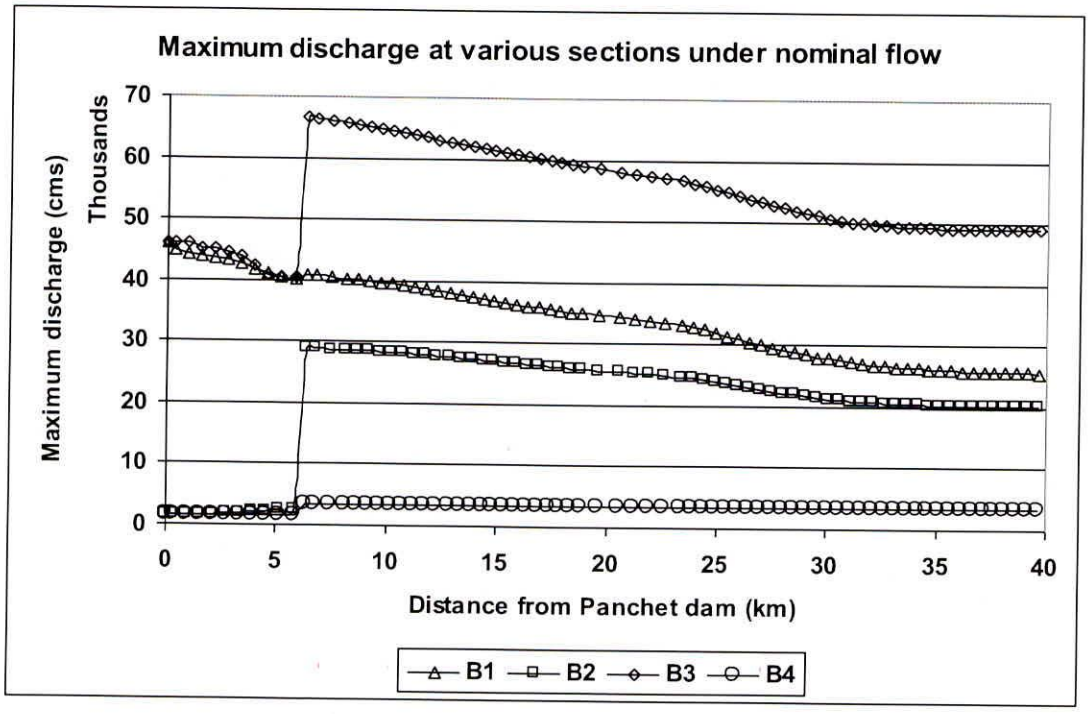

Fig. 5.13 Maximum discharge at various croo sections.

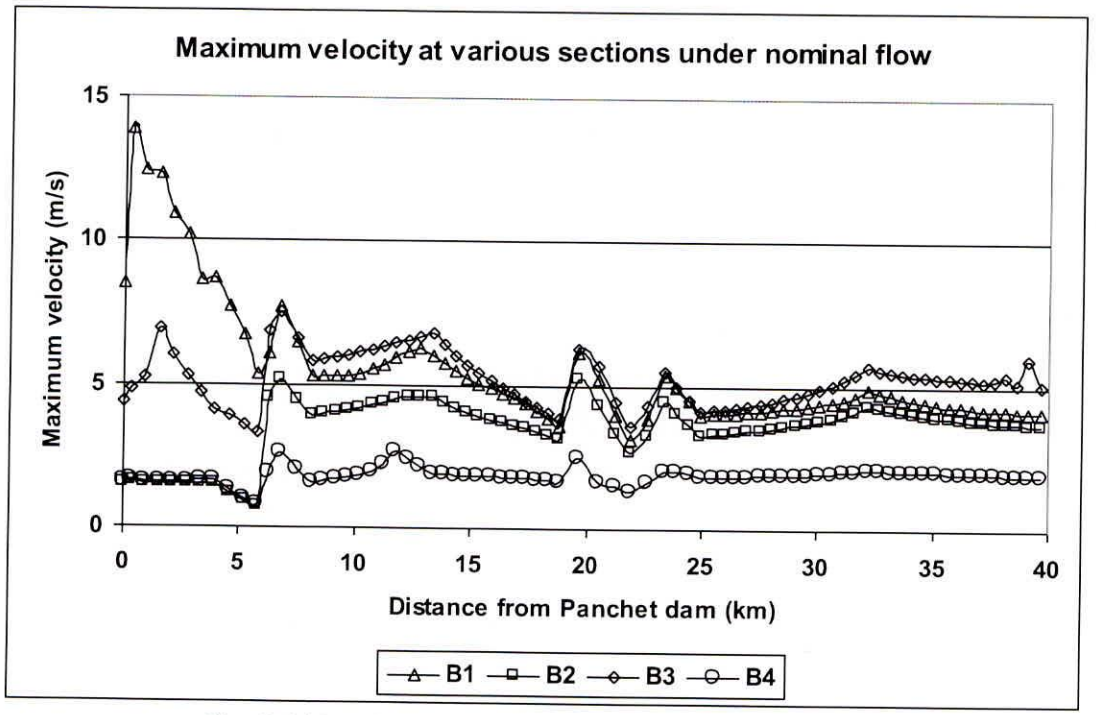

Fig. 5.14 Maximum velocity of flow at various sections.

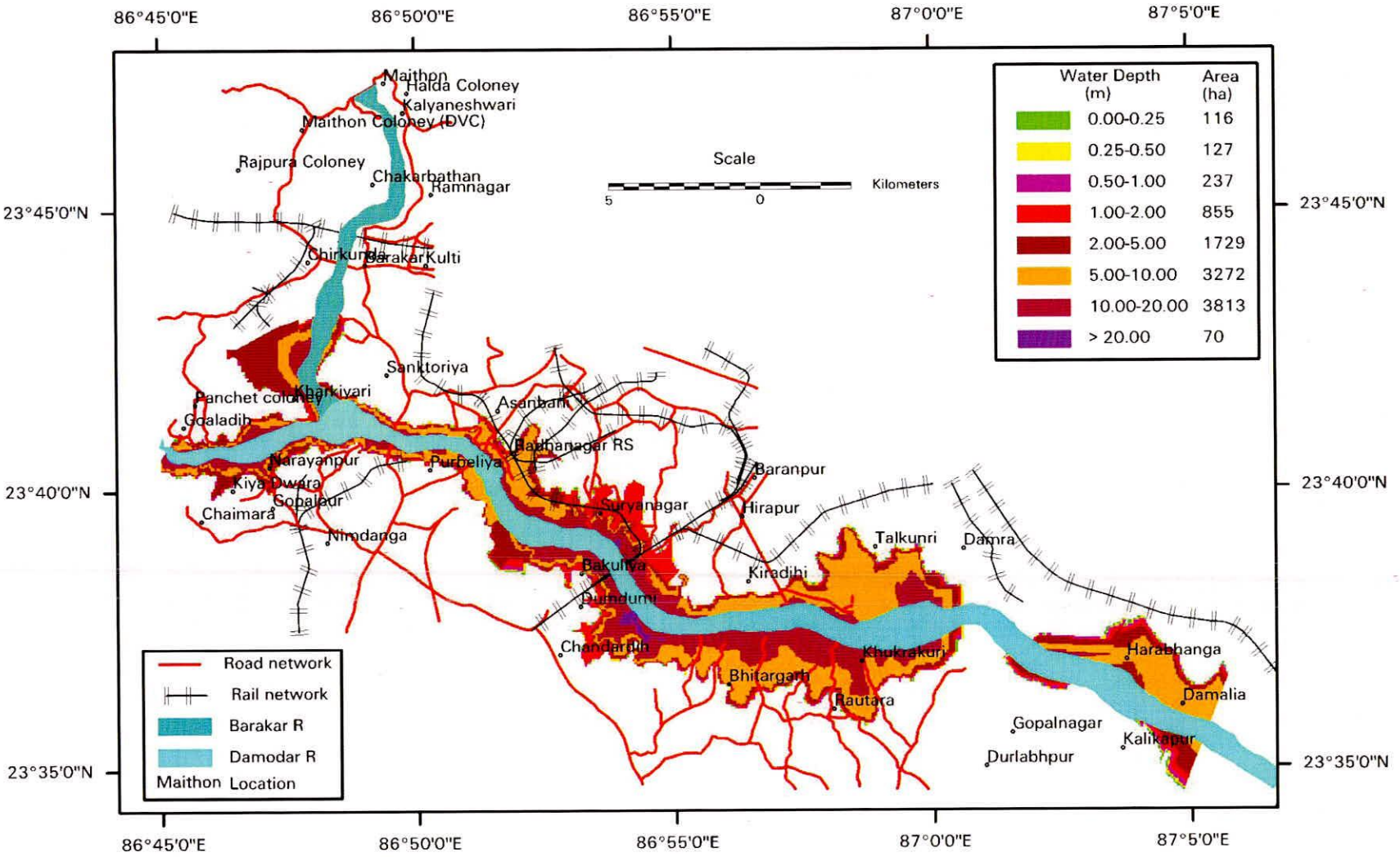

Fig. 5.15 (a) Inundation map for case B1 (Panchet dam fails while Maithon dam remains intact).

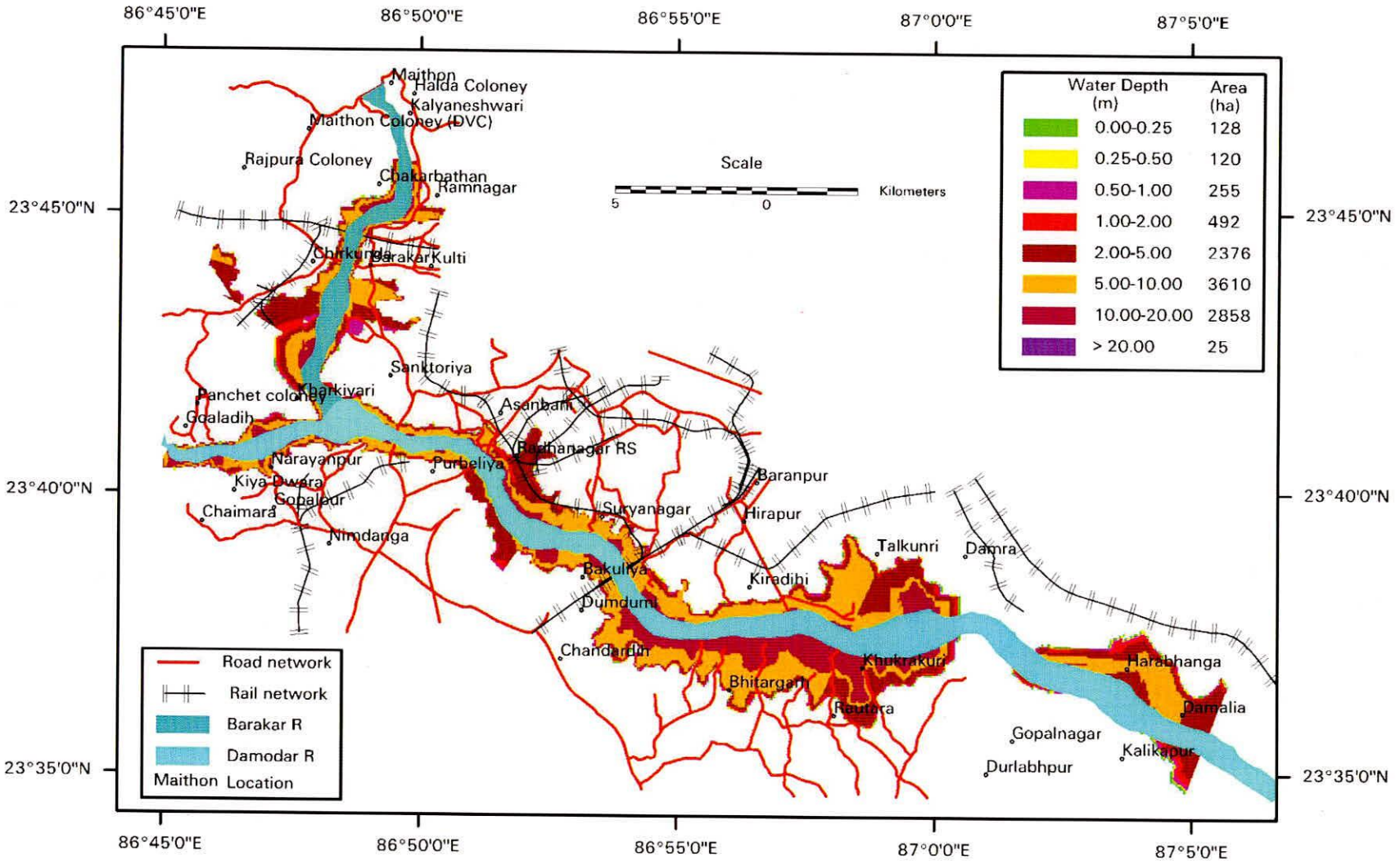

Fig. 5.15 (b) Inundation map for case B2 (Maithon dam fails while Panchet dam remains intact).

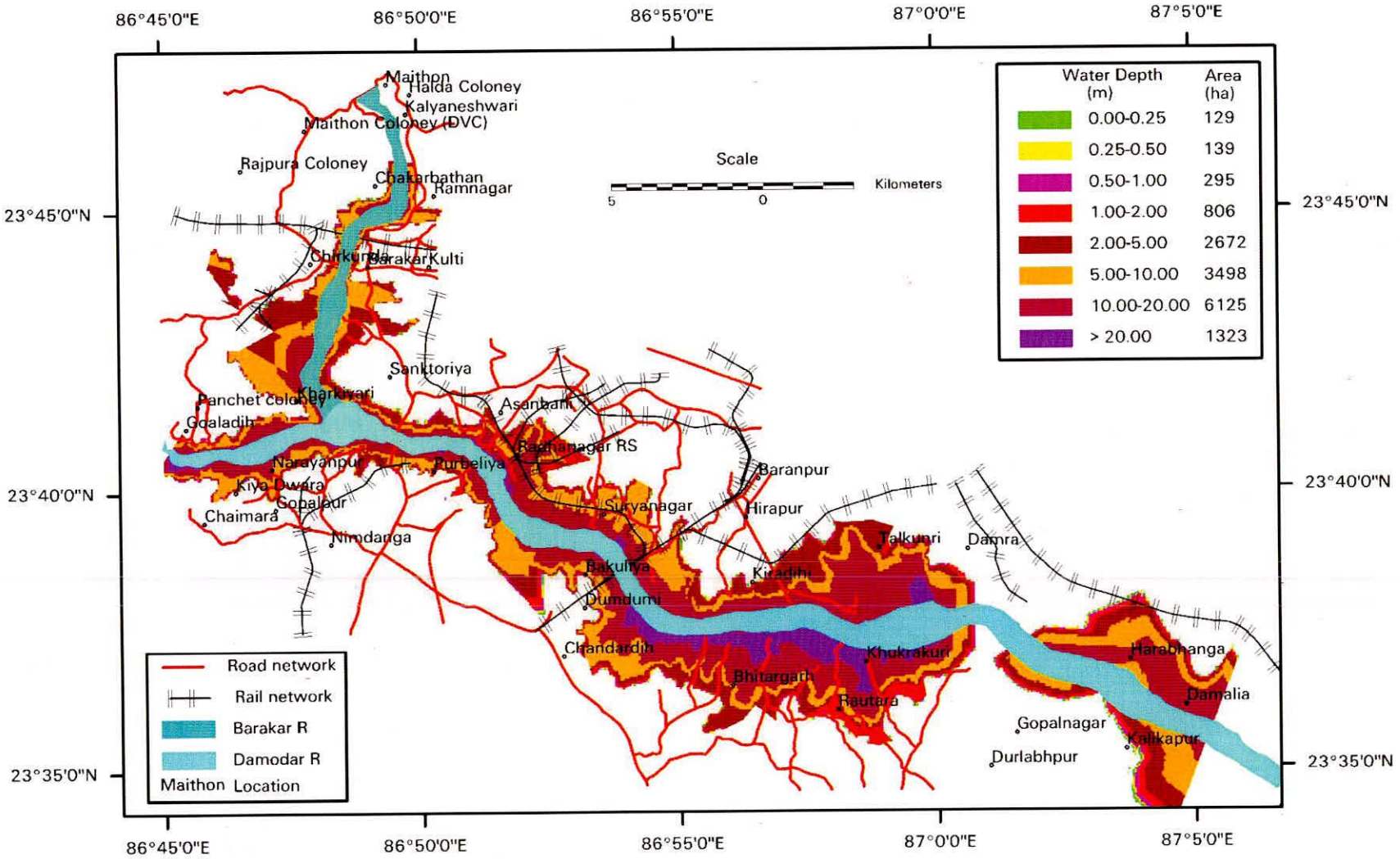

Fig. 5.15 (c) Inundation map for case B3 (both Panchet and Maithon dams fail).

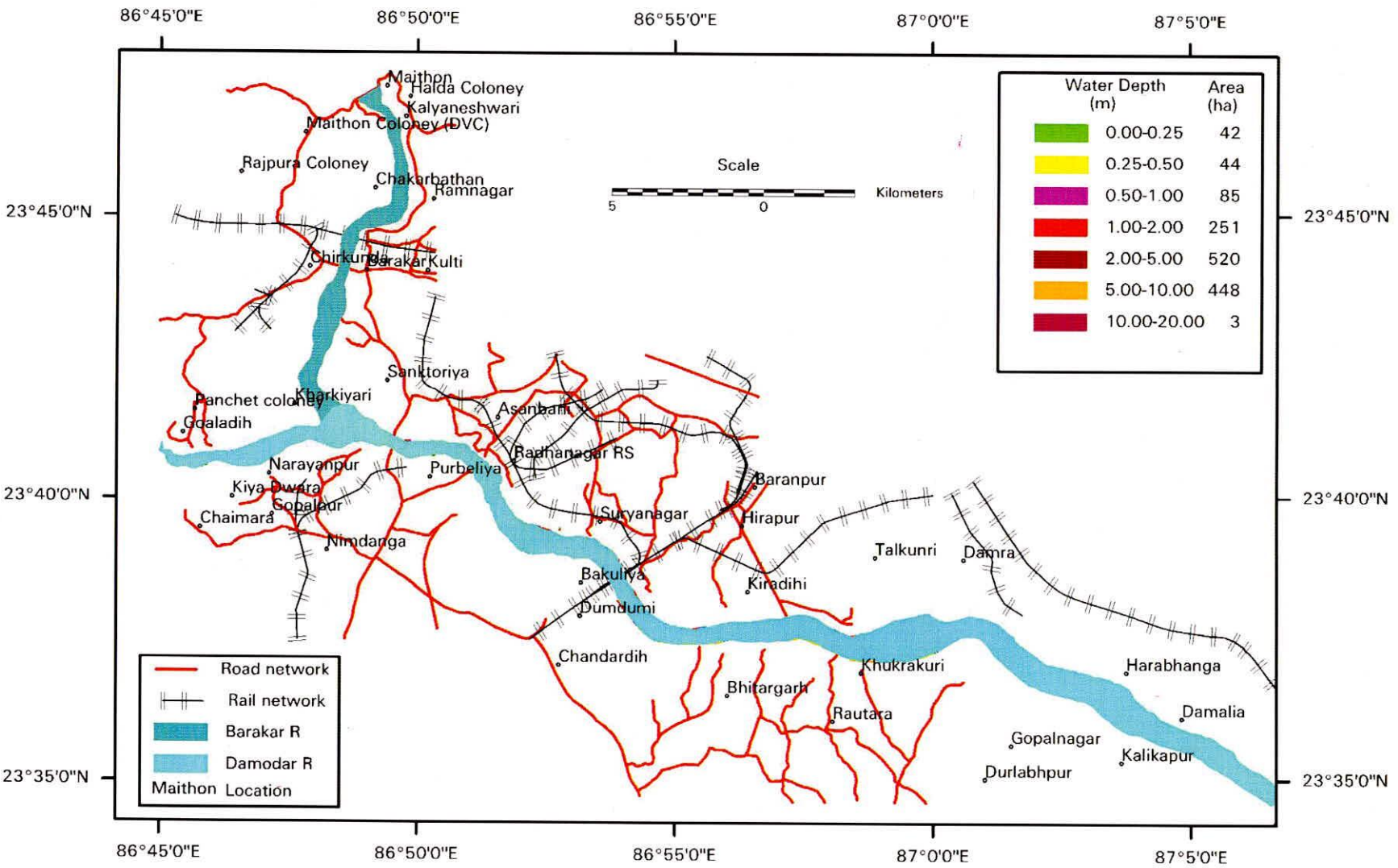

Fig. 5.15 (d) Inundation map for case B4 (Neither Panchet nor Maithon dam fails).

5.5 Sensitivity of Breach Parameters

Sensitivity analysis for three model parameters namely; breach width, side-slope of breach and time of breach has been done for failure of both the dams separately. During the sensitivity analysis, outflow is computed by varying one parameter while the others are kept constant. The initial model parameters for both the dams are breach width = 1.0 km, slope of breach = 1:1 and time of breach = 1 hr.

5.5.1 Sensitivity of breach parameters for Panchet dam failure

Breach width - The dam break model for Panchet dam has been simulated with changed breach width of 0.5 km, 1.5 km, 2.0 km and 2.5 km and the outflow at various downstream sections are computed. The effect of breach width on the maximum discharge at 1.55 km, 5.8 km, 6.8 km, 21.95 km and 39.64 km has been computed as shown in Table: 5.2 (a). The maximum discharge for various breach width at different downstream sections are plotted and shown in Fig. 5.16 (a). Comparatively low values of maximum discharge at sections 1.55 and 5.8 km are due to the fact that uopto Ch- 5.8 km, the river discharge consists of flow of Damodar river only while after Ch- 5.8 km, flow from Maithon enters the Damodar river and therefore the discharge increases enormously. It is observed that It has been observed that when breach width increases, maximum discharge at any section also increases. But the rate of increase in maximum discharge is comparatively higher in lower value of breach width as shown by the steeper slope of the curve up to breach width of 2 km. When breach width increases beyond 2 km, the curves seems to be flat, it means breach width beyond 2 km does not result in appreciably change in maximum discharge at any section.

Time of Breach - The sensitivity of the breach time has been studied by changing the time of breach to 0.5, 1.5, 2, 2.5 and 3 hours. The effect of breach time on maximum discharge at various sections can be observed from Table: 5.2 (b) and Fig. 5.16 (b). It has been observed that when the breach time increases, the maximum discharge decreases upto Ch- 5.8 km while increases afterwards, though the changes are not very appreciable.

Slope of Breach Section -The sensitivity of the slope of breach section has been studied by changing the value of S to 0.5, 1.5, 2 and 2.5. Their effect on maximum discharge at various sections can be observed from Table: 5.2 (c) and Fig. 5.16 (c). It has been observed that when the slope of breach section increases, the maximum discharge increases in general though the increases is not very appreciable

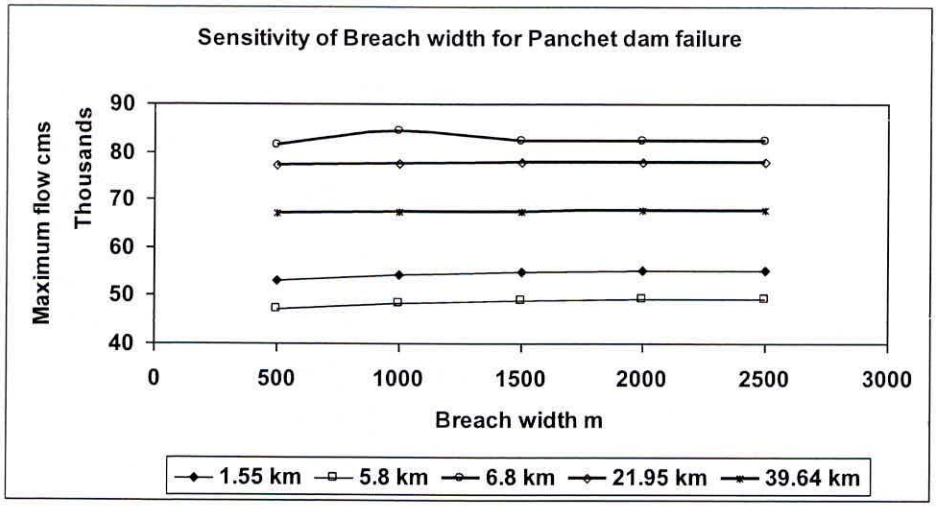

Fig. 5.16 (a) Sensitivity of breach width for Panchet dam failure.

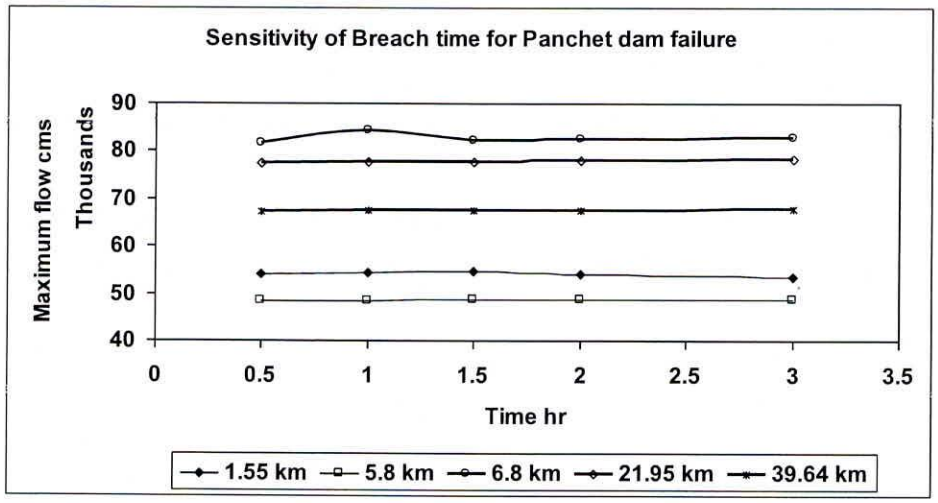

Fig. 5.16 (b) Sensitivity of breach time for Panchet dam failure.

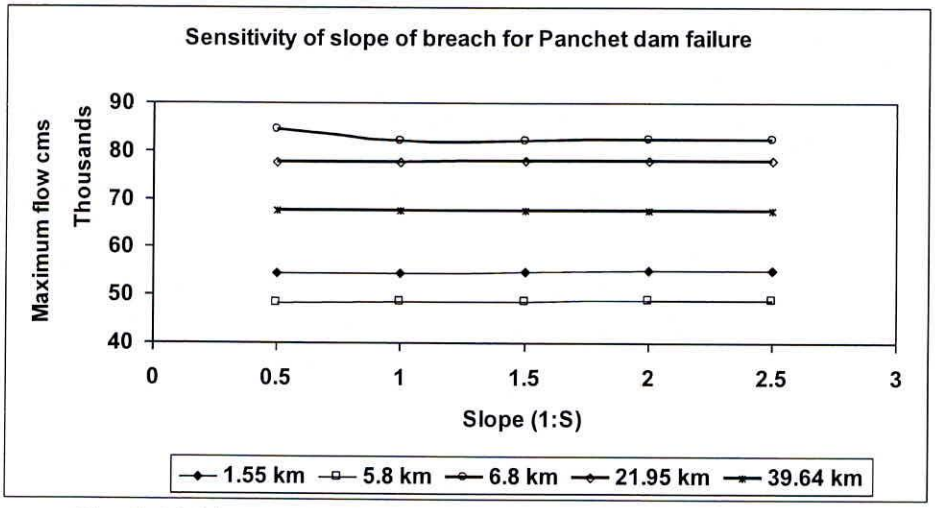

Fig. 5.16 (c) Sensitivity of slope of breach for Panchet dam failure.

5.5.2 Sensitivity of breach parameters for Maithon dam failure

Breach width - The dam break model for Panchet dam has been simulated with changed breach width of 0.5 km, 1.5 km, 2.0 km and 2.5 km and the outflow at various downstream sections are computed. The effect of breach width on the maximum discharge at 3.35 km, 5.35 km, 7.75 km, 10.15 km and 12.75 km has been computed as shown in Table: 5.3 (a). The maximum discharge for various breach width at different downstream sections are plotted and shown in Fig. 5.17 (a). It is observed that It has been observed that when breach width increases, maximum discharge at any section also increases. But the rate of increase in maximum discharge is comparatively higher in lower value of breach width as shown by the steeper slope of the curve up to breach width of 2 km. When breach width increases beyond 2 km, the curves seems to be flat, it means breach width beyond 2 km does not result in appreciably change in maximum discharge at any section.

Time of Breach - The sensitivity of the breach time has been studied by changing the time of breach to 0.5, 1.5, 2, 2.5 and 3 hours. The effect of breach time on maximum discharge at various sections can be observed from Table: 5.3 (b) and Fig. 5.17 (b). It has been observed that when the breach time increases, the maximum discharge decreases. In fact the breach time signifies the total time elapsed in forming a breach section of specified breach width. If the time of breach increases, the process of development of breach section slows down and the breach outflow will decrease. These effects are very much appreciable at nearer sections from dam site, while on moving farther in downstream direction, this effect diminishes due to attenuation of hydrograph.

Slope of Breach Section -The sensitivity of the slope of breach section has been studied by changing the value of S to 0.5, 1.5, 2 and 2.5. Their effect on maximum discharge at various sections are mentioned in Table: 5.3 (c) and Fig. 5.17 (c). It has been observed that when the slope of breach section increases, the maximum discharge increases.

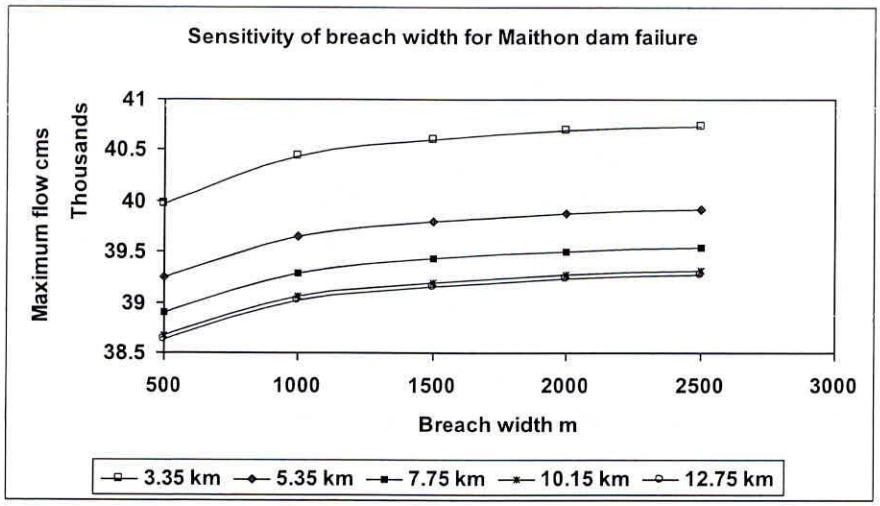

Fig. 5.17 (a) Sensitivity of breach width for Maithon dam failure.

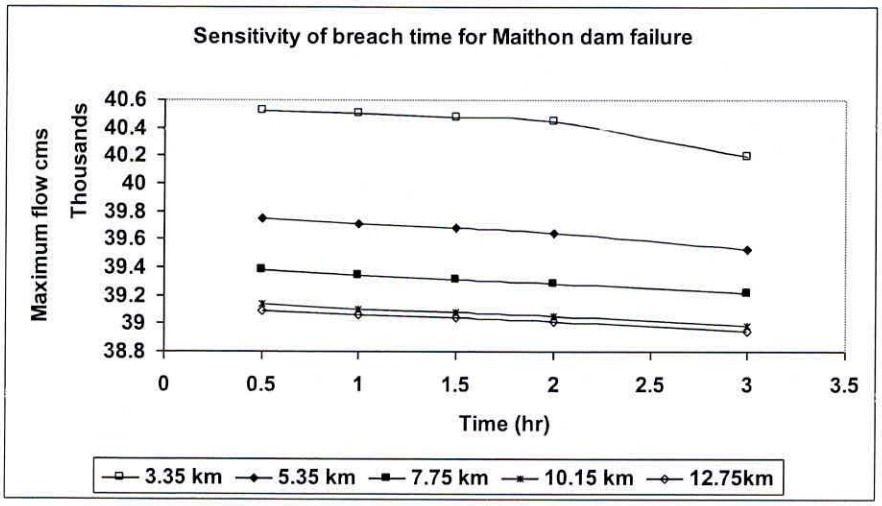

Fig. 5.17 (b). Sensitivity of breach time for Maithon dam failure.

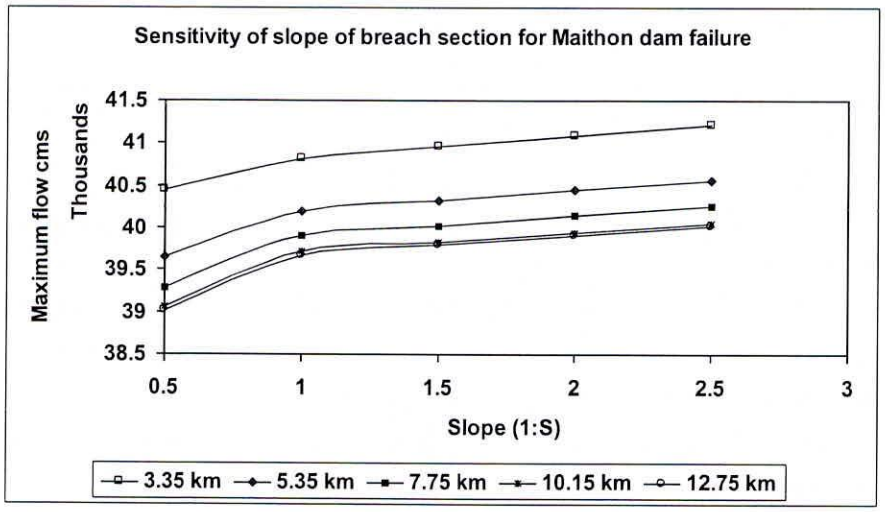

Fig. 5.17 (c). Sensitivity of slope of breach for Maithon dam failure.

5.6 Limitations of the Study

The dam break model requires huge amount of field data. Though the NWS DAMBRK model has capability to simulate various cases of dam break, in absence of necessary data, the model gives a much generalized output. For simulation of failure in Maithon-Panchet dam system, attempt has been taken to collect most of the relevant required data, some of them could not be find out. In this regard, the study are subject to the following limitations:

(i) The cross sectional details could be collected upto 39.64 km downstream of Panchet dam, but not at regular interval. Further, survey data of all sections for a particular year could not be collected. Some of the sections are surveyed during 1980 while others in 1984 and 1990. Due to this, in case of sedimentation in river bed during this period, the longitudinal profile of the river may change and the used data may not reflect the actual nature of river. The cross sectional details just downstream of dam location are not available for Maithon as well as for Panchet, which is an essential boundary condition for simulation. Though the nearest available cross section with suitable extrapolation are used in the study. Further, the surveyed sections are limited within the banks of the river and no information is available for the flood plain. As the dam break flood submerges the flood plain, the cross sections beyond the river banks along with hydraulic characteristics of the flood plain are also required for the dam break simulation. In this study, the sections are extended to the flood plain as per the information available from toposheets. For some of the stretch along the downstream river, the toposheet at 1:25,000 scales is available and river sections could be extrapolated with sufficient accuracy. But for a considerable stretch of river, the river sections have been extrapolated with 1:50,000 scale toposheet with inadequate contour information.

(ii) For preparation of digital elevation model of the area, contours from toposheet have been used. The area for which 1:25,000 scale toposheet are available provides contours at 10 m interval while for rest of the area; contours at 20 m interval are available. This induces error in the DEM and therefore in the inundation maps.

(iii) NWS DAMBREK model is one dimensional flow model and therefore is capable of simulating the river valley flow in Panchet and Maithon in most of its stretch. But at the confluence of the two rivers and other locations when river passes though the plain areas, the flow does not remain necessarily one dimensional and therefore the simulation inhibit error.

(iv) The details of any infrastructure in the river course could not be collected and therefore have not been considered in the study. Further, no information is available about the land use/nature of soils/rocks along the river for estimation of the value of Manning's coefficient, n. For carrying out this study, the value of n has been adopted, based on the comments made in the survey book (but limited to river sections only and not to flood plains) and in accordance with the guidelines mentioned in standard textbooks.

5.7 Conclusions

The following conclusion can be drawn from this study.

(i) NWS DAMBRK model can be applied with the limited data availability and yields useful information. In this study, the model is run and maximum discharge, maximum stage are estimated at various river cross sections. The inundation map is also prepared for various cases of dam break flood.

(ii) For finalization of the model parameters simulations have been carried out with various combinations of breach width and breach time to identify these parameters for the severe most flood resulting from failure of the dams. In case of the Maithon dam; which is an earthen dam of length 4.5 km the breach width has been assumed as 1 km and time of breach as 1 hours. This combination of breach width and breach time has resulted into a severe flood and therefore has been considered appropriate for dam break study. Similarly for the Panchet dam breach width of 1 km and breach time of 1 hr simulates the severe flood and therefore have been considered in the study.

(iii) The model can be applied for simulating the dam break failure condition under PMF condition as well as under the condition of earthquake or some terrorist attack by assuming suitable parameters.

(iv) The maximum stage reached at any section is of vital importance as it determines whether that section will be inundated or not. The inundation map prepared for each case provides information about the extent of inundation and also the magnitude of inundation.

(v) The geographical information system (GIS) like ERDAS serves as an important tool for preparation of the digital elevation model (DEM) of the downstream river reach and mapping the area inundated due to dam break flood by coupling the DEM with

the water levels computed using the DAMBRK package. Manual estimation of such purposes is a tedious and cumbersome process and often discourages the field engineers from carrying out the flood inundation studies resulting from the failure of a dam. At times, it also leads to erroneous estimates. On the other hand, modern techniques like the GIS serve as an efficient approach for storage, processing and retrieval of large amount of database. Its spatial modelling and tabular databases constitute a powerful tool for the data analysis. Also, the database created and stored in GIS system may be updated as and when required.

REFERENCES

Banerjee, S. and A. K. Das, (2003), Review of Floods in Damodar Valley Projects, Proceedings of International Conference on Water Related Disaster (ICWRD-2002), Kolkata, Volume –I, pp. 96-99.

Bruce, H., (1982), Asymptotic Solutions for Dam Break Problems, Journal of Hydraulic Division, American Society of Civil Engineers, Vol. 108 (1/4), pp115.

Chen, C. and L. A. Druffel, (1977), Dam break flood computation by method of characteristics and linearized implicit scheme, Proceedings, Dam-break flood modeling workshop, U.S. Water Resources Council, Washington, D.C., pp 312-345.

Cheng Lung Chen, (1985), Hydraulic concepts in debris flow simulation, Proceedings of Specialty Conference on delineation of Landslide, flash flood and Debris flow hazards in Utah, Utah State University, Logan, Utah, pp. 236-259.

Cristofano, E.A., 1965, Method for computing rate for failure of earth fill dams, Bureau of Reclamation, Denver, Colorado.

CWC, 2002, Regulation Manual for Damodar Valley Reservoirs, 2nd Edition, November, 2002, Central Water Commission.

Fread, D. L., (1987), Breach: An erosion model for Earthen Dam Failures, Hydrologic Research Laboratory, NOAA, NWS, U.S. Department of Commerce, Silver Spring, Maryland.

Fread, D.L., (1984), DAMBRK Model – The NWS Dam-Break Flood Forecasting Model, Hydrologic Research Laboratory, National Weather Services, Silver Spring, Maryland, 56pp.

Froehlich, D. C., (1987), Embankment-Dam Breach Parameters, Proceeding s of 1987 National Conference on Hydraulic Engineering, American Society of Civil Engineers, New York, pp. 570-575.

Gundalach, D. L. and W.A. Thomas, (1977), Guidelines for Calculating and Routing Dam Break Flood, Research Note No. 5, Corps of Engineers, U.S. Army, The Hydrologic Engineering Centre.

Hagen, V. K., (1982), Re-evaluation of Design Floods and Dam Safety, paper presented at Fourteenth ICOLD Congress, Rio De Janeiro.

Harris, G.W. and D. A. Wagner, (1967), Outflow from Breached Dams, University of Utah.

Hydrologic Engineering Centre, (HEC-1), (1981), Flood Hydrograph package, User Manual, U.S. Army Corps of Engineers, Davis, California.

Katopodes, N. D. and D. R. Schambar, (1982), Application of Dam Break Flood Wave Models, Journal of Hydraulic Division, American Society of Civil Engineers, Vol 109 (5/8),

Kjelds, J. and M. Rungo, (2002), Dam Breach Modeling and Inundation Mapping,

MacDonald, T. C. and J Langridge-Monopolis, (1984), Breaching Characteristics of Dam Failures, Journal of Hydraulic Division, American Society of Civil Engineers, 110, No. 5, pp. 567-586.

National Institute of Hydrology, 1985-86 Report No. CS-16, Dam break analysis for Machhu dam-II.

National Institute of Hydrology, 1987-88 Report No. TR-34, Development of dimensionless flood hydrographs from Machhu dam – II failure using dambrk model.

National Institute of Hydrology, 1990-91 Report No. CS 49, Application of NWS dam break program using data of Gandhi Sagar Dam.

National Institute of Hydrology, 1992-93 Report No. CS 89, Application of dam break program MIKE 11 to Machhu II dam and its comparison with NWS DAMBRK application results.

National Institute of Hydrology, 1996-97 Report No. CS (AR)-20, Dam break study of Barna dam.

National Institute of Hydrology, 2001 Report No. CS/AR-1/2000-2001, 'Dam Break Study of Myntdu Leska Dam Using DAMBRK Model.

National Institute of Hydrology, 2004 Dam break flow simulation study of Lower Manner dam in Andhra Pradesh, India.

National Institute of Hydrology, 2004 Dam break flow simulation study of Sri Ram Sagar dam in Andhra Pradesh, India.

Ponce, V. M. and A. J. Tsivoglou, (1981), Modeling of Gradual Dam Breaches, Journal of Hydraulics Division, American Society of Civil Engineers, 107, HY6, pp. 829-838.

Regulation manual for Damodar valley reservoirs, 2002, Central Water Commission, New Delhi.

Ritter, A., 1892, The propagation of water waves. Ver. Deutsch Ingenieure Zeitschr. (Berlin), 36, pt.2, No. 33, pp 947-954.

Sakkas, J. G., (1980), Dimensionless Graphs of Flood from Rupture Dam, Research Note No. 8, Hydrologic Engineering Centre, Davis, California.

Sakkas. J. G., and T. Strelkoff, (1973), Dam break flood in a prismatic dry channel, Journal of Hydraulic Division, American Society of Civil Engineering, 99, HY12, pp 2195-2215.

Singh, K.P., and A. Snorrason (1982), Sensitivity of outflow peaks and Flood Stages to the Selection of Dam Breach Parameters and Simulation Models, University of Illinois State Water Survey Division, Surface Water Section, Champaign, Illinois.

Subramanya, K., (1986), Flow in Open Channels, First revised edition, Tata McGraw-Hill Publishing Company Limited, New Delhi, pp. 68-69.

Terzidis, G., and T. Strelkoff (1970), Computation of Open Channel Surges and Shocks, Journal of hydraulic Division, American Society of Civil Engineers, 96, HY 12, pp. 2185-2610.

U.S. Army Corps of Engineers, (1960), Floods resulting from suddenly breached dams-conditions of minimum resistance, Hydraulic Model Investigation., Miscellaneous paper 2-374, Report 2, WES 121 pp.

Users Manual, 'DAMBRK', 1989. The N.W.S, Dam Break Flood Forecasting Model.

Wurbs R. A., (1987), Comparative Evaluation of Dam-Breach Flood Wave Models, Texas, A&M University, College Station, Texas, pp. 13-20.

Table 3.1: Annual Runoff at different dam sites (value in thousands)

Name of dam site	Minimum on Record (In acre feet)	Maximum on record (In acre feet)
Tilaiya	64	660
Maithon	655	5009
Konar	111	690
Tenughat	608	2,644
Panchet	1,108	7,351
Durgapur	1,965	15,272

(Regulation Manual for Damodar Valley Reservoirs, CWC, 2002)

Table 3.2: Salient Features of Maithon Project

A. General	
Location	Jharkhand State Latitude - 23^0 47' Longitude - 86^0 49'
District	Dhanbad
Nearest City/Town	Maithon and Kumardhubi (6.5 km),
Purpose	Multi-purpose
River	Barakar, major tributary of river Damodar
Year of comencement	December 1951
Year of completion	September 1957
B. Hydrology	
Catchment Area	6293.7 Sq. km including area intercepted by Tilaiya dam.
Maximum Observed Flood peak (27-09-1978)	10449 Cumec
Average annual runoff	2614.99 Million Cubic Meter
Spillway Design Flood	13,592 Cumecs
Average Annual rainfall	114.17 cm
C. Reservoir Levels	
River bed level	103.63 m
Full Reservoir Level (F.R.L)	152.4 m
Maximum Water Level (M.W.L)	150.88 m
Crest level of spillway	140.21 m
Height of Dam	Earth dam = 49.99 m Concrete dam = 56.08 m
Top of Dam (road elevation)	156.06 m
Width of Roadway	6.71 m
D. Reservoir Capacity Data	
Gross capacity @ F.R.L.152.40 m	1093.54 Million Cubic Meter
Gross capacity @ M.W.L.150.88 m	896.79 Million Cubic Meter
Dead storage @ E.L 132.59 m	93.17 Million Cubic Meter
Live storage between 132.59 m & 150.88 m	803.62 MM^3
E. Submergence	
Total area of submergence at F.R.L.	107.16 sq.km
F. Details Of Dam	
Spillway Crest Level	EL 140.21 m
Spillway Gate details	(12 Gates of 12.5 × 12.19 m)
Under Sluices	5 Nos. each of 3.05 m x 1.73 m size Sill Level E.L.121.01 m
Total length of Dam (Concrete + Earth)	362.41 + 4064.35

Table 3.3: Salient Features of Panchet Project

A. General	
Location	Jharkhand State Latitude - 23^0 40' Longitude - 86^0 46'
District	Dhanbad
Nearest City/Town	Kumardhubi (17.7 km),
Purpose	Multi-purpose
River	Damodar
Year of comencement	November 1952
Year of completion	November 1959
B. Hydrology	
Catchment Area	10,966 Sq. km including area intercepted by Konar and Tenughat reservoirs.
Maximum Observed Flood peak (04-10-1959)	12432 Cumec
Average annual runoff	4539.23 Million Cubic Meter
Spillway Design Flood	17,840 Cumec
Average Annual rainfall	114.17 cm
C. Reservoir Levels	
River bed level	97.54 m
Full Reservoir Level (F.R.L)	135.64 m
Maximum Water Level (M.W.L)	132.59 m
Crest level of spillway	123.45 m
Height of Dam	Earth dam = 40.84 m Concrete dam = 47.85 m
Top of Dam (road elevation)	139.30 m
Width of Roadway	9.75 m
D. Reservoir Capacity Data	
Gross capacity @ F.R.L.135.64 m	1358.08 Million Cubic Meter
Gross capacity @ F.R.L.132.59 m	939.19 Million Cubic Meter
Dead storage @ E.L 119.48 m	119.14 Million Cubic Meter
Live storage between 119.48 & 132.59 m	820.05 Million Cubic Meter
E. Submergence	
Total area of submergence at F.R.L.	153.38 sq.km
F. Details Of Dam	
Spillway Crest Level	EL 123.45 m
Spillway Gate details	(15 Gates of 12.19 × 12.19 m)
Under Sluices	10 Nos. each of 3.05 m x 1.73 m size Sill Level E.L.104.24 m
Total length of Dam (Concrete + Earth)	370 + 6407 m

Table 4.1: Probable maximum flood hydrograph at Maithon dam site

Time (hr)	Flow (Cumec)	Time (hr)	Flow (Cumec)	Time (hr)	Flow (Cumec)	Time (hr)	Flow (Cumec)
0	100	30	4800	60	26246	90	4000
3	100	33	5200	63	25250	93	3000
6	100	36	8500	66	24700	96	2500
9	100	39	12000	69	19200	99	2200
12	100	42	13500	72	15000	102	2000
15	100	45	16000	75	10000	105	1500
18	100	48	18500	78	7000	108	1000
21	500	51	22000	81	5100	111	800
24	1000	54	25000	84	4900	114	700
27	2400	57	25500	87	4700	117	400

Source: Banerjee et al, 2003.

Table 4.2: Probable maximum flood hydrograph at Panchet dam site

Time (hr)	Flow (Cumec)	Time (hr)	Flow (Cumec)	Time (hr)	Flow (Cumec)	Time (hr)	Flow (Cumec)
0	1000	24	12000	48	38875	72	6000
6	1100	30	20000	54	35000	78	4000
12	1400	36	28000	60	19750	84	2000
18	4500	42	36000	66	9900	90	1100

Source: Banerjee et al, 2003

Table 4.3: Survey of India toposheets used in preparation of DEM

Toposheet No.	Scale
73I/13	1:50,000
73M/2	1:50,000
73I/14 NW	1:25,000
73I/14 NE	1:25,000
73I/14 SE	1:25,000

Table: 5.1 Inflow details from Barakar for various failure cases of Panchet & Maithon dam

Failure case type	Failure condition of dam		Type of flow in Barakar at confluence
	Panchet	Maithon	
A1	fails	safe	C2
A2	safe	fails	C1
A3	fails	fails	C1
A4	safe	safe	C2
B1	fails	safe	C4
B2	safe	fails	C3
B3	fails	fails	C3
B4	safe	safe	C4

Table 5.2 (a): The maximum discharge at various d/s sections of Panchet river due to variation in breach width

Width (m) \ Sections	1.55	5.8	6.8	21.95	39.64
500	53006	47064	81422	77105	67122
1000	54434	48415	84296	77586	67430
1500	54958	48896	82137	77743	67529
2000	55184	49101	82221	77818	67577
2500	55304	49223	82266	77857	67610

Table 5.2 (b): The maximum discharge at various d/s sections of Panchet river due to variation in breach time

Time (hr) \ Sections	1.55	5.8	6.8	21.95	39.64
0.5	54096	48337	81707	77366	67309
1	54434	48415	84296	77586	67430
1.5	54533	48556	82214	77803	67551
2	54123	48597	82463	78015	67671
3	53539	48630	82936	78416	67897

Table 5.2 (c): The maximum discharge at various d/s sections of Panchet river due to variation in breach slope

Slope (S) \ Sections	1.55	5.8	6.8	21.95	39.64
0.5	54434	48415	84296	77586	67430
1	54613	48629	82046	77659	67472
1.5	54788	48675	82132	77734	67515
2	54956	48833	82210	77803	67555
2.5	55120	48981	82293	77874	67595

Table 5.3 (a): The maximum discharge at various d/s sections of Maithon river due to variation in breach width

Width (m) \ Sections	3.35	5.35	7.75	10.15	12.75
500	39972	39244	38895	38670	38631
1000	40444	39645	39285	39055	39015
1500	40605	39795	39431	39198	39158
2000	40690	39872	39506	39272	39232
2500	40733	39911	39544	39309	39269

Table 5.3 (b): The maximum discharge at various d/s sections of Maithon river due to variation in breach time

Time (hr) \ Sections	3.35	5.35	7.75	10.15	12.75
0.5	40521	39749	39376	39134	39092
1	40506	39707	39339	39103	39061
1.5	40479	39678	39314	39081	39041
2	40444	39645	39285	39055	39015
3	40197	39524	39212	38988	38949

Table 5.3 (c): The maximum discharge at various d/s sections of Maithon river due to variation in breach time

Slope (S) \ Sections	3.35	5.35	7.75	10.15	12.75
0.5	40444	39645	39285	39055	39015
1	40821	40194	39898	39705	39666
1.5	40957	40320	40021	39826	39787
2	41086	40441	40139	39942	39904
2.5	41211	40559	40253	40054	40016